IN THE UNITED STATES PATENT AND TRADEMARK OFFICE

In re Patent of	:	Wilhelm, et al.
Patent No.	:	6,680,320
For	:	UROKINASE INHIBITORS
Control No.	:	90/007,935
Filed	:	July 26, 2002
Issued	:	January 20, 2004
TC/A.U.	:	3991
Examiner	:	Bennett Celsa
Docket No.	:	2923-236
Customer No.	:	6449
Confirmation No.	:	6102

DECLARATION

Commissioner for Patents
P. O. Box 1450
Alexandria, VA 22313-1450

Sir:

I, John Foekens, declare as follows.

1. I am listed as coinventor of the above-captioned U.S. patent. I am B.Sc., MS.C. and Ph.D. in Biochmemistry. I am currently Head of the Laboratory of Tumor Endocrinology of the Department of Medical Oncology at the Erasmus Medical Center Rotterdam, Netherlands. My group has been involved in the study of the clinical relevance of the urokinase system of plasminogen activation for over 15 years. The studies, which have mainly been carried out in patients with breast cancer, have been published in over 30 peer-reviewed scientific publications, in journals like the Journal of the National Cancer Institute, Journal of Clinical Oncology, and Cancer Research. For over 10 years we have been collaborating with various companies on drugs aimed at inhibiting primary tumor growth and metastasis in our experimental in vivo models,

mainly syngeneic rat breast and colon cancer models. The drugs studied involve metalloproteinase inhibitors, and urokinase inhibitors.

2. I understand that Nα-(2,4,6-Triisopropyl-phenylsulfonyl)-3-amidino-(L)-phenylalanine-4-ethoxycarbonyl-piperazide ("(L) isomer") and Nα-(2,4,6-Triisopropyl-phenylsulfonyl)-3-amidino-(D,L)-phenylalanine-4-ethoxycarbonyl-piperazide ("racemate") are disclosed in the 1997 and 1998 Pentapharm Product Catalogues as a low molecular weight synthetic inhibitor for uPA. However, I do not see any indication that either of the racemate and (L) isomer is a "selective" uPA inhibitor in either of the Catalogues. Nor do I see any indication that either of the racemate and (L) isomer is acceptable for a pharmaceutical use, particularly an anti-invasiveness or anti-proliferation use, in either of the Catalogues.

3. Rather, I see the data in the tables at page 24 of the 1997 Pentapharm Product Catalogue and page 25 of the 1998 Pentapharm Product Catalogue as strongly indicating that the racemate and (L) isomer are not selective uPA inhibitors, but instead are general serine protease inhibitors with a very broad spectrum of strong inhibitory activities with many enzymes including blood clotting cascade enzymes such as thrombin, Factor X and plasmin. For example, the Ki values of the racemate for trypsin, thrombin, Factor Xa, Faxtor XIIa, plasmin and sc-tPA taught in the 1997 Pentapharm Product Catalogue are respectively 0.2, 1.2, 2.8, 1.9, 1.0 and 17.6 times of the Ki value of the racemate for uPA. The Ki values of the (L) isomer for trypsin, thrombin, Factor Xa, Faxtor XIIa, plasmin and sc-tPA taught in the 1998 Pentapharm Product Catalogue

are respectively 0.1, 1.6, 3.7, 2.4 and 23.2 times of the Ki value of the (L) isomer to uPA. Therefore, I am of the opinion that the racemate and (L) isomer are not "selective" uPA inhibitors.

4. Further, I believe that other scientists would agree with my opinion. For example, Todd W. Rockway and Vincent L. Giranda, in their paper "Inhibitors of the Proteolytic Activity of Urokinase Type plasminogen Activator", Current Pharmaceutical Design, Volume 9, No. 19, 2003, Pp.1483-1498, state "WX-UK1 (compound 11, see below), from Wilex AG, ... is not strictly a uPA inhibitor, rather it inhibits a broad spectrum of serine proteases including uPA, plasmin, thrombin and trypsin" at page 1484, left column, third full paragraph. WX-UK1 is Nα-(2,4,6-Triisopropyl-phenylsulfonyl)-3-amidino-(D,L)-phenylalanine-4-ethoxycarbonyl-piperazide.

5. In fact, a person having ordinary skill in the art would not even have thought the naming convention of the Pentapharm Catalogues, which named the racemate and (L) isomer as Pefabloc uPA, suggested that the racemate and (L) isomer were uPA selective. Rather, one would have understood that the naming convention only indicated that the racemate and (L) isomer had the lowest Ki value for uPA among the compounds listed in the tables. Compare the Ki values in the uPA row in the tables in the Catalogues. Further, in the tables, Pefabloc uPA has a much lower Ki value for trypsin than that for uPA, and the Ki values for thrombin and plasmin are not that much higher than that for uPA, but the racemate and (L) isomer were still called Pefabloc uPA. In addition, the Ki value for uPA of Pefabloc tPA/Xa is comparable to that of

Pefabloc uPA and the Ki values of Pefabloc tPA/Xa for trypsin, Factor XII and PC are lower than that of Pefabloc tPA/Xa for sc-tPA and tc-tPA, but the Catalogues still named the compound Pefabloc tPA/Xa. In fact, the naming convention of the Catalogues is a bit arbitrary. Pefabloc TH, PL, Xa, Tryp and uPA have the lowest Ki values for the named enzymes among the compounds compared in the tables. On the other hand, the other Pefabloc compounds were named after specific enzymes, for which the compounds do not have the lowest Ki values. Therefore, it is my opinion that a person having ordinary skill in the art in view of the data presented in the tables would not have thought the name "Pefabloc uPA" suggested that the racemate and (L) isomer were selective uPA inhibitors.

6. For the reasons set forth above, I am quite confident in my opinion that the Pentapharm Catalogues would not have suggested a person having ordinary skill in the art that Pefabloc uPA is a "selective" uPA inhibitor. Rather, I believe that the Catalogues would have suggested that Pefabloc uPA is a serine protease inhibitor with strong inhibitory activities to a broad spectrum of serine proteases including trypsin, thrombin, Factor Xa, plasmin, uPA, tPA, PC and tryptase.

7. Further, based on the data in the tables of the Catalogues showing that Pefabloc uPA has inhibitory activities to a broad spectrum of blood clotting cascade enzymes including tPA and plasmin, I am of the opinion that a person having ordinary skill in the art would not have thought that the racemate or (L) isomer would be suitable for a pharmaceutical use, especially an anti-invasiveness or anti-proliferation use.

Around 1998, the generally accepted understanding among the scientists researching uPA inhibitors for an anti-invasiveness or anti-proliferation use (i.e., person having ordinary skill in the art) was as follows.

> Since both uPA and its fibrinolytic counterpart tPA share identical specificity for the Arg^{560}-$Va1^{561}$ bond in plasminogen (2-4), most low-molecular-weight protease inhibitors which inhibit uPA also inhibit tPA. Such inhibitors are unsuitable for use as antiinvasiveness drugs due to the potential undesired inhibition of tPA-mediated fibrinolysis. Similarly, antiinvasiveness uPA inhibitors should not inhibit plasmin, since both uPA- and tPA-mediated pathways converge through this enzyme. Unfortunately, such stringent selectivity requirements eliminate most of the known synthetic inhibitors of uPA. Moreover, the few remaining uPA-selective inhibitors show only moderate potency.

Towle et al., "Inhibition of urokinase by 4-substituted benzo[b]thiophene-2-carboxamidines: an important new class of selective synthetic urokinase inhibitor", Cancer Res. 53(11):2553-9 (1993), 2553, right column, the first full paragraph.

> Therapeutic inhibitors of uPA should not appreciably inhibit the closely related enzymes (thrombin and tPA [12]), which are critical components of the blood-clotting pathway.

Katz et al., "Structural basis for selectivity of a small molecule, S1-binding, submicromolar inhibitor of urokinase-type plasminogen activator", Chem Biol. 7(4):299-312 (2000), 300, left column, the paragraph bridging between pages 299 and 300.

Therefore, a person having ordinary skill in the art would have thought that Pefabloc uPA having strong inhibitory activities to many enzymes involved in blood clotting cascade, including sc-tPA and plasmin, would be unsuitable for a pharmaceutical use, particularly, an anti-invasiveness or anti-proliferation use.

8. Contrary to the generally accepted understanding among the uPA inhibitor researchers set forth above, and what a person having ordinary skill in the art would have thought as explained above, we found that the racemate and (L) isomer are not cytotoxic in pharmacologically effective concentrations (see example 5 of the patent) and the weights of lung, liver, kidney and spleen were unchanged in the tested animals through the treatment using the compounds (see example 7(a) of the patent), which indicates that the racemate or (L) isomer is clinically acceptable without a major side effect. It is noted that such measurement of weight losses of vital organs was generally accepted as a reasonable measure to test for unacceptable side effects. Further, as indicated in the Rockway paper, WX-UK1 was found pharmaceutically acceptable in Phase I human trials. Therefore, I am of the opinion that the racemate and (L) isomer are truly unexpectedly effective and acceptable for a pharmaceutical use, particularly, an anti-invasiveness or anti-proliferation use.

9. I am also of the opinion that a person having ordinary skill in the art would not have found the racemate or (L) isomer is functionally analogous to amiloride or B428 in view of the data presented in the tables of the Pentapharm Catalogues and the information available at the time of filing with regard to amiloride or B428. The Towle paper teaches that the IC_{50} values of amiloride for tPA and plasmin are at least 138 times greater than that for uPA and the IC_{50} values of B428 for tPA and plasmin are approximately 335 and 1100 times, respectively, greater than that for uPA. See Table 1. Even the Bridges reference, relied on by the Patent Office, states that the title

compounds of the reference "are 60-800-fold more active at inhibiting urokinase than tPA and are generally 400-10,000-fold selective for urokinase over plasmin." See column 10, lines 43-45. Particularly, the reference teaches the selectivity of B428 for tPA and plasmin is respectively 261 and 1067 times. See Ex#5 in table 4 of the Bridges reference. On the other hand, the Pentapharm Catalogues teach that the Ki values of the racemate for tPA and plasmin are only approximately 18 and 2 times, respectively, greater than that for uPA and the Ki values of the (L) isomer for tPA and plasmin are only approximately 24 and 2~3 times, respectively, greater than that for uPA. This level of selectivity of the racemate and (L) isomer for uPA against tPA and plasmin is not only very minimal in itself but also quite insubstantial compared with those of amiloride or B428. As explained above, selectivity for uPA against tPA and plasmin was considered critical in predicting the potential of a serine protease for a pharmaceutical use, particularly, an anti-invasiveness or anti-proliferation use. Therefore, a person having ordinary skill in the art, knowing the substantial difference in a critical property for predicting the potential for the pharmaceutical acceptability and use, would not have found the racemate or (L) isomer functionally analogous to amiloride or B428. Rather, one would have thought that amiloride and B428 are uPA inhibitors with a strong selectivity for uPA against tPA and plasmin, but the racemate and (L) isomer of the present Patent are strong, general serine protease inhibitors with a very broad spectrum of inhibitory activities and with a low selectivity for uPA against tPA and plasmin.

10. I state that all statements made herein of my own knowledge are true and that all statements made on information and belief are believed to be true; and further that these statements were made with the knowledge that willful false statements and the like so made are punishable by fine or imprisonment, or both, under Section 1001 of Title 18 of the United States Code and that such willful false statements may jeopardize the validity of the application or any patent issuing thereon.

John Foekens

Dec 27/2006
Date

D / Annex L

ent Pharmaceutical Design, 2003, 9, 1483-1498 1483

Inhibitors ytic Activity of Urokinase Type Plasminogen Activator

Todd W. Rockway[†] and Vincent L. Giranda[°]

Department of Infectious Disease Research[†] and Cancer Research[°], Abbott Laboratories, 100 Abbott Park Road, Abbott Park, IL, 60064, USA

Abstract: Urokinase type plasminogen activator (uPA) activates plasminogen to plasmin and is often associated with diseases where tissue remodeling is essential (e.g. cancer, macular degeneration, atherosclerosis). We discuss some of the mechanisms of uPA action in diseases, and evidence that some of the early uPA inhibitors can modulate the progression of these diseases. Recently, a number of research groups have discovered, with the aid of structure-based design, a new generation of uPA inhibitors. These inhibitors are much more potent and selective than their predecessors. We will review this progress here, and give particular attention to the structural rationale associated with these observed increases in potency and selectivity.

INTRODUCTION

Urokinase type plasminogen activator (uPA) is one of the two physiologically important serine proteases that can hydrolyze the zymogen plasminogen to form the active enzyme plasmin. The second serine protease is tissue plasminogen activator (tPA). These names, tPA and uPA, are somewhat of a misnomer because tPA primarily activates plasminogen within the hemodynamic spaces, while uPA primarily activates plasminogen within tissues. Once activated by either uPA or tPA, plasmin degrades fibrin, and is therefore important in the fibrin-dependent processes such as blood clotting, tissue remodeling, wound healing and inflammation [1-6]. Plasmin also degrades other components of the extracellular matrix, including laminin and fibronectin. Furthermore, plasmin can activate a number of other zymogens such as matrix metalloproteases. Because it performs many functions, the inhibition of plasmin would be expected to have a number of toxic consequences, most notably with regard to hemostasis. Seminal experiments with plasminogen knockout animals have indeed demonstrated this toxicity. These animals show a propensity towards thrombosis, and are deficient in wound healing, and have diminished macrophage and lymphocyte responses to inflammatory stimuli [7-10].

Because uPA predominates in tissues, it is thought that inhibiting uPA will have minimal toxic effects on blood clotting, but should still modulate tissue-remodeling processes. This idea is reinforced by the findings that uPA is implicated in the pathogenesis of a number of diseases that require tissue remodeling such as wound healing [11-15], cancer [5,8,9,16-18], atherosclerosis [19-23], vascular restenosis [24-27], cardiac rupture[28], and macular degeneration [29]. The fact that both the tPA and uPA knockout animals have mild phenotypes relative to the plasminogen knockout animals suggests that tPA and uPA may be able to partially compensate for each other [30-32].

uPA may also act as a growth factor, independent of its proteolytic activity. uPA binds to the uPA receptor (uPAR, CD87), and this binding is thought to focus the uPA activity into areas of active tissue remodeling. The uPAR is a glycophosphatidyl inositol linked receptor, and as such has no intracellular component [6,33-35]. In spite of this, it is clear that uPA, through uPAR, is able to activate outside-in signaling pathways that induce growth in certain cells. The signal is thought to be transmitted via integrins to which the uPA:uPAR complexes bind [36-41]. More recently, these signals have been shown to proceed through growth factor receptors such as epidermal growth factor receptor [42].

The effects of uPA have been most widely studied in the progression of cancer. Indeed, increased uPA activity is found in a wide variety of human cancers, and is often an independent poor prognostic factor [43-46]. Furthermore, the progression of experimental tumors in both plasminogen or uPA knockout animals is retarded relative to the control animals [18,47-50]. Because uPA has activities unrelated to its proteolytic activity, it is not clear that the reduction in tumor progression is related to the catalytic activity of uPA.

A number of studies have been performed examining the effects of uPA inhibitors in experimental tumors. The published results have been mixed, and even when positive, the results have not been dramatic. Amiloride, a potassium-sparing diuretic, is also a uPA inhibitor [51,52]. It has been tested independently in four laboratories with mixed results. In two of these studies, the amiloride appeared to have no effect on the growth or metastatic spread of subcutaneously implanted mouse mammary [53] or rat prostate tumors [54]. In a third study, amiloride administered in the drinking water was able to diminish the number of metastatic tumors, after an intra-jugular administration of rat mammary tumor cells. In the fourth study, amiloride was again administered in the drinking water and was able to diminish the growth of DU-145 human prostate cancer cells in immunocompromised

°Address correspondence to this author at the Department of Cancer Research, R47S, AP9A, Abbott Laboratories, 100 Abbott Park Road, Abbott Park, IL, 60064, USA: Tel: 847-937-0268; Fax: 847-938-2365; E-mail: girandav@abbott.com

1381-6128/03 $41.00+.00

mice. The other pharmacological effects (diuresis) of amiloride, combined with the modest observed anti-tumor effects, make it impossible to conclude that these effects are indeed due to inhibition of uPA.

More potent and selective uPA inhibitors (B-428 and B623, compounds 17 and 16 respectively, see below) have also shown mixed results in cancer models. In one study the compounds showed a very modest growth delay at the primary site of a subcutaneous mouse mammary tumor [53]. However, the same group showed that administration of the uPA inhibitors actually increased the number of metastases formed after injecting the tumor cells into the tail vein.

Rabbani and co-workers have also examined the effects of B-428 on experimental tumors. They have shown a modest tumor growth reduction in both rat mammary [55] and prostate tumors [56] implanted subcutaneously. They were able to show an enhancement of this effect in the mammary tumors when tamoxifen, an anti-estrogen, was added to the regime [55].

One compound, WX-UK1 (compound 11, see below), from Wilex AG, is in Phase I human trials [57]. Rodent tumor model studies have been presented at scientific meetings (92nd Annual Meeting of the American Association for Cancer Research, 2001, abstract #371), but have yet to appear in the peer-reviewed literature. This compound is not strictly a uPA inhibitor, rather it inhibits a broad spectrum of serine proteases including uPA, plasmin, thrombin and trypsin. This may be an advantage, as there are data to suggest that inhibiting multiple proteolytic paths may be more efficacious than inhibiting uPA alone [10].

A number of investigators have been able to slow the growth or spread of tumors using uPAR inhibitors or antibodies [58-61]. These data suggest that at least part of the observed phenotype in the uPA knockout animal, where tumors grew more slowly, and metastasized less frequently [18], may be due to the lack of signaling through uPAR, and thus unrelated to the catalytic activity of uPA.

These decidedly mixed results in cancer models have fostered two lines of thought. The first supposes that improved compounds will yield better results. The second is that uPA inhibition, by itself, will be insufficient to significantly effect the progression of cancer, and therefore must be combined with some other therapy (e.g. inhibition of other proteases). The resolution of this dispute regarding the efficacy of uPA inhibition will await the advance of the new generation of inhibitors into pre-clinical rodent models and ultimately into human clinical trials.

While uPA inhibitors have been studied most extensively in cancer, there is also acute interest in uPA inhibition in other diseases, particularly where the slowing of tissue remodeling may be advantageous. The uPA deficient animals show a dramatic reduction in myocardial rupture following experimental myocardial infarction [28,62]. Keloid and scar formation [10,13,63-65], restenosis following percutaneous coronary transluminal angioplasty [24,26,66-71], as well as inhibition of macular degeneration [29,72,73] are also areas of active investigation.

The ample evidence that uPA and uPAR are involved in many disease states has led many research groups to attempt to create potent and selective uPA inhibitors. While the ultimate utility of these compounds remains unknown, significant advances in inhibitor design have recently been achieved. These advances have been enabled by the use of structure-based design. Here, after a brief discussion of the historical roots of many uPA inhibitor programs, we will review recent developments in the design of reversible competitive uPA inhibitors. We will pay particular attention to the structures of these compounds when bound into the uPA active site, and discuss how these structures can help us to understand the potencies of the compounds.

THE UPA STRUCTURE

The structure of the catalytic subunit of uPA was first described Spraggon et al. [74]. Other investigators have also solved the structure of uPA, often in complex with small molecule inhibitors [75-77]. These studies provided a structural basis for understanding the similarities and differences between uPA versus other serine proteases (e.g. thrombin, factor Xa). The structures reveal that uPA has much in common with other trypsin-like serine proteases, where all have a similar protein fold. The site of catalysis, comprising the oxyanion hole plus Ser195, His57, Asp102 (the catalytic triad) are likewise similar. Another common feature of the trypsin-like serine proteases, also present in uPA, is a deep S1 pocket, which has at its base, a negative charge (the S1 pocket of the enzyme binds the amino acid, P1, on the N-terminal side of the scissile bond of the peptide substrate).

The work of Spraggon and coworkers [74] illustrated the binding of a covalent inhibitor, Glu-Gly-Arg-chloromethyl ketone (Glu-Gly-Arg-cmk), within the active site of uPA (Fig. 1). Here, the arginine side chain points towards the Asp189 carboxylate side chain at the base of the S1 subsite, presumably mimicking the natural substrate. In addition to Asp189, the guanido group of arginine also makes hydrogen bonds with the Ser190 side chain oxygen and the backbone carbonyl oxygen of Gly218. Studies described by Nienaber et al. [76] and Katz et al. [77] illustrated the binding of small molecules, such as amiloride, phenylguanidines, and amidines to uPA. The amidine or guanidine moieties are critical for the potency of these inhibitors and bind in a fashion similar to the arginine side chain (Fig. 2). Although similarities in the S1 sites predominate in the trypsin-like serine proteases, Katz and co-workers [78] have been able to identify and exploit differences at residue 190, adjacent to the Asp189 (see below). Enzymes such as uPA, trypsin and plasmin all have a Serine at position 190, whereas tPA, thrombin and factor Xa have an alanine at this position.

There are also other important differences between uPA and most trypsin-like serine proteases. In particular, the S2 and S4 subsites are smaller in uPA than in other trypsin-like serine proteases such as thrombin or factor Xa. This structural feature is due in part to a two-residue insertion at His99 that effectively reduces the size of the S2 and S4 pockets. For this reason, the peptidomimetic strategies successfully employed in the creation of thrombin inhibitors has proven more difficult in the design of uPA inhibitors.

In addition to the substrate-binding groove, there are several other subsites within the active site of uPA that are

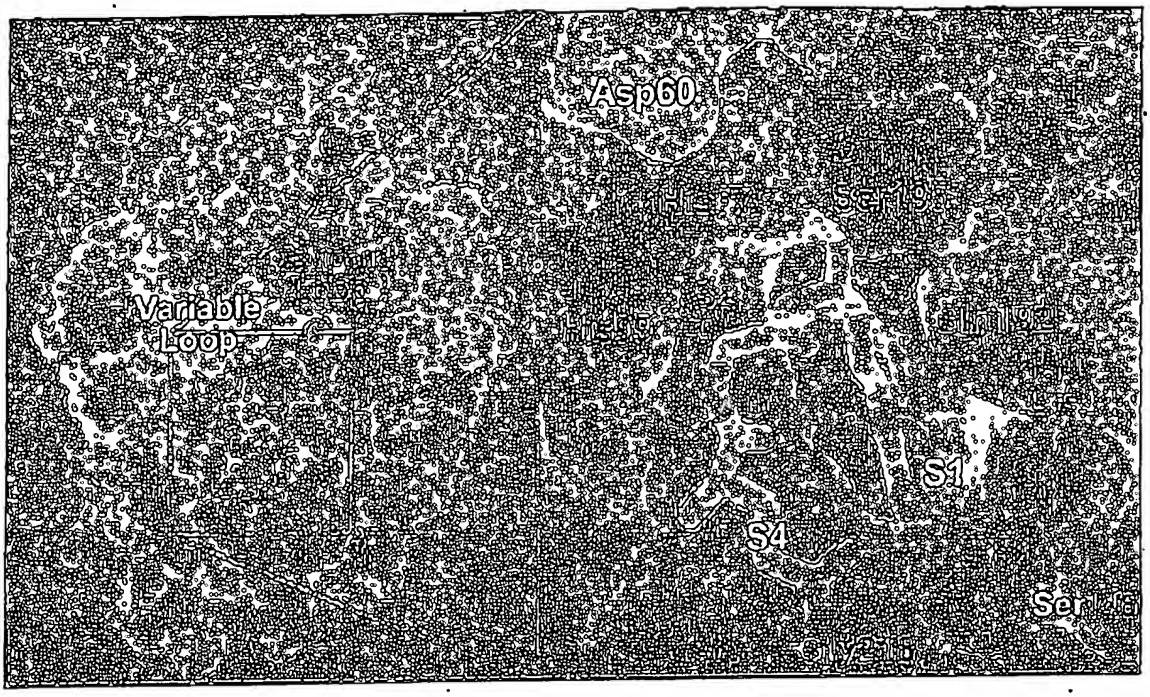

Fig. (1). The electrostatic surface of low-molecular weight uPA is depicted. Red color indicates a negative charge potential, blue positive. Glu-Gly-Arg chloromethyl ketone is docked into the active site. The structure shown here has the side chain of Gln192 rotated away from the S1β pocket. This residue is known to be rotated into different conformation depending on the bound inhibitor. The Arg residue binds into the deep S1 sub-site, and interacts with the Asp189 at the pocket's base. This critical interaction is mimicked by uPA inhibitors. Notice that the S2 and S4 subsites are relatively small, particularly when compared to other trypsin-like serine proteases.

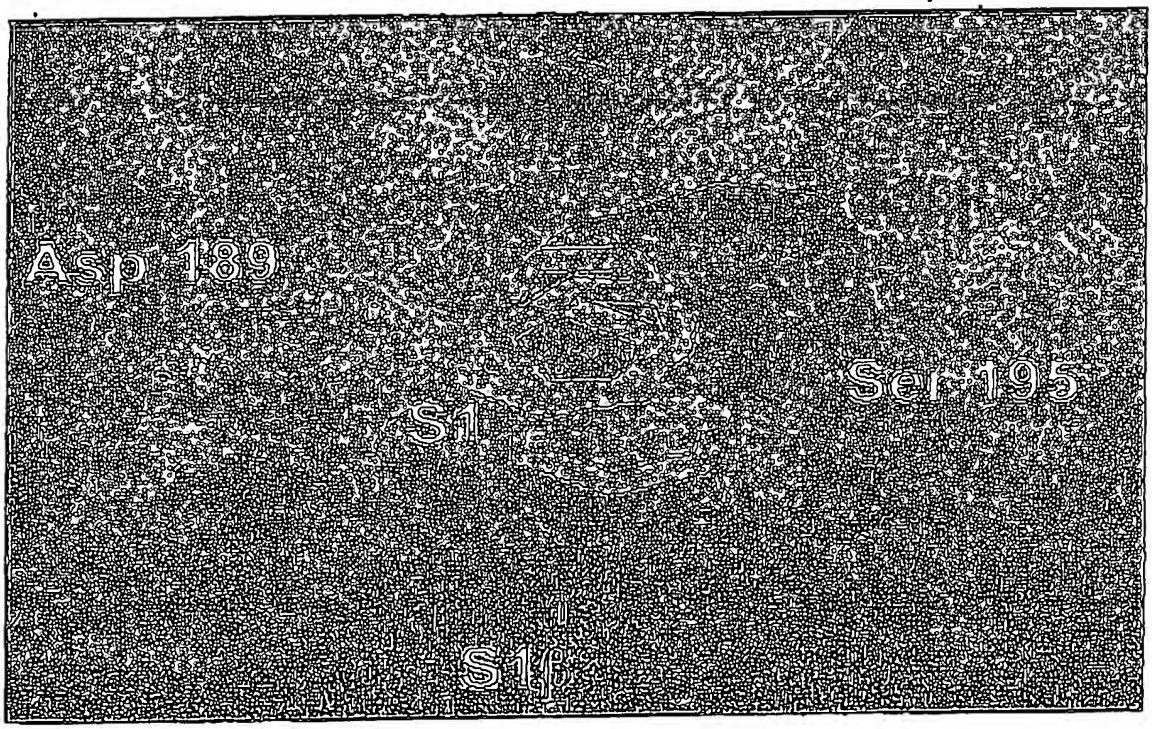

Fig. (2). Three prototype ligands are bound in the S1 subsite of uPA. Benzamidine (orange) and phenyl guanidine (magenta) both form bidentate hydrogen bonds with Asp189. The 2-amino group of 2-aminoisoquinoline forms a bifurcated hydrogen bond with Asp189. The advantage of the 2-aminoquinoline, as well as acetyl guanidines, is that they have a lower pKas than the amidines or guanidines and thus are likely to have better pharmacokinetic properties.

accessible to small molecule inhibitors and can be exploited to increase the potency and selectivity of uPA inhibitors. One such site is near the S1 pocket and is called the S1β site (Fig. 1). The floor of S1β is bounded by a disulfide bridge between Cys191 and Cys220. The sides of this site are defined by the residues Gly218 and Ser146, and the side chains both of Lys143 and Gln192 [76]. The S1β is not apparent in all structures because the side chain of Gln192 is mobile and can rotate to close off a large portion of the S1β site. The amino acids at both positions 143 and 146 vary considerably between serine proteases, and therefore interactions with the S1β pocket afford the potential for creating selective inhibitors.

The sequence between residues 58 and 64 is unique for a particular serine protease and has been called the variable loop. This loop is near the catalytic triad and has been exploited to design selective compounds. Not only is the variable loop significantly different between uPA and other serine proteases, it is also significantly different between the human and mouse uPAs [79]. These differences are substantial, and can be exploited to create mouse or human selective uPA inhibitors. Of course, this also means that investigators must be cautious when interpreting the results of their inhibitors when used in mixed systems (e.g. tumor xenografts models).

Active pursuit of small molecule uPA inhibitors began with the discovery that aryl guanidines, aryl amidines, or acyl guanidines all exhibited inhibition of the uPA catalytic domain. Initial compounds in each class exhibited modest potency and poor selectivity. Early chemical studies allowed the design of small molecule uPA inhibitors with improved potency and selectivity in each class. The subsequent structural studies of small molecule uPA inhibitor-enzyme complexes allowed the intelligent elaboration of these compounds to produce very potent and selective inhibitors. Structures of these potent compounds have been used to define and understand other interactions, which have been used in an iterative fashion to further improve the molecules.

ARYL GUANIDINES

Phenylguanidine (Fig. 2), inhibits uPA with a K_i of approximately 25 μM and exhibits selectivity over plasmin, thrombin, tPA, and plasma kallikrein (Table 1) [76,80,81]. Yang and coworkers [80] described a series of ortho, meta or para substituted phenylguanidine-based uPA inhibitors and proposed a model of binding for substituted phenylguanidines based on quantitative structure-activity relationship (QSAR) analysis. The most potent inhibitors were, 4-Chloro phenylguanidine (1, K_i = 6.1 μM) and 4-Trifluoromethyl phenylguanidine (2, K_i = 6.5 μM). These compounds also exhibited 10 to 20-fold selectivity for uPA over trypsin and greater than 100 to 1000-fold selectivity for uPA over plasmin, thrombin, plasma kallikrein and tPA (Table 1). Para-substituted phenyl guanidines appeared to have greater inhibitory potency when the para substituent was electron-withdrawing and hydrophobic, while bulky substituents decreased the potency of uPA inhibition. The ortho and meta substituted phenylguanidine analogs were approximately 10 to 100-fold less potent than the para-substituted compounds. Bulky substituents, especially ortho to the guanidine moiety, decreased further the uPA inhibitory potency.

The crystal structure of phenylguanidine has the expected interaction between the guanido group and the Asp189 at the base of the S1 pocket. A para position substituent on the phenylguanidine would be directed towards the catalytic triad. The para position is only 4 Angstroms from the catalytic Ser195 oxygen and is near the oxyanion hole. The improved potency of the 4-Cl phenylguanidine analog compared to phenylguanidine may be explained by a favorable interaction of the 4-Cl group with Ser195.

Despite the initial structure-activity relationships suggesting that substitution of the ortho or meta sites do not lead to improved potency, the crystal structures of these compounds reveal that this need not be true. The structures show that the aromatic moiety of the guanidine is sufficiently exposed at the ortho and para positions that substitutions at these positions may yield increased potency. Both of these positions point towards the S1β pocket, with the ortho position more favorable than the para.

Recently, another 4-substituted phenylguanidine analog (3) has been described by Sperl *et al.* [81,82]. The uPA inhibition for 3 is 2.4 μM. Crystallographic analysis of this compound shows the phenylguanidine moiety characteristically occupying the S1 site. The urea spacer is involved in four defined hydrogen-bonding interactions. The urea carbonyl binds to the oxyanion hole making hydrogen bonds to the backbone NH groups of Gly193 and Ser195. The urea amide hydrogens form two water-mediated hydrogen bonds to the Ser214 carbonyl and the Gln192 side chain carboxamide, respectively. This network of hydrogen bonds rigidifies the urea linkage projecting the adamantyl group toward a shallow hydrophobic pocket close to the Cys42-Cys58 disulfide bond. However, despite this extensive network of interactions, the inhibitory potency of 3 is nearly equivalent to that of the more simple 4-chloro and 4-trifluoromethyl compounds.

Amiloride (4) was reported to inhibit uPA with a K_i = 7 μM [51,52,76]. The selectivity of amiloride for uPA over similar trypsin-like serine proteases such as plasmin, thrombin, plasma kallikrein and tPA is high, however amiloride inhibited trypsin with nearly equal potency as uPA (Table 1).

An amiloride-uPA complex structure [76] reveals that amiloride occupies the S1 binding pocket as expected with the pyrazine ring extending further out of the S1 site than does phenylguanidine, due to the additional carbonyl group within the acyl guanidine moiety. The interaction of the guanidine moiety with the Asp189 in the S1 site is similar for both the amiloride and phenylguanidine. Other interactions between amiloride and the protein include a hydrogen bond between the inhibitor 3-amino and the oxygen of the Ser195 side chain. The 6-chloro group is directed toward the hydrophobic S1β site [76].

An interesting structural feature of amiloride is the acyl guanidine moiety. This moiety is less basic (pKa = 8.6) than an amidine (pKa = 10.2). For thrombin inhibitors, the high basicity of amidine or guanidine containing compounds has been shown to play a role in their poor pharmacokinetic properties [83]. Because it is likely that this same issue will arise with an amidine or guanidine containing uPA inhibitor, the less basic amiloride scaffold makes an attractive starting point for the design of an orally available uPA inhibitor.

Table 1. Inhibition Constants for uPA Inhibitors Versus Several Serine Proteases. Inhibition Constants are in μM, and are K_is Unless Noted

Compound #	uPA	tPA	Plasmin	Thrombin	Factor Xa	P-Kallikrein	Trypsin	Reference and Comments
1	6.1	>1000	>500	>1000		>2000	120	(77); 4-chloro phenylguanidine
2	6.5	>1000	>500	>1000		>2000	63	(77); 4-trifluoromethyl phenylguanidine
3	2.4	>1,000	>1,000	600	>1,000	-	-	(78,79); WX-293T
4	7.0	>1000					32	(48,49,73); amiloride
5	0.061	>60	17.4	-	-	-	-	(81-84)
6	0.17	52	>100					(81-84)
7	6.1		100					(85)
8	2.2		7.9					(85)
9	5.9	>100	51			23	7.8	(73,85); naphthamidine
11	0.41	4.9	0.39	0.49	1.7	7.2	0.037	(87); WX-UK1
12	0.64	8.7					0.6	(78)
13a	0.036		11	13	3.0		0.15	(88)
13b	0.0077		0.58	0.11	2.1		0.0033	(88)
14	0.0031	>2500	370					(91)
15	3.7	>1000	>1000					(92)
16	0.070	24	>250					(92,93); B623; IC_{50}
17	0.32 0.21	110 16.8	350	20	30		0.44	(92); B428; IC_{50} (74); APC-6860; K_i
18	0.60							(72,76)
19	0.040	48	1.6	4.9		1.4	0.33	(72,76)
20	0.035	25	3.8	3.2		10	1.7	(72,76)
21	0.63	32	2.0	5.6		2.5	0.32	(76)
22	0.040	54	16	>100		7.2	2.1	(76)
23	0.0006	0.68	0.15	0.94		0.04	0.02	(76)
24	0.0009	1.1	0.17	2.2		0.045	0.035	(76)
25	71							(96)
26	2.5 0.31							(96); pH 7.5 (96); pH 6.5
27a	0.008	0.035	0.10	0.32	0.078		0.13	(75,95,101); APC-8696
27b	0.009	8.8	0.11	60	19		0.23	(75,95,101); APC-10302
28a	1.1			6.6	4.6		2.5	(101); APC-6669
28b	2.3			4.0	2.0		3.6	(101); APC-1144
29	31			45			16	(101); APC-10273
30	3.9							(102)
31	0.06							(102)

Despite this advantage, there have been no reports of an amiloride or acyl-guanine containing uPA inhibitor beyond the parent compound.

Two heterocycle-based aryl guanidines have been reported recently by Pfizer [84-87]. The guanidino isoquinoline (5), is a potent inhibitor of uPA, K_i = 61 nM. Although no X-ray

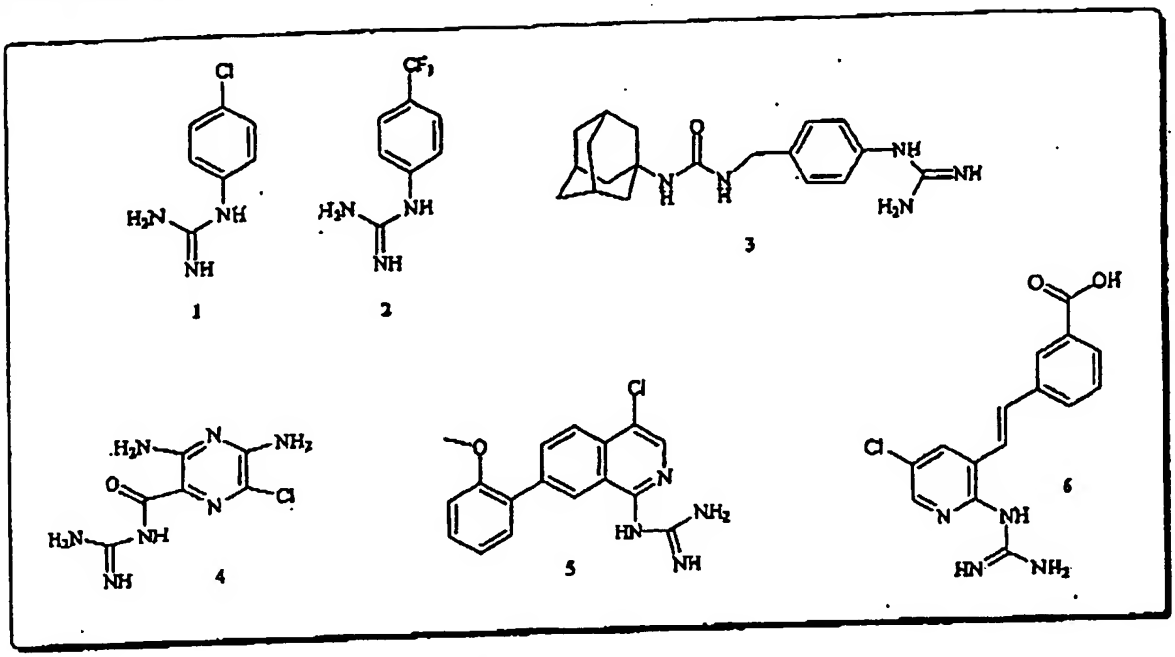

crystallographic studies have been reported for this compound, modeling of the structure suggests 5 should bind in a similar fashion as the 4-chloro phenylguanidine or amiloride. Presumably the 4-chloro group of the isoquinoline should be in close proximity to the Ser195, similar to the 3-amino group in amiloride that forms a hydrogen bond with the Ser195 hydroxyl. The 2-methoxyphenyl substituent on the 7 position of the isoquinoline ring may be directed to the S1β site in a similar fashion as the 6-chloro group of amiloride. Presumably, it occupies more of the site, thereby improving the potency of the compound. The guanidine pyridine structure (6) has a K_i is 170 nM. The molecule exhibits 300-fold selectivity for uPA over tPA and 6000-fold selectivity for uPA over plasmin. Again, modeling suggests that the 4-chloro group is near Ser195 and the phenylcarboxylate occupies the S1β site.

ARYL AMIDINES

Early Benzamidine and Naphthamidine Compounds

The discovery of substituted benzamidine (7, K_i = 6.1 μM) and naphthamidine (8, K_i = 2.2 μM) as templates for uPA inhibition was reported by Sturzebecher and Markwardt in 1978 [88]. The uPA inhibitory potency of unsubstituted benzamidine was determined to be between 30 and 180 μM [76,77,82,89]. Both 3- or 4-substituents were tolerated on the benzamidine. Unsubstituted naphthamidine (9) exhibits uPA inhibition of 5 μM. Many uPA inhibitors have been based on these aryl-amidines.

Benzamidine

Refined crystal structures of meta-substituted benzamidine-based uPA inhibitors have been described recently by Stuzebecher *et al.* [90]. This particular class of inhibitors (10) has been previously shown to inhibit thrombin and trypsin with K_i values in the nanomolar range. Inhibition of uPA, however, was weaker. Replacement of the β-Naphthylsulfonyl group in 10 with the triisopropylphenylsulfonyl group improved the uPA inhibitor potency from 6 to 10-fold. Investigation of the nature of the R group in 10 necessary for potent uPA inhibition led to a series of N-substituted piperazides. The optically active-L-enantiomer of the N-ethoxycarbonyl piperazide (11, WX-UK1) exhibited potent uPA inhibition with a K_i = 0.41 μM. This compound, however, exhibited little selectivity for uPA over the other trypsin family proteases: tPA, plasmin, thrombin, factor Xa, plasma kallekrein, and trypsin (Table 1). A related analog (12) also exhibited potent uPA inhibition (K_i = 0.64 μM), but improved selectivity against tPA. However, 12 exhibits no

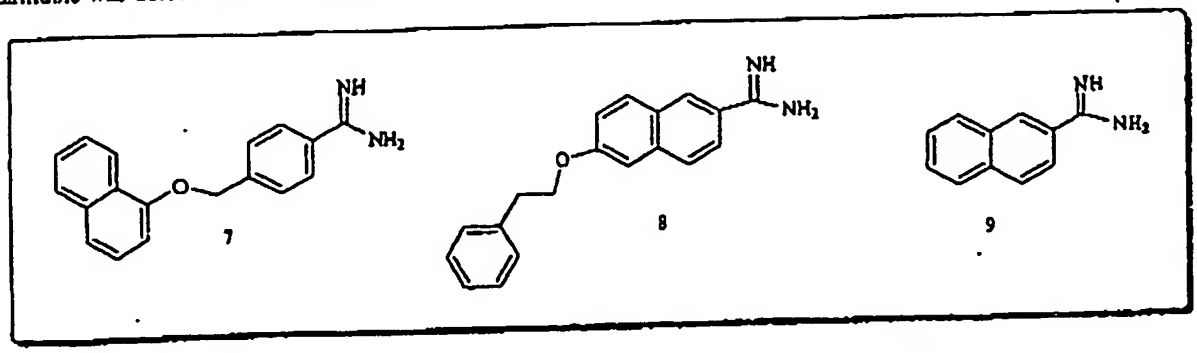

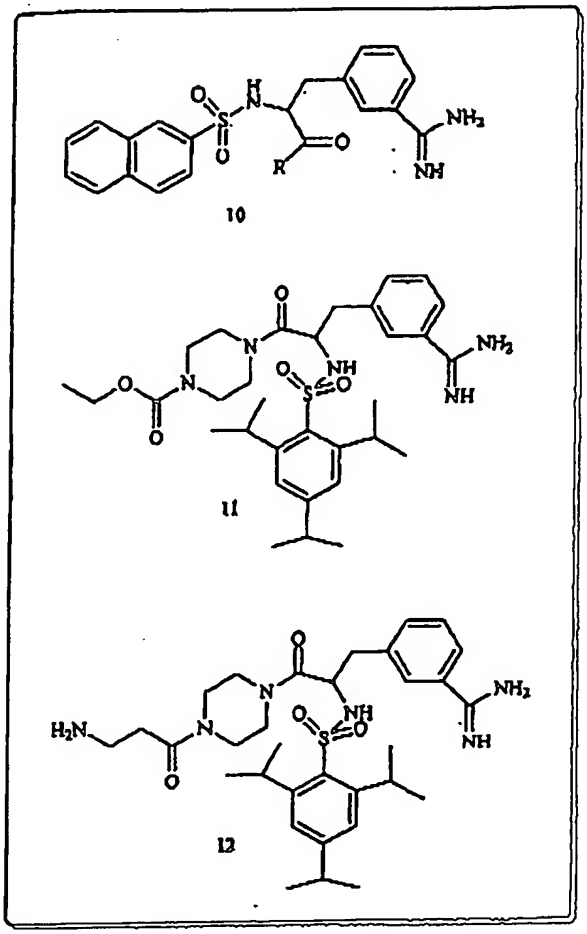

selectivity for uPA versus trypsin (Table 1). The X-ray structure of 12 was analyzed as a complex with uPA [82]. The amidino phenyl moiety binds in the S1 pocket forming the characteristic hydrogen bonds with Asp189. The β-alanine moiety is attached to the piperazine nitrogen and projects toward the indentation between His99 and the catalytic triad residue His57, forming a hydrogen bond with the Tyr94 hydroxyl group. One of the isopropyl groups of the triisopropylphenylsulfonyl moiety projects toward a small dimple situated to the left of His99 and at the edge of the S4 site (Fig. 1).

This same group has recently reported on a series of 4-substituted benzamidine (4-amidinobenzylamine) structures [91] based loosely on the structure of the thrombin inhibitor melagatran [92,93]. For these peptidomimetic compounds, the research team started with 4-amidinobenzylamine-Gly-Glu. Substitution of the P3 Glu residue with d-Ser and capping the d-Ser amino group with a benzylsulfonyl group improved potency 60-fold, to K_i = 36 nM versus uPA (13a). Substitution of the P2 with Ala (13b) or Pro further increased potency (7.7 and 13 nM K_i, respectively), but at the cost of selectivity (Table 1). These peptidomimetics had poor pharmacokinetic properties and were rapidly eliminated from plasma when administered parenterally. Some improvement in the half-life of the compounds was achieved by creating the hydroxyamidine analogue (13c) of compound 13a. This prodrug is rapidly converted to the active compound *in vivo*.

The discovery of these compounds in many ways is similar to another, preceeding, peptidomimetic strategy that had been followed by investigators at Corvas [94]. This group also found P2 and P3 were optimally Ala and d-Ser. However, the P1-substituents in this series were argininals, not amidinobenzylamines (14). Similarly, a prodrug strategy was also used, resulting in compounds with longer *in vivo* half-lives.

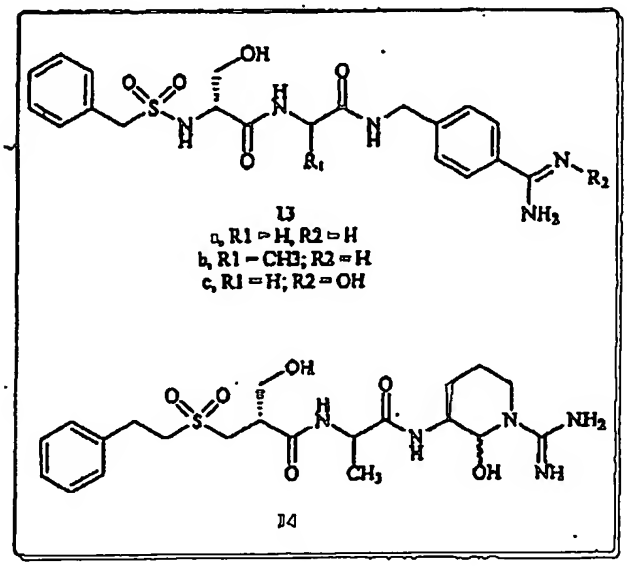

Benzo[b]thiophene-2-Carboxamidine

A major improvement in the potency of uPA aryl-amidine inhibitors was described in 1993 by Littlefield and coworkers [95,96]. They used benzo[b]thiophene-2-carboxamidine (15) as the basis for their inhibitors. The unsubstituted benzo[b]thiophene-2-carboxamidine has the nearly the same uPA potency, K_i = 3.7 μM, as naphthamidine, K_i = 5 μM. Substitution at the 4 position dramatically improved the compounds, where the best compound exhibited uPA inhibition of 70 nM (16). The 4-iodo compound, 17, is also potent with a K_i = 0.32 μM. Substitution at the 5-position [97] of the benzothiophene template provided compounds that were approximately 10-fold less potent than the 4-substituted derivatives. This 4-substituted series of inhibitors also exhibited greater than 300 to 1000-fold selectivity for uPA over tPA or plasmin. Compounds 16 and 17 were also tested for their ability to inhibit uPA catalyzed cellular basement membrane degradation. The cell surface uPA on HT-1080 human fibrosarcoma cells was inhibited with IC_{50} = 1.5 μM and IC_{50} = 0.39 μM, respectively [96].

The structure of 17 complexed with uPA, shown in (Fig. 3), reveals a strong interaction of the amidine moiety with the Asp189 carboxylate and hydrogen bond interactions with the Ser190 side chain oxygen and the Gly218 carbonyl oxygen [75,77]. There are additional hydrophobic contacts of the aromatic ring with the protein residues that define the S1 pocket. These interactions alone confer improved uPA

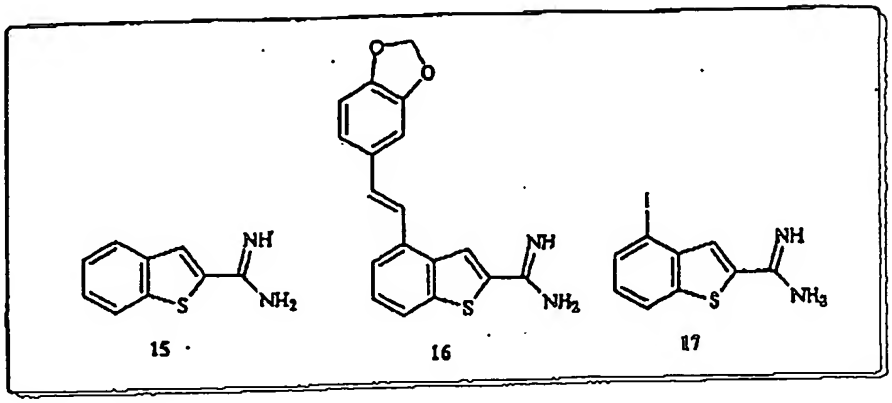

inhibition versus benzamidine, approximately 3.7 μM for the unsubstituted 2-amidino-Benzo[b]thiophene (15). However, 17 exhibited a 10-fold increase in potency over the parent compound indicating that the 4-iodo substituent must be involved in additional interactions with the protein. Indeed, the 4-Iodo group is directed toward the S1β pocket in a manner similar to the chloro-substituent of amiloride. Compound 16 is approximately 10-fold more potent in uPA inhibition (K_i = 0.07 μM) than 17, suggesting that this larger group may better occupy the S1β site than does the 4-iodo compound.

Modeling of the 17-uPA complex (Fig. 3) suggests other substitutions on the aromatic ring could result in additional potency improvements. Positions 5 and 6 are also potential sites for modification since these positions on the aromatic ring are not buried in the S1 pocket. However, uPA inhibition data published in an Eisai patent [97] of approximately 100 compounds with substitutions at position 5 or positions 4 and 5 in the benzo(b)thiophene series shows no potency improvements over compounds 16 and 17. Recently benzo(b) thiophene analogs substituted in position 6 as well as disubstituted benzo[b]thiophene analogs substituted in positions 4 and 6 have been reported [98]. These analogs exhibited uPA inhibition between 100 nM and 3μM.

6,8 Disubstituted Naphthamidines

2-Naphthamidine served as the basis for a structure-based drug design program at Abbott Laboratories [75,79]. The structure of unsubstituted naphthamidine suggested that substitutions at positions 6, 7, or 8 would be the most likely to yield improvements in the naphthamidine based series (Fig. 3). Position 6-substituents would be directed towards the catalytic Ser195 as well as the variable loop (containing Asp60A). Position 8 is directed towards the S1β pocket that had been previously used with good effect in the benzo(b)thiophene series. The remaining positions, 1,3,4,5 are all buried in the S1 pocket and could likely accommodate no (or perhaps very small) substituents. The peptide binding region, S2 and S4 sites, or the substrate-binding groove do not appear to be easily accessible from any position on the naphthamidine template (Figs. 1, 3).

The fundamental premise of the naphthamidine design strategy was to first find substituents at each position that by themselves provide potent and selective inhibition of uPA, and then combine these substituents in a single naphthamidine based molecule that would exhibit improved uPA inhibition and selectivity over each monosubstituted naphthamidine from which it was derived. This strategy was feasible, and ultimately proved successful because the naphthamidine core moved little when substituted at either the 6 or 8 position.

Position 8-substituents are directed to the S1β pocket. This site contains a water molecule that forms a hydrogen-bonded network to several residues within the S1β pocket including the Ser146 side chain hydroxyl, Lys143 side chain amine and the Gln192 side chain amide carbonyl. As demonstrated in the benzo[b]thiophene-2-carboxamidine series, large polarizable groups like Iodine or larger groups like the methylenedioxo phenyl group can fill S1β the pocket displacing the water and enhancing potency 10 to 30-fold. Alternatively, position 8-substituent groups could be used that form hydrogen bonds with the water in the S1β pocket and also improve potency.

The initial inhibitors included a naphthamidine template substituted in either position 8 alone (8-mono substituted series) or substituted in positions 7 and 8 (7,8 disubstituted series). Evaluation of approximately 50 – 100 7,8 disubstituted naphthamidines led to the discovery of 7-methoxy-8-acetamidoxy-2-napthamidine (18). This compound exhibited comparable uPA inhibitor potency (K_i = 0.60 μM) to 17. Analysis of the X-ray structure of this compound revealed a water mediated hydrogen bond from the amide carbonyl of the inhibitor side chain in position 8 and the Lys-143 residue in the S1β pocket. The effect of substitution at position 7 was variable, but typically decreased potency slightly. Crystal structures revealed that the 7-substituents were directed towards solvent, explaining their lack of effect on compound potency.

Using the structural data obtained from the 7-methoxy-8-acetamidoxy-2-naphthamidine (18), a series of alkyl carbamates substituted in position 8 was designed. Evaluation of this series of compounds for uPA inhibition revealed that the 8-methylcarbamate-2-naphthamidine (19) was a potent inhibitor of uPA, K_i = 0.04 μM, approximately 10-fold more potent than the 7-methoxy-8-acetamidoxy-2-naphthamidine and 100-fold more potent than 2-naphthamidine. Analysis of the inhibitor-protein complex shows the position 8-substituent residing in the S1β pocket and the carbonyl of the carbamate moiety involved in a water mediated hydrogen bond with the Lys143 side chain amine and the Gln192 side chain amide carbonyl group. Moreover, the NH of the

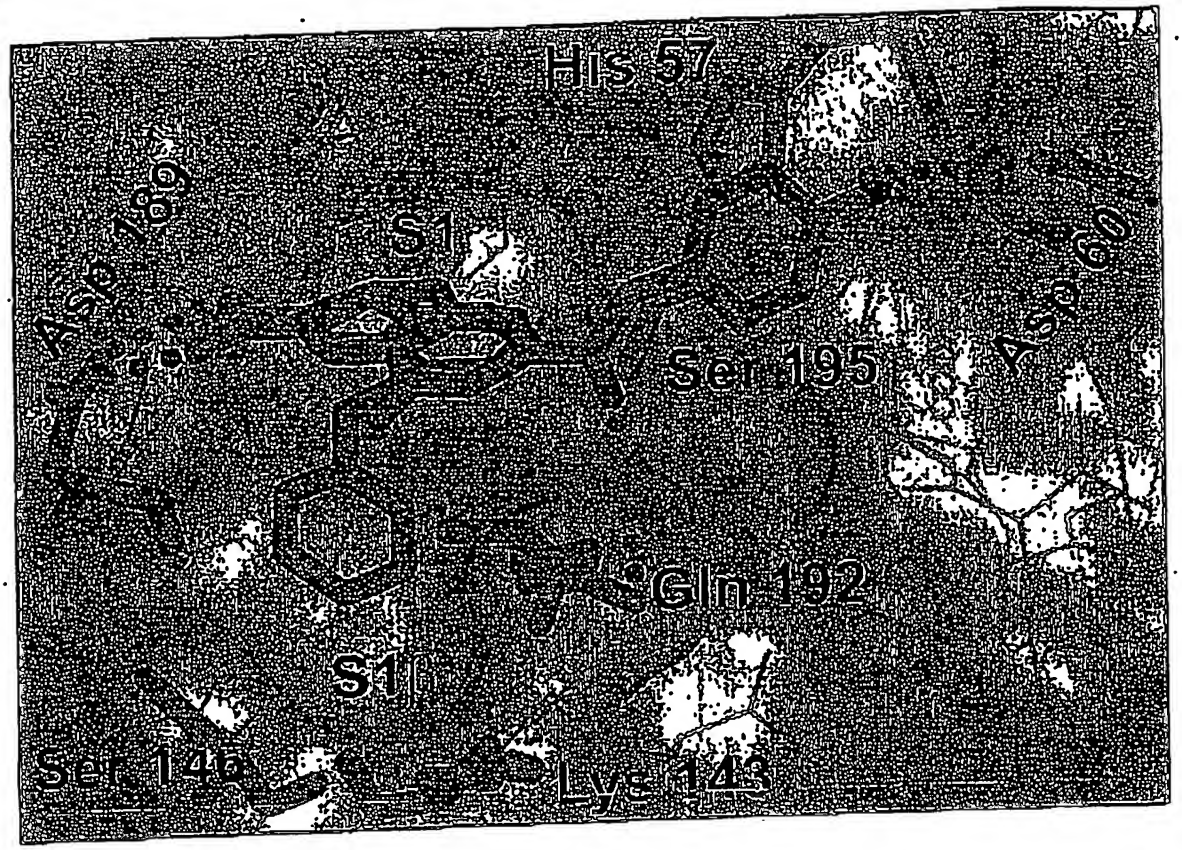

Fig. (3). An overlay of 17 (B428, orange) and 23 (magenta) in the active site of uPA. Both form hydrogen bonds between their amidine groups and Asp189. Both also have substitutions that fill the S1β pocket, 4-Iodo for 17 and 8-aminopyridine for 23. The 6-substitution of 23 also makes hydrogen bonds with Gln192 and Asp60A in the variable loop. The naphthamidine, depicted here with compound 23, remains in the same position whether unsubstituted, 6-mono, 8-mono, or 6,8 disubstituted.

carbamate group is involved in a hydrogen bond to the Gly216 residue. We investigated the size of the group tolerated in the S1β pocket by further modifying the position 8-substituents. The 8-aminopyrimidine analog (20) exhibited the same uPA inhibitor potency, K_i=0.03 μM, as the 8-methylcarbamte analog (compound 19). The crystal structure of 19 [75] reveals the position 8 amino pyrimidine group fully occupying the S1β pocket while maintaining the inhibitor amine NH hydrogen bond to the Gly216 residue of the protein. Compounds 19 and 20 also exhibited good selectivity for uPA over other trypsin family serine proteases including plasmin, tPA, plasma kallikrein, thrombin and trypsin (50-fold, Table 1).

Position 6-substituents may be directed to several remote sites within the active site. One potential site is the unique Asp60A residue (shown in Fig. 1) where a basic substituent on the inhibitor may form a hydrogen-bond interaction with the side carboxylate of the Asp. Alternatively, a position 6-substituent could be directed toward the cationic loop, containing two arginine residues, Arg35 and Arg37, whereby a salt bridge or hydrogen bond interaction with an appropriately functionalized substituent, for example a carboxylate or sulfonate, would improve the potency.

The initial inhibitor design utilized an amide linker between the naphthamidine and the position 6-substituent to direct substituents to remote regions of the active site. We initially evaluated the 6-phenylamide-linked 2-naphthamidine (21) and found it to have uPA inhibitor potency (K_i = 0.63 μM) nearly equal to 17 (K_i = 0.31 μM). Analysis of the X-ray structure of the 6-phenyl amide analog revealed a hydrogen bond interaction between the carbonyl of the amide link in the inhibitor and the amide of the Gln192 side chain. The amidine moiety is characteristically bound in the S1 pocket as has been discussed previously. The phenyl group of the inhibitor maintains a favorable van der Waals contact with the protein. Moreover, the para-position of the phenyl ring appears to be the most favorable site for attaching substituents that might interact with the Asp60A residue. This hypothesis was tested by evaluating a series of para-substituted amine functionalities on the phenyl ring for uPA inhibitor potency. The optimal substitution was the para aminomethyl substituent (22), on the phenyl ring producing a uPA inhibitor with a K_i = 0.03 μM. An X-ray structure of 22 shows the carbonyl of the amide link maintaining the hydrogen bond interaction with Gln192 side chain carboxamide, the phenyl ring maintaining favorable van der Waals contact with the protein and the para-aminomethyl group forming a favorable hydrogen bond interaction with the Asp60A. The selectivity for 22 was excellent for uPA over other trypsin family serine proteases (Table 1). Thus, directing a substituent to a particular remote site, in this case

the Asp60A residue, within the active site can indeed improve uPA inhibitor potency and selectivity.

The 6,8 disubstituted naphthamidine inhibitors, 23 and 24 were more potent than any of the mono-substituted compounds with a K_i values versus uPA of 0.0006 and 0.0009 μM respectively. These are the most potent uPA inhibitors reported to date. Compounds 23 and 24 exhibited excellent selectivity for uPA over related trypsin family serine proteases including plasmin, tPA, plasma kallikrein, trypsin, and thrombin. Compound 23 was evaluated for its ability to inhibit cell surface uPA-mediated basement membrane degradation in a human pancreatic cancer cell line that overexpresses uPA (MiaPaCa) and showed potent inhibition (IC_{50} = 3 nM) approximately 500-fold greater than 17.

The crystal structure of 23 is shown in (Fig. 3) as an overlay with 17. The most potent disubstituted naphthamidines maintain the four important interactions of the inhibitor with the protein; (1) The favorable hydrogen bonding interactions of the para-aminomethyl substituent with the Asp60A residue; (2) The amide linker carbonyl hydrogen bond with the Gln192 side chain amide group, orienting the phenyl ring toward the Asp60A residue in the protein as well as anchoring the inhibitor to the protein; (3) maximum occupancy of the 8-position 2-aminopyrimidine moiety in the S1β pocket and (4) the strong amidine-Asp189 salt bridge interaction in the S1 site.

Naphthamidine Replacements: 2-Amino-Quinolines and 2-Aminobenzimidazoles

Scientists at Abbott used novel crystallographic [99] or NMR [100] based screening methods to look for previously undiscovered S1 site binding moieties. Using these techniques they were able to identify a number of pharmocophores that bound in the S1 pocket, and had lower pKas (8.5 vs. 12) than the aryl amidines. The lower pKa should increase the possibility that the resulting compounds would be orally bioavailable. These pharmacophores are exemplified by the 2-aminoquinolines [99] (25) and 2-aminobenzimidazoles [101].

While the initial lead, 25, displayed only modest potency vs. uPA (K_i = 71 μM) Neinaber *et al.*, were able to use the S1β pocket as they had with the naphthamidine series to significantly increase potency (26, Fig. 2). The resulting N-

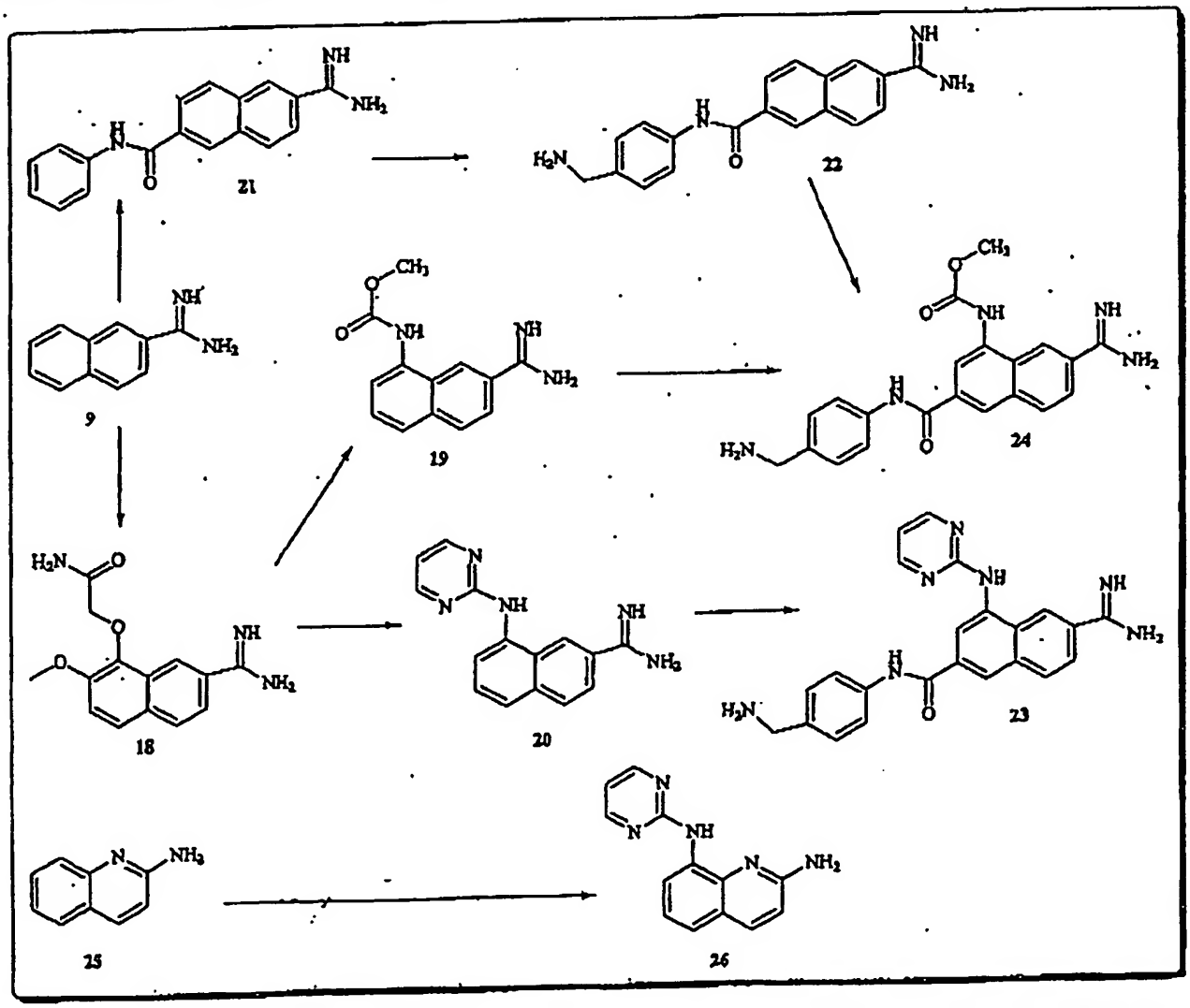

pyrimidyl 2-amino quinoline has a K_i of 2.5 μM vs. uPA at pH = 7.4 (0.31 nM at pH = 6.5). This compound, 26, also displayed improved oral bioavailability (F = 38 %, rat) versus the naphthamidine analogue (20, F = 0%, rat).

Amidino Indoles and Amidino Benzimidazoles

Recently, Axys Pharmaceuticals (now Celera) reported the development of small molecule uPA inhibitors utilizing a structure-based approach based on an amidinobenzimidazole or amidinoindole templates [78,102-104]. Compound 27a, an amidinobenzimidazole based inhibitor, exhibited uPA inhibition of 8 nM, but only modest (less than 20-fold) selectivity for tPA, factor X_a, plasmin, and trypsin (Table 1). Axys scientists proposed more selective uPA inhibitors within this class of compounds could be realized by the introduction of substituents on the aromatic moiety of the amidine [77,78]. Compound 27b, an amidinoindole based inhibitor, exhibited uPA inhibition of 9 nM and improved selectivity for uPA over tPA (1000 X), factor Xa (2000 X), thrombin (6000 X), and porcine kallekrein (90 X). However, less than 10-fold selectivity for uPA over plasmin, trypsin and Factor VII_a was exhibited by 27b. The observed improvement in selectivity for 27b over 27a is due, in part, to the chloro substituent adjacent to the amidine on the indole nucleus. In both Ala190 (factor Xa, thrombin, plasma-kallikrein) and Ser190 (uPA, Plasmin, trypsin, factor VIIa) containing enzymes, there is a water-mediated hydrogen bond between the N^1H of the amidine of the inhibitor and the protein residue in the S1 subsite. The substitution on the position adjacent to the amidine moiety with chlorine causes the displacement of the water in either Ala190 or Ser190 enzymes. The observed selectivity between the enzymes is due the hydrogen bond between N^1H^1 of the amidine and the Ser190 side chain, while a hydrogen bond in Ala190 enzymes is not possible. This proposal was confirmed by X-ray crystallography, which provided evidence for the displacement of the water by the chloro. The Axys work provided an alternative path for improving inhibitor selectivity and illustrated that selectivity improvements can be achieved through modifications of the S1 subsite without drastically increasing overall molecular weight.

Using a large number of high-resolution structures, Katz and coworkers [104] were able to distinguish a set of compounds that form an unusual network of short hydrogen bonds between a water (bound in the oxy-anion hole), their compounds and the catalytic serine (28a, 28b). What makes these compounds very interesting is that the interactions of these short hydrogen bonds are strong enough to pull the amidine moiety away from Asp189, and disrupt the canonical hydrogen bonds that occur at the pocket base (Fig. 4). There are no direct hydrogen bonds between Asp189 and the

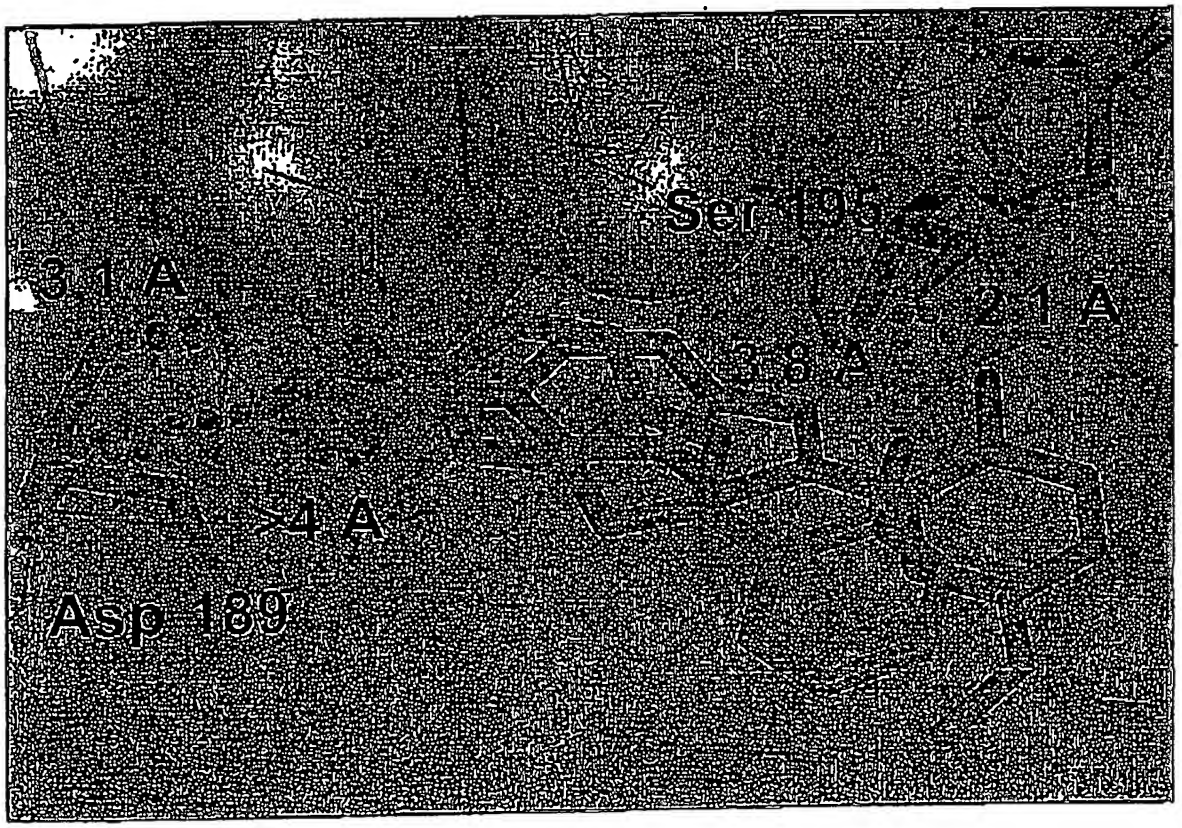

Fig. (4). An overlay of 28a (APC-6669, pink) with 29 (APC-10273, green). Although both are structurally similar, 28a makes a network of short hydrogen bonds with Ser195 and a water in the oxyanion hole (not shown), while 29 does not. The result of the short Ser195 hydrogen bond network in 28a is to pull its amidine away from Asp189 to a distance of 4 Angstroms. In spite of this poor amidine interaction, 28a is more potent than is 29.

amidine of compounds 28a,b as there are in 29, where the inhibitor does not make the network of tight hydrogen bonds at the catalytic Ser195. In spite of the loss of the Asp189 hydrogen bond, 28a,b are more potent than more typical (29) counterparts. This leaves open two possibilities: (1) compounds with no amidine moiety can be designed that would be as potent as their more polar counterparts, thus improving pharmacokinetic parameters; or (2) reintroduction of the Asp189 hydrogen bond, while maintaining the short hydrogen bond network at Ser195, could result in super-potent compounds.

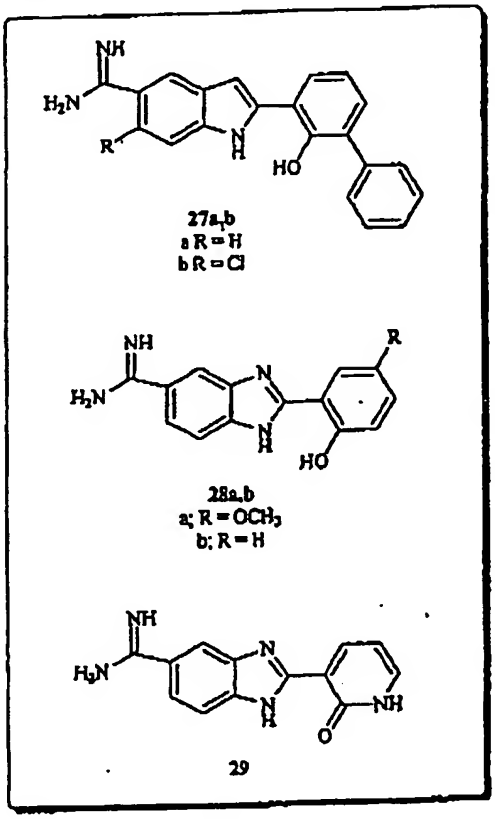

Thiophene 2-Carboxamidines

Recently, researchers at 3-Dimensional Pharmaceuticals [105,106] have discovered a new template on which to base a uPA inhibitor program. Screening of amidine libraries revealed that 5-methylthiothiophene-2 carboxamidine inhibited uPA with K_i = 6 μM, nearly equip naphthamidine[106]. Modeling, based on 17 s the 5-position of the thiophene would be nearly the 4-position of benzamidine. However, this modeling also suggested that substitutions at the 5-position would change the orientation of the thiophene ring within the S1 pocket. Therefore this site would need to be optimized first, as all other substitutions would depend on the 4-substituent. The SAR supports this, and the contribution of substituents at the 4-position varies considerably with the 5-position substituent.

Elaboration of the 4-position suggested that small aliphatic groups, methyl or ethyl, were as potent as the original S-methyl lead. It is interesting that hydrogen at this position leads to a considerable, 50-fold, decrease in potency. Larger, aromatic groups are likewise not tolerated. Although the methyl and ethyl groups do not improve potency over the S-methyl, they have the advantage of a nearly 10-fold increase in aqueous solubility.

Modeling of the thiophene 2-carboxamidine suggested that four position substituents might provide access to the S1β pocket that had been used successfully in the 4-substituted benzo[b]thiophene-2-carboxamidine or the 8-substituted 2-naphthamidine series[105]. Chemical elaboration of this hypothesis proceeded based on an aminothiazole substituent at the 4-position (30). Further elaboration via substitutions on the N-position of the aminothiazole proved valuable, with many compounds discovered with K_i values less than 1 μM. Aromatic groups proved particularly potent, and a biaryl ether substituent had a K_i = 60 nM (31). No enzyme selectivity data and no structural data have been reported for these compounds.

CONCLUSION

The development of potent and selective small molecule inhibitors of uPA possessing either an aryl amidine template or an aryl guanidine template has been realized. Utilizing available structural information, medicinal chemists have adopted different approaches, most notably in the aryl amidine template, to achieve improved potency and selectivity. This has been a long and difficult process. Studies of large numbers of aryl guanidine, aryl amidine and aryl acylguanidine templates have led to relatively few small molecule uPA inhibitors exhibiting submicromolar uPA inhibition.

The advent of routine X-ray analysis of enzyme-inhibitor complexes has allowed a detailed study of important

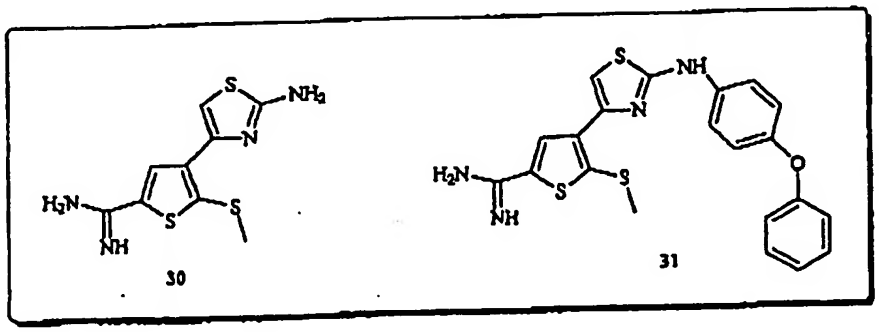

inhibitor-protein interactions of existing uPA inhibitors. The newly available structural data from different classes of inhibitors have enabled investigators to discern the most common and favorable protein-inhibitor interactions. This knowledge has, in turn allowed the development of more potent and selective uPA inhibitors.

While the goals of potency and selectivity have been achieved, the pharmacokinetic properties of many of these compounds are not sufficient to allow them to enter clinical (or even pre-clinical *in vivo*) trials. The basic amidine functionality is typically a liability for both oral bioavailability and elimination half-life. Approaches borrowed from other serine protease inhibitor programs, either pro-drugs, or less basic amidine replacements are starting to prove successful. The achievement of uPA inhibitors with desirable pharmacokinetic properties will enable investigators to achieve their ultimate goal of defining the clinical utility of uPA inhibition.

ACKNOWLEDGEMENTS

We would like to acknowledge Saul Rosenberg and Steve Fesik for their assistance in reading and editing this manuscript.

ABBREVIATIONS

uPA	=	Urokinase-Type plasminogen activator or urokinase
tPA	=	Tissue plasminogen activator
uPAR, CD87	=	Urokinase receptor
QSAR	=	Quantitative Structure-Activity Relationship

REFERENCES

References 107-109 are related articles recently published in Current Pharmaceutical Design.

[1] Behrendt, N.; Ronne, E.; Ploug, M.; Petri, T.; Lober, D.; Nielsen, L. S. et al. The human receptor for urokinase plasminogen activator. NH2-terminal amino acid sequence and glycosylation variants. *J. Biol. Chem.* 1990, *265*, 6453-6460.

[2] Duffy, M. J. Plasminogen activators and cancer. [Review] [64 refs]. *Blood Coag. & Fibrin.* 1990, *1*, 681-687.

[3] Schmitt, M.; Janicke, F.; Moniwa, N.; Chucholowski, N.; Pache. Tumor-associated urokinase-type plasminogen activator: biological and clinical significance. *Bio. Chem. Hoppe-Seyler* 1992, *373*, 611-622.

[4] Schmitt, M.; Wilhelm, O.; Janicke, F.; Magdolen, V.; Reuning, U.; Ohi, H. et al. Urokinase-type plasminogen activator (uPA) and its receptor (CD87): a new target in tumor invasion and metastasis. *J. of Obstet. & Gyn.* 1995, *21*, 151-165.

[5] Andreasen, P. A.; Egelund, R.; Petersen, H. H. The plasminogen activation system in tumor growth, invasion, and metastasis. *Cell. & Mol. Life Sci.* 2000, *57*, 25-40.

[6] Andreasen, P. A.; Kjoller, L.; Christensen, L.; Duffy, M. J. The urokinase-type plasminogen activator system in cancer metastasis: a review. *Int. J. Cancer* 1997, *72*, 1-22.

[7] Romer, J.; Bugge, T. H.; Pyke, C.; Lund, L. R.; Flick, M. J.; Degen, J. L. et al. Impaired wound healing in mice with a disrupted plasminogen gene [see comments]. *Nat. Med.* 1996, *2*, 287-292.

[8] Johnsen, M.; Lund, L. R.; Romer, J.; Almholt, K.; Dano, K. Cancer invasion and tissue remodeling: common themes in proteolytic matrix degradation. *Curr. Opin. Cell Biol.* 1998, *10*, 667-671.

[9] Dano, K.; Romer, J.; Nielsen, B. S.; Bjorn, S.; Pyke, C.; Rygaard, J. et al. Cancer invasion and tissue remodeling--cooperation of protease systems and cell types. *APMIS* 1999, *107*, 120-127.

[10] Lund, L. R.; Romer, J.; Bugge, T. H.; Nielsen, B. S.; Frandsen, T. L.; Degen, J. L. et al. Functional overlap between two classes of matrix-degrading proteases in wound healing. *EMBO J.* 1999, *18*, 4645-4656.

[11] Lotti, T.; Benci, M. Plasminogen activators, venous leg ulcers and reepithelialization. *Int. J. Dermatol.* 1995, *34*, 696-699.

[12] Schaefer, B. M.; Stark, H. J.; Fusenig, N. E.; Todd, R. F., 3rd; Kramer, M. D. Differential expression of urokinase-type plasminogen activator (uPA), its receptor (uPA-R), and inhibitor type-2 (PAI-2) during differentiation of keratinocytes in an organotypic coculture system. *Exp. Cell Res.* 1995, *220*, 415-423.

[13] Rogers, A. A.; Burnett, S.; Lindholm, C.; Bjellerup, M.; Christensen, O. B.; Zederfeldt, B. et al. Expression of tissue-type and urokinase-type plasminogen activator activities in chronic venous leg ulcers. *Vasa* 1999, *28*, 101-105.

[14] Katsoka, K.; Asai, T.; Taneda, M.; Ueshima, S.; Matsuo, O.; Kuroda, R. et al. Roles of urokinase type plasminogen activator in a brain stab wound. *Brain Res.* 2000, *887*, 187-190.

[15] Solberg, H.; Ploug, M.; Hoyer-Hansen, G.; Nielsen, B. S.; Lund, L. R. The murine receptor for urokinase-type plasminogen activator is primarily expressed in tissues actively undergoing remodeling. *Journal of Histochemistry & Cytochemistry* 2001, *49*, 237-246.

[16] Sheng, S. The urokinase-type plasminogen activator system in prostate cancer metastasis. *Cancer & Metastasis Revs.* 2001, *20*, 287-296.

[17] Blasi, F. Proteolysis, cell adhesion, chemotaxis, and invasiveness are regulated by the u-PA-u-PAR-PAI-1 system. *Thromb. Haemost.* 1999, *82*, 298-304.

[18] Shapiro, R. L.; Duquette, J. G.; Roses, D. F.; Nunes, L.; Harris, M. N.; Kamino, H. et al. Induction of primary cutaneous melanocytic neoplasms in urokinase-type plasminogen activator (uPA)-deficient and wild-type mice: cellular blue nevi invade but do not progress to malignant melanoma in uPA-deficient animals. *Cancer Res.* 1996, *56*, 3597-3604.

[19] Lupu, F.; Heim, D. A.; Bachmann, F.; Hurni, M.; Kakkar, V. V.; Kruithof, B. K. Plasminogen activator expression in human atherosclerotic lesions. *Arterioscler. Thromb. Vasc. Biol.* 1995, *15*, 1444-1455.

[20] Noda-Heiny, H.; Daugherty, A.; Sobel, B. E. Augmented urokinase receptor expression in atheroma. *Arterioscler. Thromb. Vasc. Biol.* 1995, *15*, 37-43.

[21] Plekhanova, O.; Parfyonova, Y.; Bibilashvily, R.; Domogatskii, S.; Stepanova, V.; Gulba, D. C. et al. Urokinase plasminogen activator augments cell proliferation and neointima formation in injured arteries via proteolytic mechanisms. *Atherosclerosis* 2001, *159*, 297-306.

[22] Carmeliet, P.; Moons, L.; Lijnen, R.; Baes, M.; Lemaitre, V.; Tipping, P. et al. Urokinase-generated plasmin activates matrix metalloproteinases during aneurysm formation. *Nat. Genet.* 1997, *17*, 439-444.

[23] Falkenberg, M.; Giglio, D.; Bjornheden, T.; Nygren, H.; Risberg, B. Urokinase plasminogen activator colocalizes with CD25+ cells in atherosclerotic vessels. *J. Vasc. Res.* 1998, *35*, 318-324.

[24] Christ, G.; Kostner, K.; Zehetgruber, M.; Binder, B. R.; Gulba, D.; Huber, K. Plasmin activation system in restenosis: role in pathogenesis and clinical prediction? *Journal of Thrombosis & Thrombolysis* 1999, *7*, 277-285.

[25] Kanse, S. M.; Benzakour, O.; Kanthou, C.; Kost, C.; Lijnen, H. R.; Preissner, K. T. Induction of vascular SMC proliferation by urokinase indicates a novel mechanism of action in vasoproliferative disorders. *Arterioscler. Thromb. Vasc. Biol.* 1997, *17*, 2848-2854.

[26] Quax, P. H.; Lamfers, M. L.; Lardenoye, J. H.; Grimbergen, J. M.; de Vries, M. R.; Slomp, J. et al. Adenoviral expression of a urokinase receptor-targeted protease inhibitor inhibits neointima formation in murine and human blood vessels. *Circulation* 2001, *103*, 562-569.

[27] Caccamo, D. V.; Keohane, M. E.; McKeever, P. E. Plasminogen activators and inhibitors in gliomas: an immunohistochemical study. *Mod. Pathol.* 1994, *7*, 99-104.

[28] Heymans, S.; Luttun, A.; Nuyens, D.; Theilmeier, G.; Creemers, E.; Moons, L. et al. Inhibition of plasminogen activators or matrix metalloproteinases prevents cardiac rupture but impairs therapeutic angiogenesis and causes cardiac failure [see comments]. *Nat. Med.* 1999, *5*, 1135-1142.

[29] Das, A.; McGuire, P. G.; Eriqat, C.; Ober, R. R.; DeJuan, E., Jr.; Williams, G. A. et al. Human diabetic neovascular membranes contain high levels of urokinase and metalloproteinase enzymes. *Invest. Ophthal. Vis. Science* 1999, *40*, 809-813.

[30] Carmeliet, P.; Schoonjans, L.; Kieckens, L.; Ream, B.; Degen, J.; Bronson, R. et al. Physiological consequences of loss of plasminogen activator gene function in mice. *Nature* 1994, *368*, 419-424.

[31] Carmeliet, P.; Bouché, A.; De Clercq, C.; Janssen, S.; Pollefeyt, S.; Wyns, S. et al. Biological effects of disruption of the tissue-type plasminogen activator, urokinase-type plasminogen activator, and plasminogen activator inhibitor-1 genes in mice. *Ann. N. Y. Acad. Sci.* 1995, *748*, 367-381; discussion 381-382.

[32] Carmeliet, P.; Collen, D. Development and disease in proteinase-deficient mice: role of the plasminogen, matrix metalloproteinase and coagulation system. *Thromb. Res.* 1998, *91*, 255-285.

[33] Mondino, A.; Resnati, M.; Blasi, F. Structure and function of the urokinase receptor. *Thromb. Haemost.* 1999, *82*, 19-22.

[34] Stoppelli, M. P.; Corti, A.; Soffientini, A.; Cassani, G.; Blasi, F.; Assoian, R. K. Differentiation-enhanced binding of the amino-terminal fragment of human urokinase plasminogen activator to a specific receptor on U937 monocytes. *Proc. Natl. Acad. Sci. U. S. A.* 1985, *82*, 4939-4943.

[35] Vassalli, J. D.; Baccino, D.; Belin, D. A cellular binding site for the Mr 55,000 form of the human plasminogen activator, urokinase. *J. Cell Biol.* 1985, *100*, 86-92.

[36] Degryse, B.; Orlando, S.; Resnati, M.; Rabbani, S. A.; Blasi, F. Urokinase/urokinase receptor and vitronectin/alpha(v)beta(3) integrin induce chemotaxis and cytoskeleton reorganization through different signaling pathways. *Oncogene* 2001, *20*, 2032-2043.

[37] Ossowski, L.; Aguirre-Ghiso, J. A. Urokinase receptor and integrin partnership: coordination of signaling for cell adhesion, migration and growth. *Curr. Opin. Cell Biol.* 2000, *12*, 613-620.

[38] Simon, D. I.; Wei, Y.; Zhang, L.; Rao, N. K.; Xu, H.; Chen, Z. et al. Identification of a urokinase receptor-integrin interaction site. Promiscuous regulator of integrin function. *J. Biol. Chem.* 2000, *275*, 10228-10234.

[39] Tarui, T.; Mazar, A. P.; Cines, D. B.; Takada, Y. Urokinase-type plasminogen activator receptor (CD87) is a ligand for integrins and mediates cell-cell interaction. *J. Biol. Chem.* 2001, *276*, 3983-3990.

[40] Yebra, M.; Goretzki, L.; Pfeifer, M.; Mueller, B. M. Urokinase-type plasminogen activator binding to its receptor stimulates tumor cell migration by enhancing integrin-mediated signal transduction. *Exp. Cell Res.* 1999, *250*, 231-240.

[41] Yebra, M.; Parry, G. C. N.; Strombiad, S.; Mackman, N.; Rosenberg, S.; Mueller, B. M. et al. Requirement of receptor-bound urokinase-type plasminogen activator for integrin alphavbeta5-directed cell migration. *J. Biol. Chem.* 1996, *271*, 29393-29399.

[42] Liu, D.; Ghiso, J. A.; Estrada, Y.; Ossowski, L. EGFR is a transducer of the urokinase receptor initiated signal that is required for in vivo growth of a human carcinoma. *Cancer Cell* 2002, *1*, 445-457.

[43] Duffy, M. J. Clinical uses of tumor markers: a critical review. *Crit. Rev. Clin. Lab. Sci.* 2001, *38*, 225-262.

[44] Stephens, R. W.; Brunner, N.; Janicke, F.; Schmitt, M. The urokinase plasminogen activator system as a target for prognostic studies in breast cancer. *Breast Cancer Res. Treat.* 1998, *52*, 99-111.

[45] Duffy, M. J.; Maguire, T. M.; McDermott, E. W.; O'Higgins, N. Urokinase plasminogen activator: a prognostic marker in multiple types of cancer. *J. Surg. Oncol.* 1999, *71*, 130-135.

[46] Brunner, N.; Pyke, C.; Hansen, C. H.; Romer, J.; Grondahl-Hansen, J.; Dano, K. Urokinase plasminogen activator (uPA) and its type 1 inhibitor (PAI-1): regulators of proteolysis during cancer invasion and prognostic parameters in breast cancer. *Cancer Treat. Res.* 1994, *71*, 299-309.

[47] Sabapathy, K. T.; Pepper, M. S.; Kiefer, F.; Mohle-Steinlein, U.; Tacchini-Cottier, F.; Pedra, L. et al. Polyoma middle T-induced vascular tumor formation: the role of the plasminogen activator/plasmin system. *J. Cell Biol.* 1997, *137*, 953-963.

[48] Bugge, T. H.; Lund, L. R.; Kombrinck, K. K.; Nielsen, B. S.; Holmback, K.; Drew, A. F. et al. Reduced metastasis of Polyoma virus middle T antigen-induced mammary cancer in plasminogen-deficient mice. *Oncogene* 1998, *16*, 3097-3104.

[49] Gutierrez, L. S.; Schulman, A.; Brito-Robinson, T.; Noria, F.; Ploplis, V. A.; Castellino, F. J. Tumor development is retarded in mice lacking the gene for urokinase-type plasminogen activator or its inhibitor, plasminogen activator inhibitor-1. *Cancer Res.* 2000, *60*, 5839-5847.

[50] Prandsen, T. L.; Holst-Hansen, C.; Nielsen, B. S.; Christensen, I. J.; Nyengaard, J. R.; Carmeliet, P. et al. Direct evidence of the importance of stromal urokinase plasminogen activator (uPA) in the growth of an experimental human breast cancer using a combined uPA

gene-disrupted and immunodeficient xenograft model. *Cancer Res.* 2001, *61*, 532-537.

[51] Vassalli, J. D.; Belin, D. Amiloride selectively inhibits the urokinase-type plasminogen activator. *FEBS Lett.* 1987, *214*, 187-191.

[52] Lant, A. F.; Smith, A. J.; Wilson, G. M. Clinical evaluation of amiloride, a potassium-sparing. *Clinical Pharmacology & Therapeutics* 1969, *10*, 50-63.

[53] Alonso, D. F.; Farias, E. P.; Ladeda, V.; Davel, L.; Particelli, L.; Bal de Kier Joffe, E. Effects of synthetic urokinase inhibitors on local invasion and metastasis in a murine mammary tumor model. *Breast Cancer Res. Treat.* 1996, *40*, 209-223.

[54] Pilat, M. J.; Lehr, J. E.; Quigley, M. M.; Pienta, K. J. The effect of amiloride on the metastatic properties of prostate cancer in the Dunning rat model. *Oncol. Rep.* 1998, *5*, 889-892.

[55] Xing, R. H.; Mazar, A.; Henkin, J.; Rabbani, S. A. Prevention of breast cancer growth, invasion, and metastasis by antiestrogen tamoxifen alone or in combination with urokinase inhibitor B-428. *Cancer Res.* 1997, *57*, 3585-3593.

[56] Rabbani, S. A.; Harakidas, P.; Davidson, D. J.; Henkin, J.; Mazar, A. P. Prevention of prostate-cancer metastasis in vivo by a novel synthetic inhibitor of urokinase-type plasminogen activator (uPA). *Int. J. Cancer* 1995, *63*, 840-845.

[57] Sperl, S.; Mueller, M. M.; Wilhelm, O. G.; Schmitt, M.; Magdolen, V.; Moroder, L. The uPA/uPA receptor system as a target for tumor therapy. *Drug News Perspect.* 2001, *14*, 401-411.

[58] Min, H. Y.; Doyle, L. V.; Vitt, C. R.; Zandonella, C. L.; Stratton-Thomas, J. R.; Shuman, M. A. et al. Urokinase receptor antagonists inhibit angiogenesis and primary tumor growth in syngeneic mice. *Cancer Res.* 1996, *56*, 2428-2433.

[59] Rabbani, S. A.; Gladu, J. Urokinase receptor antibody can reduce tumor volume and detect the presence of occult tumor metastases in vivo. *Cancer Res.* 2002, *62*, 2390-2397.

[60] Tressler, R. T.; Pitot, P. A.; Stratton, J. R.; Forrest, L. D.; Zhua, S.; Drummond, R. J. et al. Urokinase receptor antagonists: discovery and application to in vivo models of tumor growth. *APMIS* 1999, *107*, 168-173.

[61] Wang, Y.; Liang, X.; Wu, S.; Murrell, G. A.; Doe, W. F. Inhibition of colon cancer metastasis by a 3'- end antisense urokinase receptor mRNA in a nude mouse model. *Int. J. Cancer* 2001, *92*, 257-262.

[62] Creemers, E.; Cleutjens, J.; Smits, J.; Heymans, S.; Moons, L.; Collen, D. et al. Disruption of the plasminogen gene in mice abolishes wound healing after myocardial infarction. *Am. J. Pathol.* 2000, *156*, 1865-1873.

[63] Wysocki, A. B.; Kusakabe, A. O.; Chang, S.; Tuan, T. L. Temporal expression of urokinase plasminogen activator, plasminogen activator inhibitor and gelatinase-B in chronic wound fluid switches from a chronic to acute wound profile with progression to healing. *Wound Repair Regen.* 1999, *7*, 154-165.

[64] Baker, E. A.; Leaper, D. J. Proteinases, their inhibitors, and cytokine profiles in acute wound fluid. *Wound Repair Regeneration* 2000, *8*, 392-398.

[65] Jimenez, P. A.; Telista, M.; Liu, B.; Antonaccio, M. J. Urokinase-type plasminogen activator stimulates wound healing in the diabetic mouse. *Inflamm. Res.* 1997, *46*, S169-170.

[66] Strauss, B. H.; Lau, H. K.; Bowman, K. A.; Sparkes, J.; Chisholm, R. J.; Garvey, M. B. et al. Plasma urokinase antigen and plasminogen activator inhibitor-1 antigen levels predict angiographic coronary restenosis. *Circulation* 1999, *100*, 1616-1622.

[67] Plow, E. F.; Ploplis, V. A.; Busuttil, S.; Carmeliet, P.; Collen, D. A role of plasminogen in atherosclerosis and restenosis models in mice. *Thromb. Haemost.* 1999, *82*, 4-7.

[68] Lamfers, M. L.; Lafdenoye, J. H.; de Vries, M. R.; Aalders, M. C.; Engelse, M. A.; Grimbergen, J. M. et al. In vivo suppression of restenosis in balloon-injured rat carotid artery by adenovirus-mediated gene transfer of the cell surface-directed plasmin inhibitor ATF.BPTI. *Gene Ther.* 2001, *8*, 534-541.

[69] Ikeda, U.; Hojo, Y.; Shimada, K. Plasma urokinase antigen and plasminogen activator inhibitor-1 antigen levels predict angiographic coronary restenosis. *Circulation* 2000, *102*, E167.

[70] Carmeliet, P.; Moons, L.; Stassen, J. M.; De Mol, M.; Bouche, A.; van den Oord, J. J. et al. Vascular wound healing and neointima formation induced by perivascular electric injury in mice. *Am. J. Pathol.* 1997, *150*, 761-776.

[71] Carmeliet, P.; Collen, D. Molecular genetics of the fibrinolytic and coagulation systems in haemostasis, thrombogenesis, restenosis and atherosclerosis. *Curr. Opin. Lipidol.* 1997, *8*, 118-125.

[72] Erichsen, J. T.; Jarvis-Evans, J.; Khalig, A.; Boulton, M. Oxygen modulates the release of urokinase and plasminogen activator inhibitor-1 by retinal pigment epithelial cells. *Int. J. Biochem. Cell Biol.* 2001, *33*, 237-247.

[73] Leterra, J.; Induti, R. R.; Goldstein, G. W. Regulation of in vitro glia-induced microvessel morphogenesis by urokinase. *J. Cell. Physiol.* 1994, *158*, 317-324.

[74] Spraggon, G.; Phillips, C.; Nowak, U. K.; Ponting, C. P.; Saunders, D.; Dobson, C. M. et al. The crystal structure of the catalytic domain of human urokinase-type plasminogen activator. *Structure* 1995, *3*, 681-691.

[75] Nienaber, V. L.; Davidson, D.; Edalji, R.; Giranda, V. L.; Klinghofer, V.; Henkin, J. et al. Structure-directed discovery of potent non-peptidic inhibitors of human urokinase that access a novel binding subsite. *Structure* 2000, *8*, 553-563.

[76] Nienaber, V.; Wang, J.; Davidson, D.; Henkin, J. Re-engineering of human urokinase provides a system for structure-based drug design at high resolution and reveals a novel structural subsite. *J. Biol. Chem.* 2000, *275*, 7239-7248.

[77] Katz, B. A.; Mackman, R.; Luong, C.; Radika, K.; Martelli, A.; Sprengeler, P. A. et al. Structural basis for selectivity of a small molecule, S1-binding, submicromolar inhibitor of urokinase-type plasminogen activator. *Chem. Biol.* 2000, *7*, 299-312.

[78] Katz, B. A.; Sprengeler, P. A.; Luong, C.; Verner, E.; Elrod, K.; Kirtley, M. et al. Engineering inhibitors highly selective for the S1 sites of Ser190 trypsin-like serine protease drug targets. *Chemistry & Biology* 2001, *8*, 1107-1121.

[79] Klinghofer, V.; Stewart, K.; McGonigal, T.; Smith, R.; Sarthy, A.; Nienaber, V. et al. Species specificity of amidine-based urokinase inhibitors. *Biochemistry* 2001, *40*, 9125-9131.

[80] Yang, H.; Henkin, J.; Kim, K. H.; Greer, J. Selective inhibition of urokinase by substituted phenylguanidines: quantitative structure-activity relationship analyses. *J. Med. Chem.* 1990, *33*, 2956-2961.

[81] Sperl, S.; Jacob, U.; Arroyo de Prada, N.; Sturzebecher, J.; Wilhelm, O.; Bode, W. et al. (4-Aminomethyl)phenylguanidine derivatives as nonpeptidic highly selective inhibitors of human urokinase. *Proc. Nat. Acad. Sci. USA* 2000, *97*, 5113-5118.

[82] Zeslawska, E.; Schweinitz, A.; Karcher, A.; Sondermann, P.; Sperl, S.; Sturzebecher, J. et al. Crystals of the urokinase type plasminogen activator variant beta c-uPA in complex with small molecule inhibitors open the way towards structure-based drug design. *J. Mol. Biol.* 2000, *301*, 465-475.

[83] Menear, K. Progress towards the discovery of orally active thrombin inhibitors. *Curr. Med. Chem.* 1998, *5*, 457-468.

[84] Dickenson, R. P.; Fish, P. V.; Barber, C. G. Isoquinolines. In *6093713*; Pfizer Ltd.: US, 2000.

[85] Barber, C. G.; Dickenson, R. P. 2-Pyridinylguanidine urokinase inhibitors. In *1044967A3*; Pfizer Ltd.: EP, 2000.

[86] Barber, C. G.; Dickinson, R. P. Selective urokinase-type plasminogen activator (uPA) inhibitors. Part 2: (3-Substituted-5-halo-2-pyridinyl)guanidines. *Bioorg. Med. Chem. Lett.* 2002, *12*, 185-187.

[87] Barber, C. G.; Dickinson, R. P.; Horne, V. A. Selective urokinase-type plasminogen activator (uPA) inhibitors. Part 1: 2-Pyridinylguanidines. *Bioorg. Med. Chem. Lett.* 2002, *12*, 181-184.

[88] Sturzebecher, J.; Markwardt, F. [Synthetic inhibitors of serine proteinases. 17. The effect of benzamidine derivatives on the activity of urokinase and the reduction of fibrinolysis]. *Pharmazie* 1978, *33*, 599-602.

[89] Sturzebecher, J.; Markwardt, F. Synthetische Inhibitoren der Serinproteinasen. *Pharmazie* 1978, *33*, 599-602.

[90] Sturzebecher, J.; Vieweg, H.; Steinmetzer, T.; Schweinitz, A.; Stubbs, M. T.; Renatus, M. et al. 3-Amidinophenylalanine-based inhibitors of urokinase. *Bioorg. Med. Chem. Lett.* 1999, *9*, 3147-3152.

[91] Kunzel, S.; Schweinitz, A.; Reissmann, S.; Sturzebecher, J.; Steinmetzer, T. 4-Amidinobenzylamine-Based inhibitors of urokinase. *Bioorg. Med. Chem. Lett.* 2002, *12*, 645-648.

[92] Gustafsson, D.; Antonsson, T.; Bylund, R.; Eriksson, U.; Gyzander, E.; Nilsson, I. et al. Effects of melagatran, a new low-molecular-weight thrombin inhibitor, on thrombin and fibrinolytic enzymes. *Thromb. Haemost.* 1998, *79*, 110-118.

[93] Gustafsson, D.; Nystrom, J.; Carlsson, S.; Bredberg, U.; Eriksson, U.; Gyzander, E. et al. The direct thrombin inhibitor melagatran and its oral prodrug H 376/95: intestinal absorption properties, biochemical and pharmacodynamic effects. *Thrombosis Research.* 2001, *101*, 171-181.

[94] Tumura, S. Y. Synthesis and biological activity of peptidyl aldehyde urokinase inhibitors. *Bioorg. Med. Chem. Lett.* 2000, *10*, 983-987.

[95] Towle, M. J.; Lee, A.; Maduakor, E. C.; Schwartz, C. E.; Bridges, A. J.; Littlefield, B. A. Inhibition of urokinase by 4-substituted benzo[b]thiophene-2-carboxamidines: an important new class of selective synthetic urokinase inhibitor. *Cancer Res.* 1993, *53*, 2553-2559.

[96] Bridges, A. J.; Lee, A.; Schwartz, C. E.; Towle, M. J.; Littlefield, B. A. The synthesis of three 4-substituted benzo[b]thiophene-2-carboxamidines as potent and selective inhibitors of urokinase. *Bioorg. Med. Chem.* 1993, *1*, 403-410.

[97] Bridges, A.; Littlefield, B. A.; Schwartz, C. E. Urokinase inhibitors. In *5340833*; Eisai Co. Ltd.: US, 1994.

[98] Dellaria, J. F. Urokinase inhibitors. In *6207701*; Abbott Laboratories: US, 2001.

[99] Nienaber, V. L.; Richardson, P. L.; Klighofer, V.; Bouska, J. J.; Giranda, V. L.; Greer, J. Discovering novel ligands for macromolecules using X-ray crystallographic screening. *Nat. Biotechnol.* 2000, *18*, 1105-1108.

[100] Shuker, S. B.; Hajduk, P. J.; Meadows, R. P.; Fesik, S. W. Discovering high-affinity ligands for proteins: SAR by NMR. *Science.* 1996, *274*, 1531-1534.

[101] Hajduk, P. J.; Boyd, S.; Nettesheim, D.; Nienaber, V.; Severin, J.; Smith, R. et al. Identification of novel inhibitors of urokinase via NMR-based screening. *J. Med. Chem.* 2000, *43*, 3862-3866.

[102] Mackman, R. L.; Hui, H. C.; Breitenbucher, J. G.; Katz, B. A.; Luong, C.; Martelli, A. et al. 2-(2-Hydroxy-3-alkoxyphenyl)-1H-benzimidazole-5-carboxamidine derivatives as potent and selective urokinase-type plasminogen activator inhibitors. *Bioorg. Med. Chem. Lett.* 2002, *12*, 2019-2022.

[103] Mackman, R. L.; Katz, B. A.; Breitenbucher, J. G.; Hui, H. C.; Verner, E.; Luong, C. et al. Exploiting subsite S1 of trypsin-like serine proteases for selectivity: potent and selective inhibitors of urokinase-type plasminogen activator. *J. Med. Chem.* 2001, *44*, 3856-3871.

[104] Katz, B. A.; Elrod, K.; Luong, C.; Rice, M. J.; Mackman, R. L.; Sprengeler, P. A. et al. A novel serine protease inhibition motif involving a multi-centered short hydrogen bonding network at the active site. *J. Mol. Biol.* 2001, *307*, 1451-1466.

[105] Wilson, K. J.; Illig, C. R.; Subasinghe, N.; Hoffman, J. B.; Rudolph, M. J.; Soll, R. et al. Synthesis of thiophene-2-carboxamidines containing 2-aminothiazoles and their biological evaluation as urokinase inhibitors. *Bioorg. Med. Chem. Lett.* 2001, *11*, 915-918.

[106] Rudolph, M. J.; Illig, C. R.; Subasinghe, N. L.; Wilson, K. J.; Hoffman, J. B.; Randle, T. et al. Design and synthesis of 4,5-disubstituted-thiophene-2-amidines as potent urokinase inhibitors. *Bioorg. Med. Chem. Lett.* 2002, *12*, 491-495.

[107] Jiang, S.; Zhao, Q. and Debnath, A. K. Peptide and non-peptide HIV fusion inhibitors. *Curr. Pharm. Des.* 2002, *8*(8), 563-80.

[108] Kurowska, E. M. Nitric oxide therapies in vascular diseases. *Curr. Pharm. Des.* 2002, *8*(3), 155-66.

[109] Rockway, T. W.; Nienaber, V. and Giranda, V. L. Inhibitors of the protease domain of urokinase-type plasminogen activator. *Curr. Pharm. Des.* 2002, *8*(28), 2541-58.

Structural basis for selectivity of a small molecule, S1-binding, submicromolar inhibitor of urokinase-type plasminogen activator

Bradley A Katz, Richard Mackman, Christine Luong, Kesavan Radika, Arnold Martelli, Paul A Sprengeler, Jing Wang, Hedy Chan and Lance Wong

Introduction: Urokinase-type plasminogen activator (uPA) is a protease associated with tumor metastasis and invasion. Inhibitors of uPA may have potential as drugs for prostate, breast and other cancers. Therapeutically useful inhibitors must be selective for uPA and not appreciably inhibit the related, and structurally and functionally similar enzyme, tissue-type plasminogen activator (tPA), involved in the vital blood-clotting cascade.

Results: We produced mutagenically deglycosylated low molecular weight uPA and determined the crystal structure of its complex with 4-iodobenzo[*b*]thiophene-2-carboxamidine ($K_i = 0.21 \pm 0.02\ \mu M$). To probe the structural determinants of the affinity and selectivity of this inhibitor for uPA we also determined the structures of its trypsin and thrombin complexes, of apo-trypsin, apo-thrombin and apo-factor Xa, and of uPA, trypsin and thrombin bound by compounds that are less effective uPA inhibitors, benzo[*b*]thiophene-2-carboxamidine, thieno[2,3-*b*]-pyridine-2-carboxamidine and benzamidine. The K_i values of each inhibitor toward uPA, tPA, trypsin, tryptase, thrombin and factor Xa were determined and compared. One selectivity determinant of the benzo[*b*]thiophene-2-carboxamidines for uPA involves a hydrogen bond at the S1 site to $O\gamma_{Ser190}$ that is absent in the Ala190 proteases, tPA, thrombin and factor Xa. Other subtle differences in the architecture of the S1 site also influence inhibitor affinity and enzyme-bound structure.

Conclusions: Subtle structural differences in the S1 site of uPA compared with that of related proteases, which result in part from the presence of a serine residue at position 190, account for the selectivity of small thiophene-2-carboxamidines for uPA, and afford a framework for structure-based design of small, potent, selective uPA inhibitors.

Address: Axys Pharmaceutical Corporation, 385 Oyster Point Boulevard, Suite 3, South San Francisco, CA 94080, USA.

Correspondence: Bradley A Katz
Email: brad_katz@axyspharm.com

Key words: S1 structure, thrombin, tPA, trypsin, uPA

Received: **5 November 1999**
Revisions requested: **13 December 1999**
Revisions received: **14 January 2000**
Accepted: **11 February 2000**

Published: **23 March 2000**

Chemistry & Biology 2000, 7:299–312

1074-5521/00/$ – see front matter

Introduction

One of the basic hurdles in the development of enzyme inhibitors as drugs involves the achievement of selectivity toward the target enzyme and against its closely related counterparts. In serine proteases specificity of a physiological substrate is conferred by the combination of interactions at a series of sites, designated S3, S2, S1, S1′, S2′ and S3′, that bind successive peptide sidechains designated P3, P2 and P1 prior to the susceptible scissile peptide bond, and P1′, P2′ and P3′ after it [1]. Most inhibitors of a subset of trypsin-like serine proteases (which includes trypsin, tryptase, factor Xa, thrombin, urokinase-type plasminogen activator and tissue-type plasminogen activator) have a basic group that makes hydrogen-bonded salt bridges with the Asp189 carboxylate at the base of the S1 pocket, as for the arginine residue of a substrate. Interactions at the S1 site enable substrates or inhibitors to discriminate between the class of trypsin-like serine proteases with an aspartate residue at position 189 and other families such as chymotrypsin-like proteases, with a serine residue at position 189.

Selectivity of inhibitors for individual members within the family of trypsin-like serine proteases is often achieved through interactions of inhibitor groups at subsites such as S1′, S2 and S3, whose sequences and structures differ significantly from one member to the next [2–5]. Because of the high structural similarity in the S1 sites of the trypsin-like serine proteases with an aspartate residue at position 189, small-molecule inhibitors that achieve specificity for trypsin-like serine protease drug targets through interactions at this site alone merit close scrutiny. One such inhibitor is 4-iodobenzo[*b*]thiophene-2-carboxamidine, a lead compound from a series of over 90 4-substituted benzo[*b*]thiophene-2-carboxamidines reported in 1993 [6]. This compound stands out as a submicromolar competitive inhibitor of urokinase-type plasminogen activator (uPA), exhibiting selectivity for uPA and against plasmin, thrombin and tissue-type plasminogen activator (tPA).

Because of its involvement in tumor metastasis and invasion, uPA has emerged as a drug target for development of

therapeutics for prostate, breast and other cancers [7–11]. Therapeutic inhibitors of uPA should not appreciably inhibit the closely related enzymes (thrombin and tPA [12]), which are critical components of the blood-clotting pathway. Both uPA and tPA share the same primary physiological substrate (plasminogen) and inhibitor (plasminogen activator inhibitor), exhibit stringent specificity, and share similar sequences and three-dimensional structures [12,13]. Determination of the structural basis for the affinity and selectivity of 4-iodobenzo[*b*]thiophene-2-carboxamidine for uPA and against tPA and other related proteases is therefore expected to provide insight for structure-based design of selective, potent inhibitors of uPA and other trypsin-like protease targets.

To this end we determined the crystal structures of the uPA, trypsin and thrombin complexes of 4-iodobenzo[*b*]thiophene-2-carboxamidine, and the K_i values of this inhibitor for trypsin-like serine protease drug targets and anti-targets: uPA, tPA, thrombin, factor Xa, tryptase and trypsin. Structural determinants of the binding of this scaffold were further examined by quantitating inhibition of each of the enzymes by structurally related analogs that are less effective inhibitors of uPA, benzo[*b*]thiophene-2-carboxamidine, thieno[2,3-*b*]pyridine-2-carboxamidine, and benzamidine, and by determining and comparing the structures of the uPA, trypsin and thrombin complexes. Finally, structures of inhibitor-free trypsin, factor Xa and thrombin were determined to delineate and compare features of the apo-enzymes, such as the ordered solvent structure at the S1 site that mediates the binding of the inhibitors investigated. The uPA–small-molecule structures of this study, involving fully reversible active site inhibitors, are among the first reported to date [11].

Although the S1 sites of uPA and tPA are structurally very similar, the identity of residue 190 is an important feature that distinguishes one from the other. uPA and tPA can be considered archetypes of two classes of trypsin-like serine proteases, those with a serine residue at position 190, such as uPA, trypsin and tryptase, and those with an alanine residue at position 190, such as tPA, thrombin and factor Xa. The differences in the architectures and hydrogen-bonding potentials of the S1 sites of these two protease families, as visualized in the structures of representative members determined here, both in the presence and absence of S1-bound inhibitors, provide a basis for selectivity development. Comparison within this set of structures of distinguishing features in the S1 site, such as its width and depth, its spatial relationship to the active site, and the nature and degree of its structural plasticity, yields clues for achieving inhibitor selectivity. The complementary structural and inhibition data of this study not only form a framework for the structure-based development of potent, selective uPA inhibitors, but also provide insight into the design of inhibitors that discriminate between these two large important classes of trypsin-like serine proteases.

Results

Affinity and selectivity of benzo[*b*]thiophene-2-carboxamidine analogs for uPA and for other trypsin-like serine proteases

We observed competitive inhibition by 4-iodobenzo-[*b*]thiophene-2-carboxamidine of each member of a panel of trypsin-like serine proteases comprising uPA, trypsin, tryptase, tPA, thrombin and factor Xa. The inhibition constant (K_i value) determined here for uPA at pH 7.4 is 0.21 ± 0.02 μM (Table 1), compared with 0.53 ± 0.07 μM determined at pH 7.5 by Towle *et al.* [6]. The K_i value for tPA, an anti-target closely related structurally and functionally to uPA, is 16.8 ± 0.4 μM, yielding a selectivity ratio for tPA versus uPA of 80. Also listed in Table 1 are the K_i values for benzo[*b*]thiophene-2-carboxamidine, thieno[2,3-*b*]pyridine-2-carboxamidine and benzamidine toward each protease. Our determined selectivity ratios of 4-iodobenzo[*b*]thiophene-2-carboxamidine toward uPA

Table 1

Inhibition constants of amidine inhibitors toward selected trypsin-like serine proteases.

	Ser190 proteases			Ala190 proteases		
Inhibitor	uPA	Trypsin	Tryptase	tPA/uPA	Thrombin/uPA	Factor Xa
APC-6860*	**0.21 ± 0.02**	**0.44 ± 0.1**	1.5 ± 0.1	16.8 ± 0.4	**20 ± 2**	30 ± 2
APC-7377†	2.3 ± 0.2	**1.0 ± 0.1**	9.9 ± 0.8	15 ± 1	58 ± 5	21 ± 2
APC-7538‡	**63 ± 5**	**80 ± 5**	34 ± 2	1800 ± 100	1600 ± 200	360 ± 110
Benzamidine	**97 ± 9**	**21 ± 2**	20 ± 2	**750 ± 70**	**320 ± 25**	110 ± 20
None		**apo**			**apo**	**apo**

All K_i values in μM. Bold values denote structures determined here or elsewhere (tPA–benzamidine) [12]. *4-Iodobenzo[*b*]thiophene-2-carboxamidine. Competitive inhibition was demonstrated and K_i values determined rigorously for each enzyme by varying both the substrate and the inhibitor concentrations. For the other compounds, K_i values were determined at one substrate concentration (per enzyme) set near the determined K_m value (see text). †Benzo[*b*]thiophene-2-carboxamidine. ‡Thieno[2,3-*b*]pyridine-2-carboxamidine.

and against plasmin (15, data not shown), thrombin and tPA (95 and 80, respectively) are significantly less than the corresponding values in the study of Towle *et al.* (1100, > 780 and 330, respectively) [6].

4-Iodobenzo[*b*]thiophene-2-carboxamidine is a significantly better inhibitor of the Ser190 proteases listed in Table 1, uPA, trypsin and tryptase (K_i = 0.2–1.5 μM), than the Ala190 counterparts, tPA, thrombin and factor Xa (K_i = 17–30 μM). In general, the other inhibitors in Table 1 show a similar trend. Factors other than the identity of residue 190 can also influence inhibitor potency, however. For example, benzo[*b*]thiophene-2-carboxamidine is a 9.9-fold better inhibitor of trypsin (1.0 μM) than of tryptase (9.9 μM), both of which have a serine residue at position 190. In addition, uPA (with Ser190) is inhibited by benzamidine (K_i = 97 μM) about as weakly as is factor Xa (with Ala190; K_i = 110 μM).

Benzo[*b*]thiophene-2-carboxamidine is a poorer inhibitor of uPA and tryptase than the 4-iodo analog, by factors of 11 and 6.6, respectively (Table 1). The 4-iodo substituent has little effect on the K_i values of the other proteases. Introduction of a nitrogen into the six-membered ring of benzo[*b*]thiophene, in thieno[2,3-*b*]pyridine-2-carboxamidine, leads to a decrease in affinity toward all of the enzymes that ranges from as little as 3.4-fold for tryptase to as much as 120-fold for tPA.

Benzo[*b*]thiophene-2-carboxamidines bound to uPA make a hydrogen bond with Ser190 that is absent in Ala190 counterparts

Figure 1a shows the structure of uPA–4-iodobenzo[*b*]thiophene-2-carboxamidine, pH 6.5, superimposed on the $(2|F_o|-|F_c|)$, α_c map. The inhibitor amidine lies at the bottom of the S1 site, making two hydrogen-bonded salt bridges with the carboxylate of Asp189. One amidine nitrogen also donates a hydrogen bond to the carbonyl oxygen of Gly219. The remaining amidine hydrogen (H1) is donated in a multi-centered hydrogen-bonding interaction to $O\gamma_{Ser190}$ and to an ordered water (water1). The hydrogen-bond parameters at the S1 site for this and other structures are listed in Table 2.

In Figure 1b the structure of uPA–4-iodobenzo[*b*]thiophene-2-carboxamidine is superimposed on the corresponding thrombin complex. As in the uPA and trypsin complexes, a water co-bound at the S1 site mediates inhibitor binding. The $N1_{inhibitor}$–$O\gamma_{Ser190}$ and water1–$O\gamma_{Ser190}$ hydrogen bonds present in the uPA and trypsin complexes are absent in the thrombin complex, however, because residue 190 is an alanine in thrombin. One of the components (N1–$O\gamma_{Ser190}$) of the multi-centered enzyme–inhibitor hydrogen bond in the uPA and trypsin complexes is therefore absent in the thrombin complex. The remaining component (N1–water1) is shorter in the thrombin complex (2.9 Å at pH 7.3) than in the uPA

Figure 1

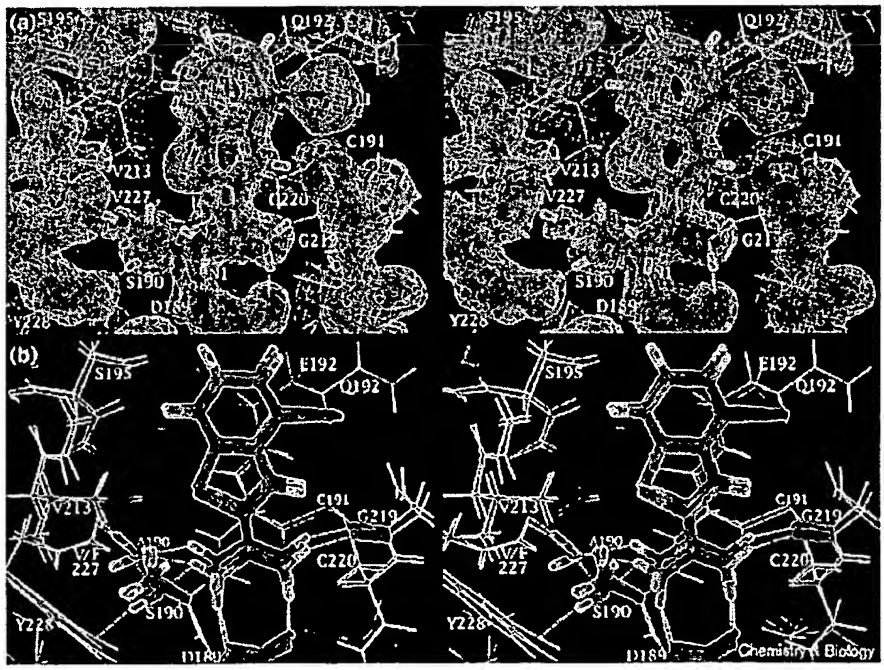

(a) Superposition of the structure of uPA–4-iodobenzo[*b*]thiophene-2-carboxamidine, pH 6.5, onto the $(2|F_o|-|F_c|)$, α_c map (1.75 Å resolution). In this and other density figures contours are at 1.0 σ (light orange), 2.4 σ (red) and 3.8 σ (pink). The shorter (N1–$O\gamma_{Ser190}$) component of the 3-centered hydrogen bond is yellow, the longer (N1–water1) component is cyan. **(b)** Superposition of the thrombin– and uPA–4-iodobenzo[*b*]thiophene-2-carboxamidine complexes. In this and other figures comparing uPA with another structure, carbon, oxygen and nitrogen atoms are green, red and blue, respectively, for uPA, and light green, orange and purple, respectively, for the other complex. Residues common to both structures are labeled in white, those unique to uPA in light blue and those unique to the other enzyme in orange. Hydrogen bonds at S1 are light blue for uPA, and orange for the other enzyme. The long (3.21 Å) N1–water hydrogen bond in the uPA complex is cyan. The directionalities of the hydrogen bonds involving $O\gamma_{Ser190}$ and $O\eta_{Tyr228}$ in the uPA complex can be inferred from the following: a well-ordered water donates one proton to O_{Ala183}, and the other to $O\delta1_{Asp189}$ (data not shown). The other hydrogen bond to this water, involving $O\eta_{Tyr228}$, is therefore donated by $O\eta_{Tyr228}$, the $H\eta_{Tyr228}$ proton lying in the aromatic plane. $O\eta_{Tyr228}$ therefore accepts the hydrogen bond from $O\gamma_{Ser190}$.

Table 2

Hydrogen bond lengths and angles, inhibitor dihedrals, and temperature factor of co-bound water at the S1 site.

(a) uPA, tPA, trypsin and thrombin complexes of benzo[*b*]thiophene-2-carboxamidine analogs and of benzamidine.

	pH	N2–$O\delta2_{Asp189}$	N2–O_{Gly219}	N1–$O\delta1_{Asp189}$	N1–$O\gamma_{Ser190}$	N1–H1–$O\gamma_{Ser190}$	Inhibitor dihedral
uPA–APC-6860*	5.5	2.85(02)	2.77(02)	2.83(03)	2.72(05)	121(2)	11(3)
Thrombin–APC-6860	7.3	2.81	2.62	3.13			−1
Trypsin–APC-6860	8.2	2.87	2.76	3.09	2.92	111	5
Trypsin–APC-6860	5.5	2.85	2.66	2.81	2.77	129	18
Trypsin–APC-7377†	8.2	2.80	2.72	2.85	2.91	127	4
uPA–APC-7538‡	5.5	2.83	2.79	2.80	2.63	116	9, 2‡
Trypsin–APC-7538	5.5	2.80	2.73	2.83	2.84	124	−11, −11‡
Trypsin–APC-7538	8.2	2.90	2.76	2.89	2.87	119	−11, −9‡
Trypsin–benzamidine§	7.5	2.93(05)	2.68(09)	2.90(04)	2.88(11)	120(2)	−20(2)
Thrombin–benzamidine	7.3	2.76	2.59	2.95			−7
uPA–benzamidine	5.5	2.94	2.74	2.88	2.52	115	5
tPA–benzamidine#	7.5	3.00	2.82	2.96			−3

(b) complexes plus inhibitor-free trypsin, thrombin, and factor Xa.

	pH	N1–OH_2	N1–H1–OH_2	$O\gamma_{Ser190}$–OH_2	$O_{Val/Phe/Ile227}$–OH_2	O_{Trp215}–OH_2	B (H_2O)
uPA–APC-6860	5.5	3.21(04)	130(8)	3.01(11)	3.18(13)	3.42(02)	29(1)
Thrombin–APC-6860	7.3	2.91	130		3.07	3.60	19
Trypsin–APC-6860	8.2	3.12	142	3.16	2.98	3.39	25
Trypsin–APC-6860	5.5	3.47	118	3.18	2.89	3.32	24
Trypsin–APC-7377	8.2	3.15	119	2.91	3.05	3.20	24
uPA–APC-7538	5.5	3.26	130	3.19	3.11	3.20	20
Trypsin–APC-7538	5.5	3.16	128	3.12	2.98	3.08	18
Trypsin–APC-7538	8.2	3.07	131	3.21	2.87	3.01	20
Trypsin–benzamidine	7.5	3.04(06)	142(6)	3.14(06)	2.87(05)	3.06(06)	18(2)
Thrombin–benzamidine	7.3	2.73	150		3.25	3.29	16
uPA–benzamidine	5.5	2.96	136	2.84	3.26	3.41	19
tPA–benzamidine	7.5	3.06	154		2.83	3.36	26
apo-trypsin	5.0			2.70	3.33	3.22	29
apo-trypsin	7.7			3.00	3.02	3.12	29
apo-thrombin	7.8				3.06	3.36	34
apo-factor Xa	7.5				2.76	3.20	41

Distances are in Å, temperature factors (B-values) in Å^2, and the ring-amidine dihedral in degrees. Standard deviations are in parentheses. *APC-6860, 4-Iodobenzo[*b*]thiophene-2-carboxamidine. †APC-7377, Benzo[*b*]thiophene-2-carboxamidine. ‡APC-7538, Thieno-[2,3-*b*]pyridine-2-carboxamidine. The dihedral angles are for conformations 1 and 2 (see text) §Ten structures (pH 7.00 to 8.25) of resolutions higher than 1.5 Å. #1rtf [12].

complex (3.2 Å at pH 6.6) or than in the trypsin complex (3.1 Å at pH 8.2, or 3.5 Å at pH 5.5). The N1–H1–O_{water1} angle of this interaction is nonoptimal (~130°) and similar in all complexes (Table 2).

The decrease in the N1–water1 hydrogen bond length in thrombin–4-iodobenzo[*b*]thiophene-2-carboxamidine from that in the corresponding uPA complex is accomplished by a rotation of the inhibitor amidine group by 12° around the thiophene–amidine bond; in the thrombin complex the amidine is virtually coplanar with the thiophene (dihedral = −1°). The change in the inhibitor geometry to planarity in the thrombin complex is associated with an increase in the N1–$O\delta1_{Asp189}$ hydrogen bond from 2.8 Å in the uPA complex to 3.1 Å in the thrombin complex.

Interactions and environment of the iodo group in 4-iodobenzo[*b*]thiophene-2-carboxamidine complexes

The density corresponding to the iodo group is very strong (23 σ in the uPA and trypsin complexes). The iodo group occupies a cavity, making van der Waals contacts with $C\delta_{Gln192}$ (3.7 Å), $S\gamma_{Cys220}$ (4.2 Å), O_{Gly216} (3.9 Å), and

N_{Gly219} (4.3 Å) in the uPA complex, and similar contacts in the trypsin and thrombin complexes. The structure of trypsin–benzo[*b*]thiophene-2-carboxamidine is virtually identical to that of the 4-iodo analog complex.

Variability in the structures of bound amidine inhibitors

Comparison of the structures of the inhibitor complexes of uPA, tPA, trypsin and thrombin denoted by the bold entries in Table 1 reveals a remarkable diversity in the binding of such small inhibitors. The complexes can be divided roughly into two groups based on the orientations of the aromatic planes of the bound inhibitors. The inhibitors in the first set are rotated by ~20° from those in the second set around their long symmetry axis. Consequently the amidines in the first set are rotated around the amidine-aromatic bond by ~−20° from those in the second set in order to maintain hydrogen-bonding interactions at S1. The first set includes trypsin–, thrombin– and uPA–4-iodobenzo[*b*]thiophene-2-carboxamidine, uPA–thieno[2,3-*b*]pyridine-2-carboxamidine, and uPA– and tPA–benzamidine; the second set trypsin– and thrombin–benzamidine, and trypsin–thieno[2,3-*b*]pyridine-carboxamidine. The aromatic amidine dihedrals for the bound inhibitors range from −20° to +18° (Table 2).

Diversity in the S1 site architectures of the trypsin-like serine proteases complexes

Differences in the bound structure of benzamidine or of other small amidine inhibitors among the trypsin-like protease complexes reflect subtle but significant changes in the corresponding S1 site architectures. In uPA–benzamidine there are shifts (of ~0.5 Å) in the position of $O\gamma_{Ser190}$, $O\eta_{Tyr228}$, and water1 from the respective locations in trypsin–benzamidine (Figure 2a, Table 3a). In trypsin–benzamidine (and in many other trypsin–amidine complexes) water1 makes four hydrogen bonds. In the hydrogen-bonding scheme of Figure 2a, water1 accepts hydrogen bonds from $O\gamma_{Ser190}$, (3.14 ± 0.06 Å) and from $N1_{benzamidine}$ (3.04 ± 0.06 Å), and donates hydrogen bonds to O_{Trp215} (3.06 ± 0.06 Å) and to O_{Val227} (2.87 ± 0.05 Å;

Figure 2

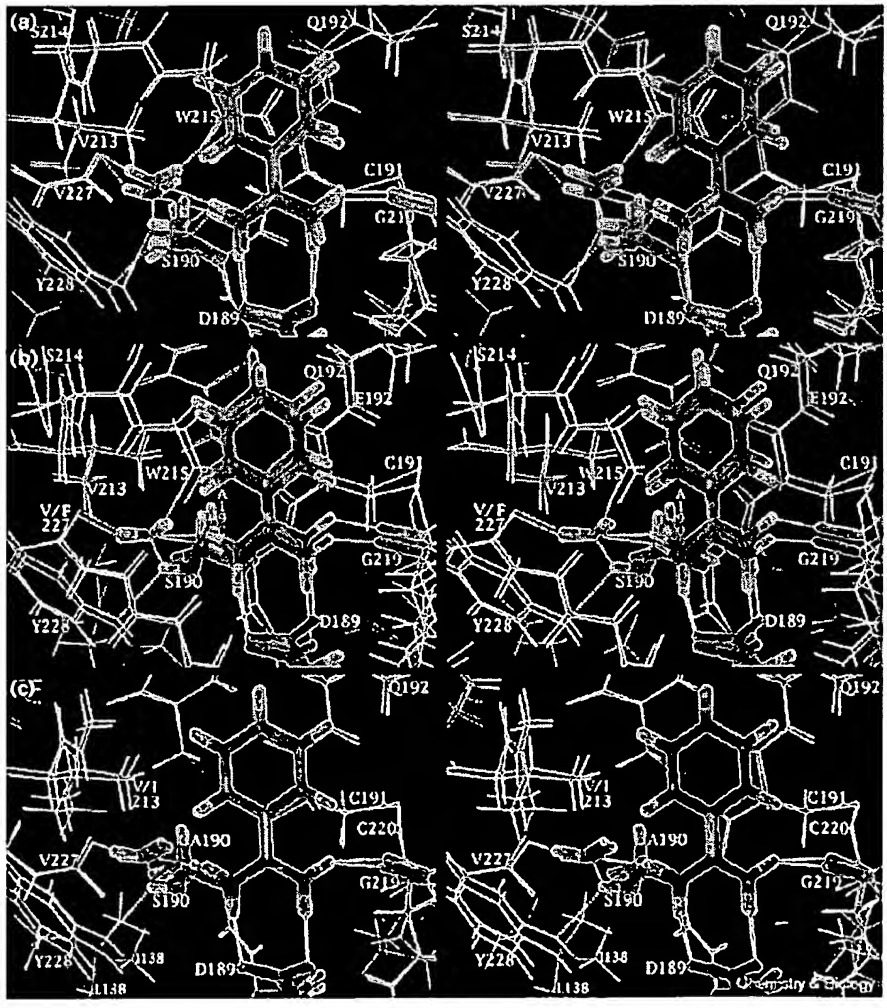

(a) Superposition of the structures of trypsin–benzamidine, pH 7.5, at 1.21 Å resolution, and uPA–benzamidine, pH 6.5, at 1.85 Å resolution. Hydrogen bonds for the trypsin and uPA complexes are yellow and light blue, respectively. The long water1–O_{Val227} interaction in uPA–benzamidine (3.26 Å) is darker cyan. In addition to any hydrogen bonds accepted from water1, the carbonyl oxygens of residues 215 and 227 also accept β-sheet hydrogen bonds, with better angular components, from the peptide nitrogens of residues 227 and 215, respectively, in these and other structures. In the hydrogen-bonding scheme shown, $O\gamma_{Ser190}$ donates a multi-centered hydrogen bond to water1 and to $O\eta_{Tyr228}$. Other orientations of water1 and alternate hydrogen bonding $O\gamma_{Ser190}$–water1 directionalities are possible, especially in cases where hydrogen bonds to the carbonyl oxygens of residues 215 and/or 227 are absent, as in Figure 1. **(b)** Superposition of thrombin–benzamidine onto uPA–benzamidine using corresponding mainchain atoms from residues 43–45, 53, 54, 191–197, 212–221 and 227–229 yields a 0.25 Å rms deviation between these two sets of atoms. **(c)** Superposition of tPA–benzamidine (1rtf [12]) onto uPA–benzamidine.

Table 2). In uPA–benzamidine, however, the latter hydrogen bonds are absent (water1–O_{Trp215} = 3.4 Å, water1–O_{Val227} = 3.3 Å). Their absence is associated with shorter N1–$O\gamma_{Ser190}$ and water1–$O\gamma_{Ser190}$ hydrogen bonds (2.5 Å and 2.8 Å) than in the other trypsin and uPA complexes (Table 2). The difference in hydrogen-bonding interactions involving water1 between uPA– and trypsin–benzamidine is not seen between uPA– and trypsin–4-iodobenzo[*b*]thiophene-2-carboxamidine. In both of the latter complexes water1 makes hydrogen bonds with $O\gamma_{Ser190}$, N1 and $O_{Val/Phe227}$, but not with O_{Trp215} (Table 2).

Table 3a lists the overall root mean square deviations (rmsds) and selected individual atomic differences between the superimposed inhibitor-binding sites of pairs of benzamidine complexes of trypsin, uPA, thrombin and tPA, along with the percent of sequence identity between the catalytic domains (heavy chains) of each pair or between their structural cores. There is a rough correlation between overall (and core) sequence similarity and similarity in the S1 site architecture. The two most structurally similar S1 sites (rmsd 0.29 Å) belong to the pair of proteases with the highest overall sequence identity, uPA/tPA (45.6%). The largest structural variations (rmsd 0.41 Å) occur for the pair with the second lowest overall sequence identity, thrombin/tPA (31.5%, Table 3a).

In each of the structures of this study the S1, S1′ and active-site residues Cys42, His57, Asp189, Ser195 and Tyr228, common to uPA, tPA, trypsin, tryptase, thrombin, and factor Xa, are well determined by density and have low temperature factors (Table S1b in the Supplementary material section). The relative locations of selected atoms of these residues vary significantly between complexes, however, by as much as 1 Å (Table 3a), irrespective of the identity of residue 190. The differences between proteases in the sidechain position and conformation of Tyr228 can be seen in Figure 2a–c for the comparisons of the benzamidine complexes of uPA, trypsin, thrombin and tPA. These types of subtle differences define a unique set of S1 site dimensions (Table S1a) that distinguish one protease from another, providing a fingerprint of each particular protease.

Table 3c also summarizes some control comparisons. Overall, there are minor differences between the benzamidine-binding sites of trypsin crystal forms $P3_121$ and $P2_12_12_1$, although some moderate and highly reproducible differences do occur. Because neighboring protein molecules do not directly contact any of the bound inhibitors or inhibitor-binding sites in either crystal form, the differences must reflect indirect, and relatively long-range effects of crystal packing. Identical structures independently determined in the same crystal form exhibit negligible structural differences (rmsd 0.05 Å; Table 3c), and emphasize the accuracy of the structural determinations.

A dramatic increase in the depth of the S1 site of uPA compared with that of thrombin is apparent in the comparison of the structures of uPA– and thrombin–benzamidine (Figure 2b). Bound benzamidine is shifted by 0.5 Å, and the Asp189 sidechain is correspondingly shifted by ~0.6 Å (Table 3a). The relative positions of the bound inhibitors and of the Asp189 sidechain are significantly different in many of the comparisons that involve a common bound inhibitor. The largest differences occur between uPA and thrombin. By contrast, the structures of the S1 sites of uPA and tPA are highly similar (Figure 3c) and have the lowest overall rms deviations from one another, 0.29 Å (Table 3a). Benzamidine binds in a similar relative position and orientation, and with a similar planarity to these two related proteases (Figure 3c). The high similarity of the uPA– and tPA–benzamidine complexes underscores the effect of residue 190 on inhibitor potency. The most obvious difference between the complexes, the absence of the Ser190 sidechain and of the associated hydrogen bond to benzamidine in the tPA complex, is strongly implicated in the 7.7-fold decrease in potency.

Discrete conformational disorder in thieno[2,3-*b*]pyridine-2-carboxamidine bound to uPA and trypsin

In uPA–thieno[2,3-*b*]pyridine-2-carboxamidine, pH 6.5, and in the corresponding trypsin complex, pH 5.5 and 8.2, the inhibitor is discretely disordered between two conformations involving a 180° rotation of the thieno[2,3-*b*]pyridine moiety about the amidine–thiophene bond. The disorder was discovered and verified as described in the Supplementary material section. Figure 3a shows the structure and ($2|F_o|-|F_c|$), α_c map for uPA–thieno[2,3-*b*]-pyridine-2-carboxamidine, pH 6.5. In the first conformation the sulfur is in a favorable location, as in bound benzo[*b*]thiophene-2-carboxamidines. Water1 is shifted, by 0.5 Å, from its position in uPA–4-iodobenzo[*b*]thiophene-2-carboxamidine, donating a shorter hydrogen bond to the thiophene sulfur (3.0 Å versus 3.3 Å), and coming into hydrogen-bonding range of O_{Trp215} (3.2 Å versus 3.4 Å). In the first conformation of bound thieno[2,3-*b*]pyridine-2-carboxamidine, the inhibitor nitrogen is not in a favorable location, buried without hydrogen bonds, 3.6 Å from $O\gamma_{Ser195}$. In the second conformation, the nitrogen is in a more favorable location, exposed to solvent but the sulfur is in a less favorable location, making a close S–O_{Gly219} contact (3.3 Å; Figure 3a).

In trypsin–thieno[2,3-*b*]pyridine-2-carboxamidine, the nitrogen of the second conformer does make a hydrogen bond (3.1 Å) with $O\gamma_{Ser195}$, because the bound inhibitor is 0.5 Å higher in the S1 site than in the uPA complex (Figure 3b). At pH 8.2 it can be inferred that $O\gamma_{Ser195}$ is the hydrogen-bond donor to both $N\varepsilon2_{His57}$ and to the inhibitor nitrogen. Consequently there is a deficit in hydrogen-bonding interactions involving the buried inhibitor nitrogen, $O\gamma_{Ser195}$ and $N\varepsilon2_{His57}$. At pH 5.5 a

Table 3

Comparison of structures of benzamidine complexes of trypsin, uPA, thrombin, and tPA, and of apo-trypsin and apo-thrombin.

Sub-site	S1									
Residue	Ser/Ala190	Asp189			Tyr228		Gly219	Inhibitor		$H_2O(1)$
Atom	Oγ	Cβ	Oδ1	Oδ2	Oη	Cε2	O	N1	N2	O
(a) Thrombin/uPA		**0.52**	0.33	**0.75**	0.22	0.23	**0.59**	0.41	**0.61**	0.09
Thrombin/tPA		**0.64**	0.18	**0.61**	0.31	0.17	0.26	0.21	0.31	0.29
Trypsin/thrombin		**0.50**	0.22	**0.55**	**0.82**	**0.67**	0.35	0.21	0.22	**0.65**
Trypsin/uPA	**0.52**	0.22	0.30	0.38	**0.52**	**0.49**	0.20	**0.50**	0.31	**0.45**
Trypsin/tPA		**0.65**	0.16	0.21	**0.77**	**0.58**	0.25	0.25	0.28	**0.46**
uPA/tPA		0.43	0.25	0.29	**0.54**	0.37	0.37	**0.55**	0.10	0.30
(b) Trypsin/apo-trypsin	**0.57**	0.44	0.14	0.29	0.15	0.16	0.16			0.19
Thrmb/apo-thrombin		0.14	0.37	0.42	0.20	0.15	0.34			**0.55**
(c) Trypsin*, $P3_121/P2_12_12_1$	0.14	0.11	0.19	0.16	0.12	0.10	0.19	0.37	0.33	0.22
Trypsin†, $P3_121/P3_121$	0.12	0.05	0.05	0.05	0.05	0.02	0.10	0.05	0.06	0.05
Trypsin‡, $+SO_4^{-2}/-SO_4^{-2}$	0.09	0.05	0.05	0.04	0.03	0.06	0.05	0.05	0.04	0.04

Sub-site	S1′	Active site							Sequence	
Residue	Cys42	Ser195		His57	Gln/Glu192	Residues withheld			identity	
Atom	N	Oγ	Cβ	Nε2	Cα	from superposition§	rmsi§	rmsf§	Overall	Core#
(a) Thrombin/uPA	0.40	**1.07**	0.24	**1.07**	**0.56**	42, 57–58, 189–190, 192–193	0.36	0.25	27.8	44.1
Thrombin/tPA	**0.74**	**0.99**	**0.48**	**0.54**	**0.65**	42, 44–45, 57–58, 190, 192¶	0.41	0.33	31.5	47.5
Trypsin/thrombin	0.41	**0.59**	**0.46**	0.39	**0.65**	53, 58, 189–190, 192	0.37	0.33	34.4	49.2
Trypsin/uPA	**0.76**	**0.52**	0.39	**0.89**	0.38	42, 57	0.35	0.28	35.2	48.3
Trypsin/tPA	**0.72**	**0.59**	**0.64**	0.30	0.31	42, 53, 190, 193, 195	0.38	0.38	36.9	52.5
uPA/tPA	0.26	0.23	0.28	**0.57**	0.06	43–45, 53–54	0.29	0.25	45.6	61.9
(b) Trypsin/apo-trypsin	0.09	**0.54**	0.20	0.32	0.29	190–192	0.14	0.12		
Thrmb/apo-thrombin	0.17	**0.56**	0.25	0.12	**0.61**	191–192	0.27	0.25		
(c) Trypsin*, $P3_121/P2_12_12_1$	0.05	0.32	0.14	0.35	**0.50**	192	0.13	0.12		
Trypsin†, $P3_121/P3_121$	0.06	0.14	0.12	0.12	0.02		0.05	0.05		
Trypsin‡, $+SO_4^{-2}/-SO_4^{-2}$	0.06	0.37	0.22	0.17	0.02		0.05	0.05		

Differences are in Å, and sequence identity is in %. Differences greater than 0.45 Å are in bold. In **(a)** and **(b)** all trypsin–benzamidine comparisons involve $P3_121$ trypsin–benzamidine-sulfate, pH 7.50, 1.21 Å resolution. Sulfate and citrate are co-bound at the active sites of tPA– and uPA–benzamidine, respectively. *Trypsin–benzamidine, both forms at pH 8.2, with no co-bound sulfate. The $P2_12_12_1$ form is the 'small cell' form (a = 54.8 Å, b = 58.7 Å, c = 67.6 Å). †Trypsin–benzamidine, pH 7.0 and 7.5, sulfate co-bound at each pH. ‡Trypsin–benzamidine, both in form $P3_121$, one at pH 7.7, with co-bound sulfate, and the other at pH 8.25 (and otherwise identical soaking conditions) without co-bound sulfate. §Mainchain atoms of residues 42–45, 53–54, 57–58, 189–197, 212–221 and 227–229 were used for initial superpositions of S1, S1′ and active sites, yielding overall initial rmsd, rmsi. Residues with significant differences in mainchain positions between corresponding atom pairs were withheld from final superpositions (for Figures and final comparisons), yielding 'rmsf'. #Core residues are 26–34, 41–58, 65–71, 81–91, 102–108, 117–124, 135–144, 154–164, 180–183, 189–200, 210–215 and 226–240. ¶Also excluded were residues 193, 195, 213 and 216–219.

sulfate is co-bound with partial occupancy (60%) at the active site, receiving hydrogen bonds from $N\varepsilon2_{His57}$, $O\gamma_{Ser195}$, and N_{Gly193}, as in trypsin–benzamidine-sulfate, or –BABIM-sulfate [14] (Figure 3b). The Hγ proton of Ser195 is disordered, donating partial hydrogen bonds to two of the oxygens of the co-bound sulfate in one location, and donating a hydrogen bond to the nitrogen of conformer 2 of the inhibitor in the other location (Figure 3b). (The pK_a of the thieno[2,3-*b*]pyridine nitrogen is estimated to be ~4.9 [15].) The aromatic planes of the inhibitor conformers in uPA–thieno[2,3-*b*]pyridine-2-carboxamidine are rotated ~17° from those in the trypsin–thieno[2,3-*b*]pyridine-2-carboxamidine (Figure 3b), but are oriented similarly to those in uPA– and trypsin–4-iodobenzo[*b*]thiophene-2-carboxamidine. No binding of thieno[2,3-*b*]pyridine-2-carboxamidine to thrombin was observed crystallographically at an inhibitor concentration of 1 mM.

Figure 3

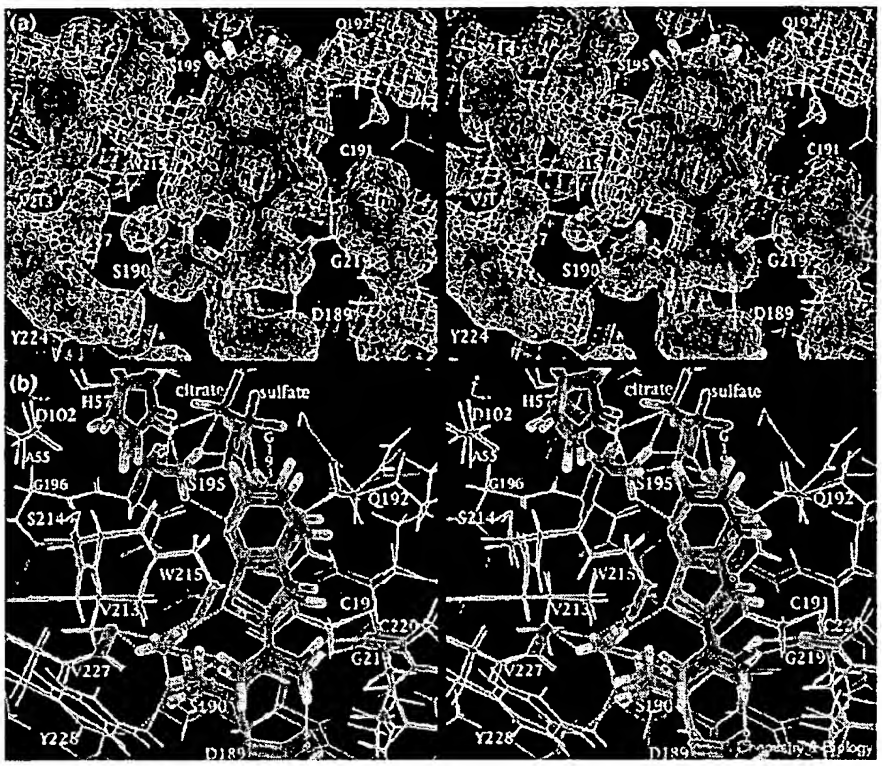

(a) Structure of uPA–thieno[2,3-*b*]pyridine-2-carboxamidine, pH 6.5, at 1.65 Å resolution, on the $(2|F_o|-|F_c|)$, α_c map. The occupancies of conformation 1 (with green carbons) and 2 (light green carbons) are 66% and 34%, respectively. In the trypsin complex the corresponding occupancies are 54% and 46% at pH 5.5, and 31% and 69% at pH 8.2. (b) Superposition of uPA– and trypsin–thieno[2,3-*b*]pyridine-2-carboxamidine, pH 5.5. For clarity only the first conformation of the bound inhibitors is shown. In each complex the aromatic rings of the two bound conformations of the inhibitors lie in the same plane as one another (see Figure 4a). The two locations of the Hγ proton of Ser195 for the trypsin complex are shown.

Structural comparison of inhibitor complexes with corresponding inhibitor-free enzymes

The B factors of protein groups making hydrogen bonds with trypsin ($O\delta1,2_{Asp189}$, $O\gamma_{Ser190}$ and O_{Gly219}) decrease significantly upon inhibitor binding (Table S1b), and the $O\gamma_{Ser190}$ atom undergoes a large shift, 0.5 Å in trypsin–benzamidine (Table 3b). Binding of benzamidine to thrombin decreases the B factors of $N\varepsilon2_{His57}$, $O\delta1,2_{Asp189}$ and $C\beta_{Ala190}$ (Table S1b). Binding of inhibitors to thrombin incurs greater and more extensive structural changes than does binding of the same inhibitors to trypsin. The rms deviations between the superimposed inhibitor-binding sites of thrombin–benzamidine and apo-thrombin is 0.27 Å, compared with 0.14 Å for trypsin–benzamidine/apo-trypsin (Table 3b). Binding of benzamidine induces a major contraction of the S1 site of thrombin, by 0.8 Å, along the $C\alpha_{Glu192}$–$C\alpha_{Trp215}$ vector, compared with only 0.2 Å for trypsin (Table S1a). In thrombin the contraction is reflected in a 0.6 Å change in the position of $C\alpha_{Glu192}$ (Table 3b).

The water (water1) that mediates inhibitor binding at S1 in the complexes is bound in a similar location in the structures of apo-trypsin (Figure 4a), apo-thrombin (Figure 4b) and apo-factor Xa. In apo-trypsin water1 makes hydrogen bonds with $O\gamma_{Ser190}$, O_{Val227}, O_{Trp215}, as in trypsin–benzamidine, and trypsin–thieno[2,3-*b*]pyridine-2-carboxamidine, and makes a fourth hydrogen bond with another ordered water (Figure 4a). Although there is a moderate increase in mobility of this water (29 Å^2) compared with that in the complexes (B = 18–25 Å^2), it is well ordered in apo-trypsin in terms of both location and orientation.

In thrombin, water1 undergoes a more pronounced decrease in B factor, from 16–19 Å^2 to 34 Å^2, upon inhibitor binding. In apo-thrombin, water1 makes only one hydrogen bond with the protein (with O_{Phe227}) and one with another water (B = 47 Å^2; Figure 4b). In apo-factor Xa water1 is in a similar environment, and not well ordered (B = 41 Å^2). There are more possible orientations of water1 in the Ala190 apo-proteases, thrombin and factor Xa because water1 lacks the hydrogen-bonding interactions provided by $O\gamma_{Ser190}$ and O_{Trp215} in apo-trypsin. Upon inhibitor binding to the Ala190 proteases, acceptance by water1 of the hydrogen bond donated by N1 of the inhibitor amidine causes an increase in the positional and/or rotational order of water1 (reflected by a large decrease in B factor) that represents an unfavorable entropy component to inhibitor binding.

Comparison of the uPA structures of this study with that published previously

Some of the differences between the uPA structures of this study (space group C2, resolutions up to 1.65 Å) and the previously published structure (space group R3, 2.5 Å resolution, 1lmw [13] in the Brookhaven Database [16]) occur

on the surface and are due to differences in crystal packing. Other significant differences, however, reflect the higher resolution and level of refinement of these new uPA structures (see Table 4 and Table S2 in the Supplementary material section for refinement statistics). For example, in the R3 structure the loop comprising residues 185A–186 has very high B values, > 100 Å^2 for Trp186 which is completely solvent-exposed, whereas in our structure, this loop is well determined with Trp186 well packed and well ordered (B = 30 Å^2). It was also necessary to reverse the directionality of the A chain from that in the R3 structure in order to fit the strong, well-defined density observed for several residues before, after, and including the disulfide that links the A chain to the B chain.

Many of the asparagine and glutamine sidechains in the R3 structure were re-oriented with respect to the flip of the sidechain amide; of these 18 sidechains, 16 are unambiguously orientable because of hydrogen bonds to neighboring residues. The two that are not orientable are mobile surface residues that do not make hydrogen bonds. Of the ten histidine sidechains, all are well determined, and nine have unambiguous orientations with respect to the flip of the imidazoles.

In the C2 uPA structures of this study determined from crystals grown in the presence of citrate, there are three citrate molecules at intermolecular regions including one near the active site. One acid group of the latter citrate occupies a region near the oxyanion hole, its carboxylate oxygens accepting a hydrogen bond from N_{Gly193} and from $O\gamma_{Ser195}$. Another acid group makes a hydrogen-bonded salt bridge with $N\varepsilon2_{His57}$.

Discussion

Hydrogen-bonding differences between the S1 sites of Ser190 and Ala190 serine proteases that impart inhibitor selectivity

Most trypsin-like serine protease targets for drug design fall into three classes: those with serine, threonine or alanine at position 190. The S1 sites of the Ser190 and Ala190 sets of proteases, compared in this study, exhibit steric and electrostatic differences that can be exploited to engineer inhibitor selectivity. One factor contributing to the selectivity of 4-iodobenzo[*b*]thiophene-2-carboxamidine for uPA and against tPA is an additional hydrogen bond between the inhibitor amidine and $O\gamma_{Ser190}$ that is absent in the Ala190 proteases. This difference in hydrogen bonding at the S1 site is reflected in a marked trend of greater potency of each of the four amidine inhibitors for the Ser190 proteases than for the Ala190 counterparts (Table 1).

The more important component of the multi-centered N1–$O\gamma_{Ser190}$–water1 hydrogen-bonding network in the uPA– and trypsin–inhibitor complexes of this study is the N1–$O\gamma_{Ser190}$ interaction. In uPA– and trypsin–4-iodobenzo[*b*]thiophene-2-carboxamidine, pH 6.5 and

Figure 4

Structures and associated $(2|F_o|-|F_c|)$, α_c maps for (a) apo-trypsin, pH 7.7; and (b) apo-thrombin, pH 7.5, 1.47 Å resolution. In (b), the long water1–O_{Trp215} distance (3.4 Å) is indicated in cyan.

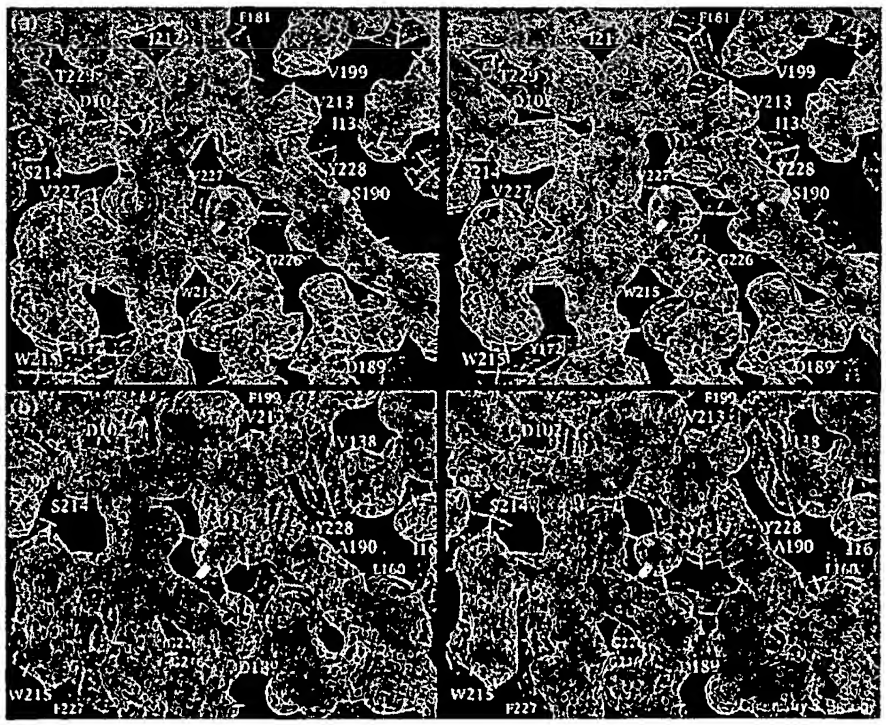

5.5, respectively, the N1–$O\gamma_{Ser190}$ length is shorter than the N1–water1 length by 0.5 and 0.7 Å, respectively (Table 2). To compensate for the absence of the N1–$O\gamma_{Ser190}$ hydrogen bond in thrombin–4-iodobenzo-[*b*]thiophene-2-carboxamidine, the N1–water1 hydrogen bond is shortened, by 0.3 Å, from the value in the corresponding uPA complex, and by 0.2 Å and 0.6 Å from the values in the trypsin complex at pH 5.5 and 8.2, respectively (Table 2). The N1–H1–water1 angle is nonoptimal, 130°, in both the uPA and thrombin complexes. The single nonoptimal hydrogen bond involving H1 in thrombin–4-iodobenzo[*b*]thiophene-2-carboxamidine is, therefore, expected to provide less binding affinity than the multi-centered hydrogen-bonding interactions in the corresponding uPA and trypsin complexes. The increase in free energy of binding of 4-iodobenzo[*b*]thiophene-2-carboxamidine in the Ser190 proteases, can be estimated from the ratios of the K_i values in Table 1. The increase in free energy of binding of 4-iodobenzo[*b*]thiophene-2-carboxamidine in the Ser190 proteases can be estimated from the ratios of the K_i values in Table 1 ($\Delta\Delta G_{binding}$ in kcal/mol for a pair of complexes with K_i values of K_i1 and $K_i2 = 1.1335 \times \log(K_i1/K_i2)$). The increase ranges from 1.4 ± 0.1 kcal/mol (for the tryptase, tPA pair) to 2.9 ± 0.2 kcal/mol (for the uPA, factor Xa pair).

The decrease in the N1–water1 hydrogen bond length to 2.9 Å in the thrombin–4-iodobenzo[*b*]thiophene-2-carboxamidine complex from 3.2 Å in the uPA complex is associated with other changes unfavorable for inhibitor binding: a lengthening of the N1–$O\delta1_{Asp189}$ hydrogen bond from 2.8 to 3.1 Å, and a change in the thiophene–amidine dihedral angle from 11° to –1°. The greater planarity of the inhibitor in the thrombin complex is associated with an unfavorable contact between the thiophene hydrogen and an amidine hydrogen. The resulting increase in conformational energy of the thrombin-bound inhibitor from that of the uPA-bound inhibitor is estimated from *ab initio* calculations to be 0.5 kcal/mol.

A final factor favoring the binding of 4-iodobenzo[*b*]thiophene-2-carboxamidine to uPA over Ala190 counterparts involves the degree of order in the apo-enzymes of the water (water1) that mediates inhibitor binding. Because there is no hydrogen bond between water1 and the sidechain of residue 190 in the Ala190 proteases (Figure 4b), hydrogen-bond formation between water1 and the amidine inhibitors involves an increase in the order (and decrease in the entropy) of water1, reflected in a sizable decrease in its B-factor, by 15 Å^2, in the case of thrombin. In the inhibitor-free Ser190 counterparts, the position and orientation of water1 is more constrained by the hydrogen bond with $O\gamma_{Ser190}$ (Figure 4a), and thus less unfavorable entropy changes occur upon inhibitor binding; the decrease in its B factor is only 4 Å^2 in the case of trypsin.

Other structural differences among the S1 sites of trypsin-like serine proteases that impart inhibitor selectivity

In addition to the direct influence of residue 190 on the structure and character of the S1 site, other longer-range forces exert indirect, but significant effects. For example, the rms mainchain positional difference, 0.35 Å, between a set of residues (at and near S1) of the superimposed S1 sites of uPA– and trypsin–4-iodobenzo[*b*]thiophene-2-carboxamidine (each having Ser190), is similar to the corresponding difference between the uPA (Ser190) and thrombin (Ala190) complexes (0.36 Å; Table 3a). These variations, determined by more global sequence differences (Table 3a), affect the relative locations, orientations and dihedral angles of bound inhibitors, and consequently the resulting hydrogen-bond lengths and van der Waals interactions between the protease and the inhibitor. The preference of small amidine inhibitors for Ser190 proteases over Ala190 counterparts observed in Table 1 is not, therefore, expected nor observed to be completely general.

Diversity in the binding of small amidine inhibitors at the S1 sites of trypsin-like serine proteases

Within the set of protease–amidine complexes in this study, there are significant differences that involve the binding of a single inhibitor to different enzymes (Figure 2a–c, Table 3a), as well as the binding of different inhibitors to a single enzyme. These differences include the relative orientations of the bound inhibitors, their degree of planarity and their depths in the S1 pocket. There is a corresponding variability in the relative position and conformation of Asp189, and in the position and hydrogen-bonding interactions of the water co-bound at S1.

The structures of thrombin– and tPA–benzamidine [12] provide insight into the poor benzamidine potencies for these proteases (K_i = 320 μM and 750 μM, respectively, Table 1). When bound to thrombin and tPA, benzamidine not only lacks a hydrogen bond with residue 190 (alanine in these cases), but also has considerable conformational strain (the phenyl-amidine dihedral is –7° in thrombin, and –3° in tPA).

An example of how structural features other than residue 190 can influence inhibitor affinity can be seen by comparing the structures and associated K_i values for uPA– and trypsin–benzamidine, both of which have serine at position 190. The S1 site of uPA is deeper than that of trypsin; the $O\gamma_{Ser190}$–$C\alpha_{Ser195}$ distance is 0.5 Å shorter in trypsin–benzamidine than in uPA–benzamidine. The S1 site of uPA is also wider, by 0.7 Å, along the $C\alpha_{Asp189}$–N_{Gly226} vector (Table S1a). These enlargements in the S1 pocket of uPA compared with that of trypsin result in the loss of the water1–O_{Phe227} and water1–O_{Trp215} hydrogen bonds in uPA–benzamidine compared with trypsin–benzamidine. The shift in the position of water1 in uPA–benzamidine, by 0.5 Å, from its location in

trypsin–benzamidine, is accompanied by an unfavorable change in the phenyl-amidine dihedral, from $-20 \pm 2°$ in trypsin–benzamidine, to 5° in uPA–benzamidine. The dihedral change corresponds to a calculated increase in conformational strain of 1.9 kcal/mol, larger than the actual decrease in binding energy of 0.9 kcal/mol calculated from the 4.6-fold decrease in affinity (Table 1). Favorable changes that may partially offset the conformational strain in uPA-bound benzamidine include the significantly shorter (by 3.3 σ and 5.0 σ, respectively) $N1–O\gamma_{Ser190}$ and $water1–O\gamma_{Ser190}$ hydrogen bonds (Table 2).

Comparison of the structures of the amidine complexes of uPA, tPA, trypsin and thrombin show, even with the simplest serine protease inhibitor (benzamidine), the important role of ordered solvent in mediating inhibitor binding, and the intricate partitioning of structural perturbations between changes in hydrogen bond lengths and in conformational strain. In Ser190 proteases, formation of the additional enzyme–inhibitor hydrogen bond involving Ser190 concurs with other interactions, including the $O\eta_{Tyr228}–O\gamma_{Ser190}$ and $water1–O\gamma_{Ser190}$ hydrogen bonds. These and other short- and long-range steric and electrostatic interactions at S1, determined from the local and global sequence, are often intricately coupled and cooperatively determine the structure and interactions of the bound inhibitor, its conformational strain and its affinity. The coupling renders the precise difference in the binding energy of the multi-centered ($O\gamma_{Ser190}$, water1, $N1_{inhibitor}$) hydrogen bond in Ser190 proteases versus the water1–N1 hydrogen bond in Ala190 proteases difficult to assess. Clearly, to determine and exploit the subtle structural differences at the S1 site that are important for inhibitor design requires high-resolution X-ray crystal structures of complexes involving both the target and the anti-target(s), even when their sequences are identical and their structures highly similar in the vicinity of inhibitor binding.

Significance

Involved or implicated in numerous disease states, trypsin-like serine proteases are rational, well-studied targets for therapeutic inhibition. Most of these targets and their anti-targets fall into three categories: those with threonine, serine or alanine residues at position 190. The ability to discriminate among these protease classes via small S1 recognition elements would provide a powerful basis for the design of small-molecule inhibitors that are both potent and specific for individual drug targets, such as urokinase-type plasminogen activator (uPA).

The K_i values of 4-iodobenzo[*b*]thiophene-2-carboxamidine for uPA and for other trypsin-like serine proteases along with the structures of the associated complexes show that considerable specificity for uPA can be achieved through interactions at the S1 site alone. Although the S1 sites of uPA and tPA are highly similar to one another, they differ at position 190: alanine in tissue-type plasminogen activator (tPA), and serine in uPA. Ser190 is capable of making an additional hydrogen bond with S1-bound amidine inhibitors that can impart an increase in affinity of amidine inhibitors for uPA over Ala190 counterparts.

Comparison of the structures of the S1 sites of members of the Ala190 and Ser190 classes of trypsin-like serine proteases indicates that these sites are as different from one another within each class as they are between the two classes. Structural features in addition to the sidechain of residue 190 therefore differentiate the S1 sites of trypsin-like serine proteases and constitute a distinct fingerprint of each enzyme. Structural differences between S1 sites formed from identical segments of local sequence are imposed by the flanking sequence and structure. Specificity determinants at this site reside not only in its local structure but also in the degree and extent of its structural plasticity, determined by the sequence and structure of the neighboring regions. The depth, width, electrostatic character and spatial relationship of the S1 site to the active site and to other nearby binding sites such as S1′ constitute a unique signature of the target. When properly tuned to these parameters remarkably small inhibitors can attain considerable specificity.

Urokinase has emerged as a rational drug target for the treatment of breast and prostate cancer. The uPA–inhibitor complexes in this study are among the first small-molecule–uPA complexes reported, and are at resolutions significantly higher (1.7 Å) than the previously published uPA–peptide hemi-ketal structure (2.5 Å). Along with the related trypsin, thrombin and factor Xa structures described here they form part of a database that promises to expedite structure-based design of potent and specific small-molecule uPA inhibitors.

Materials and methods

Preparation of deglycosylated low molecular weight human uPA
Cloning of LMW uPA. The DNA fragment coding for LMW uPA was generated by polymerase chain reaction (PCR) amplification of pET-20HMUK, which contains the cDNA sequence of high molecular weight uPA (HMW uPA) cloned from a kidney cDNA population (Clontech, Palo Alto, CA). The amino terminus of our recombinant LMW uPA starts at residue 135 in the HMW uPA sequence. Amplification of LMW uPA was performed under standard conditions with a 5′ primer (5′-LMW-uPA = 5′-AAAAAACCGTCCTCTCCGCCGGAAGAAT-3′) coding for the amino acids KKPSSPPEE and a 3′ primer (3′-uPA-AvrII = 5′-CGC**CTAGG**TCAGAGGGCCAGGCCATTCTCTT-3′) containing an *Avr*II restriction site (bold). The PCR-amplified product was treated with Klenow fragment, digested with *Avr*II, and cloned into the *P. pastoris* expression vector pPIC9K (Invitrogen, San Diego, CA) linearized with *SnaB*I and *Avr*II. The sequence of LMW uPA in the expression construct (pPIC9KLMWuPA) was confirmed by sequencing.

Construction of deglycosylated LMW uPA expression vector. Deglycosylated LMW uPA (LMW uPA-N145A) has an Asn→Ala substi-

tution at position 302 in HMW uPA, or residue 145 of LMW uPA (chymotrypsin numbering scheme). The DNA fragment coding for LMW uPA-N145A was generated by amplifying upstream and downstream of the mutagenic site with primers, 5′-Ala-HindIII (5′-CC*AAGCTT*CTACCGACTATCTCTATCCGGAGCAGCT-3′) and 3′-Ala-*Hind*III (5′-CCA*AGCTT*CTTTTCCAAAGCCAGTGATCTCACA-3′) coding for the Asn145→Ala substitution (bold type). Both mutagenic primers contain a new *Hind*III site (italicized) facilitating construction of the full-length DNA fragment coding for LMW uPA-N145A. The PCR-amplified LMW uPA(Ala145)-HindIII product (generated with 5′-LMW-uPA and 3′-Ala-HindIII primers) was treated with Klenow fragment and digested with *Hind*III. The HindIII-uPA(Ala156)-AvrII PCR product (generated with 5′-Ala-HindIII and 3′-uPA-AvrII primers) was digested with both *Hind*III and *Avr*II. The digested PCR fragments were then cloned into the *P. pastoris* expression vector pPIC9 (Invitrogen, San Diego, CA) linearized with *SnaB*I and *Avr*II. The sequence of the insert in the expression construct, pPIC9LMWuPA(N145A), was verified by sequencing.

Transformation of P. pastoris *and screening for expression of LMW uPA-N145A.* The pPIC9LMWuPA(N145A) expression construct was linearized with *Bgl*II, and used to transform the histidine-deficient *P. pastoris* strain GS115 by electroporation as described (*P. pastoris* expression kit instruction manual). Recombinant clones were cultured in buffered glycerol-complex (BMGY) medium and induced in buffered complex medium containing 0.5% methanol (BMMY). Cell-free culture supernatants were isolated, and the expression of recombinant enzyme was determined by silver-stained sodium dodecyl sulfate–polyacrylamide gel electrophoresis (SDS–PAGE) on a 12% acrylamide gel and by immunoblotting with a human uPA monoconal antibody (Oncogene Science). After activation with human plasmin, enzyme activity was assayed with the chromagenic substrate, Spectrozyme UK (American Diagnostica, Greenwich, CT).

Purification of LMW uPA-N145A. Purification of LMW uPA-N145A was based on affinity chromatography involving binding to p-aminobenzamidine [17]. Clarified *P. pastoris* supernatant was dialyzed into 20 mM MES (pH 6.0) with Amicon S1Y10 and passed through CM-Sepharose (Pharmacia). Urokinase in the gradient elution fractions was activated with plasmin at pH 8.5, 37°C for 2 h. The activated fractions were adjusted to pH 7.0 and made 1.0 M in NaCl before loading on a benzamidine-sepharose column (Pharmacia Biotech). Activated LMW uPA-N145A was eluted with 100 mM citric acid (pH 3.5), giving a single band on nonreduced SDS gel (data not shown).

Synthesis of inhibitors. Benzamidine was purchased from Sigma, and the starting materials and reagents for other compounds from Aldrich. 4-Iodobenzo[*b*]thiophene-2-carboxamidine and the corresponding noniodo analog, benzo[*b*]thiophene-2-carboxamidine were synthesized as described by Bridges *et al.* [18]. A similar procedure [19,20] was used to synthesize thieno[2,3-*b*]pyridine-2-carboxamidine (see Scheme 1 in the Supplementary material section). Synthetic details are described in the Supplementary material section.

Enzymology

Purchased enzymes were HMW uPA (American Diagnostica), tPA (Sigma), trypsin (Worthington), tryptase (Athens Research Technologies), thrombin (Calbiochem) and factor Xa (Haematological Technologies, Inc). The substrates for trypsin, tryptase, and thrombin (tosyl-Gly–Pro–Lys-p-nitroanilide), for factor Xa (CH_3OCO-D-CHA-Gly–Arg-pNA·AcOH, 'Pefachrome Xa') and one of the two substrates for HMW uPA (Bz-Ala–Gly–Arg-p-nitroanilide-AcOH, 'Pefachrome UK') were from Centerchem, Inc. The alternative substrate for HMW uPA (Cbz-L-(γ)Glu(α-t-BuO)-Gly-Arg-pNA, 'Spectrozyme UK') and the substrate for tPA (CH_3-SO_2-D-HHT-Gly–Arg-pNA, 'Spectrozyme tPA') were from American Diagostica Inc. Enzymes were assayed spectrophotometrically at ambient temperature in 50 mM Tris, 150 mM NaCl, 0.05% (v/v) Tween-20, 10% (v/v) DMSO, 0.002% antifoam, pH 7.4. The thrombin and factor Xa assays also contained 5.0 mM $CaCl_2$. The final concentrations of uPA, tPA, trypsin, factor Xa, tryptase and thrombin in the respective assays were 30, 11, 7.0, 3.0, 1.0 and 6.0 nM. The substrate concentrations of 100 μM (uPA), 200 μM (tPA), 100 μM (trypsin), 1000 μM (factor Xa), 500 μM (tryptase) and 250 μM (thrombin) were chosen based on the determined K_m values of 85, 430, 100, 1000, 1620 and 280 μM, respectively. The rate of change in absorbance at 405 nm was measured immediately after addition of enzyme. Apparent inhibition constants (K_i'), were calculated by nonlinear least-squares regression analysis of the absorbance time course data using the software package BatchKi (developed and provided by Petr Kuzmic, Biokin Ltd., Madison, Wisconsin) using methodology similar to that described previously [21] for tight-binding inhibitors. These values were converted to K_i values by the formula, $K_i = K_i'/(1 + S/K_m)$.

The K_i values for inhibition of each enzyme by 4-iodobenzo[b]thiophene-2-carboxamidine were performed under assay conditions similar to those described above, except that concentrations of both the inhibitor and the substrate were varied (see the Supplementary material section), and the uPA substrate was Cbz-L-(γ)Glu(α-t-BuO)-Gly–Arg-pNA ('Spectrozyme UK') from American Diagnostica. Assay data were fitted to the equations describing competitive, noncompetitive and uncompetitive inhibition using the computer programs COMPO, NONCOMPO and UNCOMPO [22] and the K_i values were obtained. The goodness of fit showed that inhibition was competitive.

Crystallization and preparation of inhibitor-free proteases and of protease–inhibitor complexes

Human uPA complexes. LMW human uPA-N145A was concentrated to 10 mg/ml using an Amicon Centricon-10 system and incubated in 50 mM HEPES, 5.0 mM NaCl, pH 7.4, 1.4 mM 4-iodobenzo[*b*]thiophene-2-carboxamidine for 15 min on ice. Potential crystallization conditions were screened in vapor diffusion drops with sparse matrix screening [23] kits purchased from Hampton Research, Laguna, CA. The complex was crystallized by vapor diffusion in hanging drops containing equal volumes of protein–inhibitor solution (0.28 mM LMW uPA-N145A, 1.4 mM inhibitor) and well solution (20% 2-propanol, 20% PEG 4K, 100 mM sodium citrate, pH 6.5) sealed over the well. Diamond plate crystals grew in 2 days. Other complexes were crystallized by a similar protocol at inhibitor concentrations at least tenfold higher than the K_i values.

Human thrombin–acetyl-hirudin and co-complexes. Thrombin was purchased from Haematologic Technologies, Inc. and acetyl-hirudin from Bachem. Thrombin-acetyl-hirudin was prepared as described previously [24]. Thrombin (1.0 mg/ml in 50 mM HEPES, 50% glycerol, pH 7.0) was incubated with 1.0 mM acetyl-hirudin in the presence or absence of amidine inhibitors for 1 h at 4°C. The solution contained 5 equivalents of 4-iodobenzo[*b*]thiophene-2-carboxamidine, 10 mM benzamidine, or was saturated in [2,3-*b*]thienopyridine-2-carboxamidine (~2 mM). Glycerol was removed during concentration to ~10 mg/ml of the complexes with a centricon 10 (Amicon). Crystals of thrombin-acetyl-hirudin with or without co-bound small molecule inhibitors, pH 7.3 or 7.8, space group C2 (a = 71.2, b = 71.8, c = 72.7 Å, β = 100.7°) were grown in hanging drops by vapor diffusion after streak seeding. The structure without an inhibitor at the S1 site is referred to as apothrombin. The drops were made from 3 ml complex and 3 ml reservoir solution (0.10 M HEPES, 0.30 M NaCl, 22% (by volume) PEG 5K monomethyl ether, pH 7.5 or 8.2). Large single crystals of dimensions >0.2 mm in each dimension grew within 1 week.

Bovine trypsin complexes and inhibitor-free trypsin. Trypsin was crystallized as described previously [14]. A structure of $P3_121$ trypsin–benzamidine was determined at 1.20 Å resolution, in 2.02 M $MgSO_4$·7 H_2O, 100 mM MES, 1.0 mM $CaCl_2$, pH 7.5. The carboxamidine complexes were prepared by soaking trypsin–benzamidine crystals in synthetic mother liquor saturated in the inhibitors. The soaking solutions were replaced 4 times, about once a day. For the complexes determined at pH 8.2 the soaking solutions contained 1.73 M $MgSO_4$·7 H_2O, 150 mM Tris, 1 mM $CaCl_2$ and 2% dimethylsulfoxide (DMSO). For the 4-iodobenzo[*b*]thiophene-2-carboxamidine complex

Table 4

Crystallography of urokinase, trypsin, and thrombin complexed with benzo[*b*]thiophene-2-carboxamidines, thieno[2,3-*b*]pyridine-2-carboxamidine, and benzamidine, and of apo-trypsin, apo-thrombin and apo-factor Xa.

RCSB PDB Code	1C5X	1C5N	1C5R	1C5Q	1C5S	1C5U	1C5T
Protease	uPA	Thrombin	Trypsin	Trypsin	Trypsin	Trypsin	Trypsin
Inhibitor (APC #)	6860	6860	6860	6860	7377	7538	7538
pH	6.50	7.33	5.50	8.20	8.20	5.50	8.20
R_{merge} (%)*	8.8	6.3	9.1	8.7	5.0	9.0	5.7
Resolution (Å)	1.75	1.50	1.47	1.43	1.36	1.37	1.37
Completeness (%)	68	65	66	75	88	81	84
R_{cryst}(%)†	20.2	22.2	19.7	20.0	19.9	18.4	17.9
Bond dev (Å)‡	0.017	0.018	0.019	0.018	0.019	0.020	0.018
RCSB PDB Code	1C5P	1C5V	1C5L	1C5O	1C5Z	1C5Y	1C5M
Protease	Trypsin	Trypsin	Thrombin	Thrombin	uPA	uPA	Factor Xa
inhibitor	Benzamidine	(apo)	(apo)	Benzamidine	Benzamidine	7538	(apo)
pH	7.50	7.70	7.80	7.33	6.50	6.50	7.70
R_{merge} (%)*	9.0	10.7	7.1	9.0	9.3	8.7	7.2
Resolution (Å)	1.21	1.48	1.47	1.90	1.85	1.65	1.95
Completeness (%)	88	61	69	51	64	68	60
R_{cryst}(%)†	19.4	20.0	21.7	20.3	18.9	20.3	22.6
Bond dev (Å)‡	0.018	0.019	0.019	0.018	0.018	0.018	0.017

Inhibitors are coded as follows: APC-6860, 4-iodobenzo[*b*]thiophene-2-carboxamidine; APC-7377, benzo[*b*]thiophene-2-carboxamidine; APC-7538, thieno[2,3-*b*]pyridine-2-carboxamidine, . *$R_{merge} = \Sigma_h\Sigma_i |I(h)_i - \langle I(h)_i \rangle| / \Sigma_h\Sigma_i I(h)_i$. †$R_{cryst} = \Sigma(||F_o| - |F_c||)/\Sigma|F_o|$ (for reflections from 7.5 Å to the upper resolution). ‡rmsd values from ideal bond lengths.

at pH 5.5, the soaking solution was 85% saturated sodium citrate, 1 mM $CaCl_2$, 2.0% DMSO, saturated with inhibitor, pH 5.5. The pH was adjusted with saturated citric acid. For the thieno[2,3-*b*]pyridine-2-carboxamidine complex, pH 5.5, the soaking solution was 1.73 M $MgSO_4$•7 H_2O, 150 mM MES, 1 mM $CaCl_2$, 2% DMSO. To prepare inhibitor-free trypsin crystals, trypsin–benzamidine crystals were soaked at the target pH values for several weeks in 1.84 M $MgSO_4$•7 H_2O, 150 mM MES or Tris, 1.0 mM $CaCl_2$, during which the soaking solutions were periodically replaced.

Factor Xa. Lyophilized human factor Xa was purchased from Enzyme Research Laboratories Inc. The amino-terminal Gla-domain and carboxyl terminus were removed by incubation at 37°C with cathepsin G and carboxypeptidase B, and the truncated human factor Xa purified by high-performance liquid chromatography (HPLC) using a mono Q HR5/5 anion exchange column, as described previously [25]. Crystals of truncated human factor Xa (space group $P3_121$, a = b = 81.8 Å, c = 108.8 Å) were grown in hanging drops from equal volumes of protein solution (5.0 mg/ml in 20 mM HEPES, 50 mM $(NH_4)_2SO_4$, pH 8.0) and well solution (25% PEG 5K, 0.10 M Hepes, 0.2 M $(NH_4)_2SO_4$, pH 7.5). The drops were sealed over the wells. Crystals > 0.20 mm in each dimension grew after 2 weeks.

Crystallography

Crystallographic data were collected with an R-AXIS IV image plate as described in [14] and in the Supplementary material section. For trypsin–benzamidine, pH 6.5, the crystal-to-detector distance was 76.0 mm, 2θ was 15.0°, and data were collected for 10 days during which the crystal underwent minor decay. The uPA and fXa structures were solved by molecular replacement by procedures similar to those described previously [26] (see the Supplementary material section) using the uPA and factor Xa structures (1lmw [13] and 1hcg [27]), respectively, obtained from the Brookhaven Databank [16]. Initial structures of trypsin and thrombin complexes were determined as described previously [14], the latter from the isomorphous structure, 1hag [28], in the Brookhaven Database. Structures were refined with X-PLOR and with difference Fourier analysis as described previously [14,26] (see the Supplementary material section). RCSB PDB codes, and data collection and refinement statistics, are given briefly in Table 4, and in more detail in Table S2.

Superposition and comparison of structures. For each pair-wise comparison, structures were initially superimposed based on sets of S1, S1′ and active site mainchain atoms summarized in Table 3. After inspection of the initially superimposed structures, residues were then excluded from the superpositions in order to maximize similarities and differences in the inhibitor-binding sites. Averages and standard deviations in hydrogen bond lengths and other parameters were calculated for uPA–4-iodobenzo[*b*]thiophene-2-carboxamidine (for which two structures were independently determined) and for trypsin–benzamidine (for which ten structures [14,29] in two crystal forms were independently determined at resolutions of better than 1.5 Å resolution in this and other published and unpublished studies. The comparisons of the two crystal forms of trypsin in the paper involve the $P2_12_12_1$ small-cell form (a = 54.8 Å, b = 58.7 Å, c = 67.6 Å) and the $P3_121$ form (a = 54.9 Å, c = 109.3 Å).

Ab initio *calculations of amidine rotational barriers*

Ab initio calculations were performed on benzamidine and benzo[*b*]-thiophene-2-carboxamidine with Gaussian94 [30] by the Hartree-Fock method with the 6-31G* basis set. Geometry optimization with the Berny algorithm [31] used redundant internal coordinates. Calculations were carried out with no dihedral constraints or with dihedrals fixed at values of 0°, 3°, 10°, 17° and 30°. Energies were plotted as a function of dihedral angle to allow calculation of energy differences corresponding to any changes in dihedral angles.

Accession numbers

The atomic coordinates for these structures have been deposited with the Protein Data Bank with the following accession codes: 1C5X uPA–APC-6860; 1C5N, thrombin–APC-6860; 1C5R, trypsin–APC-6860; 1C5Q, trypsin–APC-6860;1C5S, trypsin–APC-7377; 1C5U, trypsin–APC-7538;1C5T, trypsin–APC-7538; 1C5P, trypsin–benzamidine; 1C5V, apo-trypsin; 1C5L, apo-thrombin ; 1C5O, thrombin–benzamidine; 1C5Z, uPA–benzamidine; 1C5Y, uPA–APC-7538; 1C5M, apo-factor Xa.

Supplementary material

Supplementary material including analysis of the discrete disorder of the inhibitor in the uPA–thieno[2,3-*b*]pyridine-2-carboxamidine complex, details of synthesis of the inhibitors, of enzymology, and of crystallography is available at http://current-biology.com/supmat/supmatin.htm.

Acknowledgements

We thank Joanna Chmielewska, Tomas Lundqvist, Erifili Mosialou, and Derek Ogg (Pharmacia and Upjohn) for the modified factor Xa, and James Janc for help with the enzymology.

References

1. Schechter, I. & Berger, A. (1967). On the size of the active site in proteinases. I. Papain. *Biochem. Biophys. Res. Commun.* **27**, 157-162.
2. Renatus, M., Bode, W., Huber, R., Stürzebecher, J. & Stubbs, M.T. (1998). Structural and functional analyses of benzamidine-based inhibitors in complex with trypsin: implications for the inhibition of factor Xa, tPA, and urokinase. *J. Med. Chem.* **41**, 5446-5456.
3. Maduskie, T.P. Jr., McNamura, K.J., Ru, Y., Knabb, R.M. & Stouten, P.F.W. (1998). Rational design and synthesis of novel, potent bis-phenylamidine carboxylate factor Xa inhibitors. *J. Med. Chem.* **41**, 53-62.
4. Gabriel, B., *et al.*, & Moroder, L. (1998). Structure-based design of benzamidine-type inhibitors of factor Xa. *J. Med. Chem.* **41**, 4240-4250.
5. Brandstetter, H., *et al.*, & Engh, R.A. (1996). X-ray structure of active site-inhibited clotting factor Xa: implications for drug design and substrate recognition. *J. Biol. Chem.* **271**, 29988-29992.
6. Towle, M.J., Lee, A., Maduakor, E.C., Schwartz, C.E., Bridges, A.J., Littlefield, B.A. (1993). Inhibition of urokinase by 4-substituted benzo[*b*]thiophene-2-carboxamidines: an important new class of selective synthetic urokinase inhibitor. *Cancer Res.* **53**, 2553-2559.
7. Dano, K., Andreasen, P.A., Grondahl-Hansen, J., Kristensen, P., Nielsen, L.S. & Shriver, L. (1985). Plasminogen activators, tissue degradation, and cancer. *Adv. Cancer Res.* **44**, 139-266.
8. Andreasen, P.A., Kjøller, L., Christensen, L. & Duffy, M.J. (1997). The urokinase-type plasminogen activator system in cancer metastasis: a review. *Int. J. Cancer* **72**, 1-22.
9. Rabbani, S.A. & Xing, R.H.M. (1998) Role of urokinase (uPA) and its receptor (uPAR) in invasion and metastasis of hormone-dependent malignancies. *Int. J. Oncol.* **12**, 911-920.
10. Stack, M.S., Ellerbroek, S.M. & Fishman, D.A. (1998). The role of proteolytic enzymes in the pathology of epithelial ovarian carcinoma. *Int. J. Oncol.* **12**, 569-576.
11. Magill, C., Katz, B.A. & Mackman, R. (1999). Emerging therapeutic targets in oncology: urokinase-type plasminogen activator system. *Emerging Therapeutic Targets* **3**, 109-133.
12. Lambda, D., *et al.*, & Bode, W. (1996). The 2.3 Å crystal structure of the catalytic domain of recombinant two-chain human tissue-type plasminogen activator. *J. Mol. Biol.* **258**, 117-135.
13. Spraggon, G., *et al.*, & Jones, E.Y. (1995). The crystal structure of the catalytic domain of human urokinase-type plaminogen activator. *Structure* **3**, 681-691.
14. Katz, B.A. & Luong, C. (1999). Recruiting Zn^{+2} to mediate potent specific inhibition of serine proteases. *J. Mol. Biol.* **292**, 669-684.
15. Perrin, D.D. (1965). Dissociation constants of organic bases in aqueous solution. Supplement to Pure and Applied Chemistry, International Union of Pure and Applied Chemistry, London, Butterworths.
16. Bernstein, F.C., *et al.*, & Tasumi, M. (1977). The Protein Data Bank: a computer-based archival file for macromolecular structures. *J. Mol. Biol.* **112**, 535-542.
17. Holmberg, L., Bladh, B. & Astedt, B. (1976). Purification of urokinase by affinity chromatography. *Biochim. Biophys. Acta* **445**, 215-222.
18. Bridges, A., Littlefield, B.A. & Schwartz, C.E. *Urokinase Inhibitors.* 23 August 1994, US Patent 5340833.
19. Bhat, B. & Bhaduri, A.P. (1984) A Novel one-step synthesis of 2-methoxycarbonylthieno[2,3-*b*]quinolines and 3-hydroxy-2-methoxycarbonyl-2-3-dihydrothieno[2,3-*b*]-quinolines. *Synthesis* **8**, 673-676.
20. Meth-Cohn, O. & Narine, B. (1978). A versatile new synthesis of quinolines, thienopyridines and related fused pyridines. *Tetrahedron Lett.* **23**, 2045-2048.
21. Kuzmic, P. (1996). Program DYNAFIT for the analysis of enzyme kinetic data: application to HIV proteinase. *Anal. Biochem.* **237**, 260-273.
22. Cleland, W.W. (1979). Statistical analysis of enzyme kinetic data. *Methods Enzymol.* **63**, 103-138.
23. Jancarik, J. & Kim, S.H. (1991). Sparse matrix sampling: a screening method for crystallization of proteins. *J. Appl. Crystallogr.* **25**, 408-411.
24. Skrzpczak-Jankun, E., Carperos, V.E., Ravichandran, K.G., Tulinsky, A., Westbrook, M. & Maraganore, J.M. (1991). Structure of the hirugen and hirulog 1 complexes of α-thrombin. *J. Mol. Biol.* **221**, 1379-1393.
25. Chmielewska, J., Lundqvist, T., Mosialou, E. & Ogg, D. *Modified human factor Xa.* 7 February 1998, International patent WO 98/28412.
26. Katz, B.A., Liu, B., Barnes, M. & Springman, E.B. (1998). Crystal structure of recombinant human tissue kallikrein at 2.0 Å resolution. *Protein Sci.* **7**, 875-885.
27. Padmanabhan, K., *et al.*, & Kisiel, W. (1993). Structure of human des(1–45) factor Xa at 2.2 Å resolution. *J. Mol. Biol.* **232**, 947-966.
28. Vijayalakshmi, J., Padmanabhan, K.P., Mann, K.G. & Tulinsky, A. (1994). The isomorphous structures of prethrombin2, hirugen- and PPACK-thrombin: changes accompanying activation and exosite binding to thrombin. *Protein Sci.* **3**, 2254-2271.
29. Katz, B.A., Finer-Moore, J.S., Mortezaei, R., Rich, D.H. & Stroud, R.M. (1995). Novel K_i ~ nanomolar inhibitors of serine proteases by binding or epitaxial chemistry on an enzyme surface. *Biochemistry* **34**, 8264-8280.
30. Frisch, M.J., et al., & Pople, J.A. (1995). *Gaussian 94, Revision E.3.* Gaussian, Inc., Pittsburgh PA.
31. Schlegel, H.B. (1982). Optimization of equilibrium geometries and transition structures. *J. Comp. Chem.* **3**, 214.

Important New Class of Selective Synthetic Urokinase Inhibitor

Murray J. Towle, Arthur Lee, Emmanuel C. Maduakor, C. Eric Schwartz, Alexander J. Bridges, and Bruce A. Littlefield[1]

Sections of Biology [M. J. T., B. A. L.] and Chemistry [A. L., E. C. M., C. E. S., A. J. B.], Eisai Research Institute, Andover, Massachusetts 01810

ABSTRACT

Urokinase-type plasminogen activator (uPA) is an important mediator of cellular invasiveness. Specifically, cell surface receptor-bound uPA activates plasminogen to the potent general protease plasmin, which then degrades extracellular matrix or basement membrane either directly or via proteolytic activation of latent collagenases. Thus, cell surface uPA initiates an extracellular proteolytic cascade with which invasive cells eliminate barriers to movement. Since cellular invasiveness plays important roles in several disease states, including cancer metastasis and invasion, arthritis and inflammation, and diabetic retinal neovascularization, the development of synthetic uPA inhibitors is an attractive therapeutic goal. Here we show that 4-substituted benzo[*b*]thiophene-2-carboxamidines represent an important new class of potent and selective synthetic uPA inhibitor. Two compounds in this class, B428 and B623, inhibit human uPA in plasminogen-linked assays with median inhibition concentration (IC_{50}) values of 0.32 and 0.07 μM, respectively. This level of inhibition represents 20- and 100-fold increases in potency, respectively, relative to the 6–7 μM potencies reported for amiloride and 4-chlorophenylguanidine, the two most potent selective synthetic uPA inhibitors previously described. Importantly, both compounds show >300-fold selectivity for uPA relative to tissue-type plasminogen activator and >1000-fold selectivity relative to plasmin. Lineweaver-Burk analyses show uPA inhibition by B428 and B623 to be competitive in nature with inhibition constants (K_i) of 0.53 and 0.16 μM, respectively. Since it is cell surface uPA and not free or secreted uPA that is primarily responsible for cellular invasiveness, biologically effective uPA inhibitors must be capable of inhibiting cell surface uPA. B428 and B623 meet this criterion by inhibiting cell surface uPA on HT1080 human fibrosarcoma cells with IC_{50} values of 0.54 and 0.20 μM, respectively. Moreover, degradation of [^{3}H]fibronectin by HT1080 cells via cell surface uPA-mediated, plasminogen-dependent mechanisms is inhibited by B428 and B623, with IC_{50} values of 1.5 and 0.39 μM, respectively. In summary, 4-substituted benzo[*b*]thiophene-2-carboxamidines such as B428 and B623 represent the most potent class of competitive synthetic uPA inhibitors currently known. Their ability to selectively inhibit both free and cell surface uPA as well as cell surface uPA-mediated cellular degradative functions suggests that this class of compounds may hold significant promise for further development as antiinvasiveness drugs.

INTRODUCTION

Cellular invasiveness is a proteolytic process by which cells move through physical barriers such as ECM[2] and BM (reviewed in Ref. 1). This process contributes to a variety of normal physiological events including trophoblast implantation, angiogenesis, movement of immune cells into inflammatory sites, wound healing, cell migration during development, tissue and organ differentiation, and bone restructuring (1). Cellular invasiveness also plays major roles in various disease processes, including tumor metastasis and invasion, arthritis, and diabetic retinopathy (1). Invasive cells degrade ECM and BM via an extracellular protease cascade which includes uPA, plasmin, and the metalloprotease family of collagenases (2–4). This cascade is initiated by uPA, which is bound to high-affinity cell surface uPAR on invasive cells (5, 6), thus ensuring high local uPA concentrations at the cell surface. Cell surface uPA cleaves the inactive zymogen plasminogen to the active serine protease plasmin, which then degrades fibronectin, laminin, and other noncollagenous ECM and BM proteins directly. In addition, plasmin activates latent collagenases, thereby initiating the degradation of ECM and BM collagen (2–4, 7–9). The role of cell surface uPA as an initiator of cellular invasiveness *in vitro* and *in vivo* has been demonstrated repeatedly in experiments in which cell surface uPA activity is blocked with anti-uPA antibodies, PA inhibitors PAI-1 and PAI-2, and uPAR peptide antagonists (10–27). Thus, blocking cell surface uPA activity presents an attractive goal for the development of antiinvasiveness pharmaceuticals. Designing low-molecular-weight synthetic protease inhibitors with appropriate potency and selectivity for uPA represents one approach to achieving this goal.

Since both uPA and its fibrinolytic counterpart tPA share identical specificity for the Arg^{560}-Val^{561} bond in plasminogen (2–4), most low-molecular-weight protease inhibitors which inhibit uPA also inhibit tPA. Such inhibitors are unsuitable for use as antiinvasiveness drugs due to the potential undesired inhibition of tPA-mediated fibrinolysis. Similarly, antiinvasiveness uPA inhibitors should not inhibit plasmin, since both uPA- and tPA-mediated pathways converge through this enzyme. Unfortunately, such stringent selectivity requirements eliminate most of the known synthetic inhibitors of uPA. Moreover, the few remaining uPA-selective inhibitors show only moderate potency. For instance, *p*-aminobenzamidine is a moderately selective, competitive uPA inhibitor, yet its potency toward uPA is only moderate ($K_i \approx$ 17–82 μM; Refs. 28–30). Somewhat better potency is shown by the potassium-sparing diuretic amiloride, which selectively inhibits uPA with a K_i value of 7 μM (31). Finally, certain 4-substituted phenylguanidines are selective, competitive uPA inhibitors; 4-chloro- and 4-trifluoromethylphenylguanidine are the most potent compounds in this series, selectively inhibiting uPA with K_i values of about 6 μM (32).

Our search for more potent selective uPA inhibitors began with modifications of amiloride and moved toward an analysis of a wide variety of mono- and bicyclic aromatic guanidines and amidines. Here we report that one class of bicyclic heteroaromatic amidines, the 4-substituted benzo[*b*]thiophene-2-carboxamidines, represents a potent new class of selective synthetic uPA inhibitor. Inhibitory characteristics of two representative compounds from this class are presented, including evidence that they block both free and cell surface uPA as well as cell surface uPA-mediated whole cell degradation of fibronectin. In summary, the 4-substituted benzo[*b*]thiophene-2-carboxamidines appear to be the most potent selective synthetic uPA inhibitors currently known. This new class of uPA inhibitor may hold

Received 11/17/92; accepted 2/25/93.

The costs of publication of this article were defrayed in part by the payment of page charges. This article must therefore be hereby marked *advertisement* in accordance with 18 U.S.C. Section 1734 solely to indicate this fact.

[1] To whom requests for reprints should be addressed, at Section of Biology, Eisai Research Institute, 4 Corporate Drive, Andover, MA 01810.

[2] The abbreviations used are: ECM, extracellular matrix; BM, basement membrane; uPA, urokinase; uPAR, urokinase receptor; tPA, tissue-type plasminogen activator; PA, plasminogen activator; PAI, plasminogen activator inhibitor; BSA, bovine serum albumin;

Synthesis of 4-substituted Benzo[*b*]thiophene-2-carboxamidines. Parent benzo[*b*]thiophene-2-carboxamidine was prepared from benzo[*b*]thiophene-2-carboxoyl acid chloride by the method of Garigipati (33). Complete descriptions of the syntheses of the 4-substituted benzo[*b*]thiophene-2-carboxamidine derivatives will be presented elsewhere.[3]

Enzyme Assays. Plasminogen-linked chromogenic assays for inhibition of purified high-molecular-weight human uPA or two-chain human tPA (both from American Diagnostica, Greenwich, CT), were performed in 96-well microtiter plates as described previously (34), using 25 IU/ml uPA or 0.5 μg/ml tPA, 25 μg/ml human glu-plasminogen (American Diagnostica), 25 μg/ml des-AA-fibrinogen (Desafib; American Diagnostica) and 1 mM *H*-D-norleucyl-hexahydrotyrosyl-lysine-*p*-nitroanilide (Spectrozyme PL; American Diagnostica) as plasmin substrate. Incubations were at room temperature in 100-μl volumes of 50 mM Tris, 0.1 M NaCl, 1 mM EDTA, and 0.01% Tween 80 (pH 7.5), and absorbance at 405 nm was read after 45–60 min using a Titertek Multiskan microtiter plate spectrophotometer. For all plasminogen-linked uPA or tPA assays, parallel sets of replicates were run in the presence and absence of plasminogen, and corrected values representing plasminogen-dependent (*i.e.*, plasminogen-activating) activity were calculated from the difference between these two parallel sets.

The effects of synthetic uPA inhibitors on plasmin activity were assessed as follows. Compounds were incubated with 125 ng/ml human plasmin (American Diagnostica) and 1 mM *H*-D-norleucyl-hexahydrotyrosyl-lysine-*p*-nitroanilide (Spectrozyme PL; American Diagnostica) as plasmin substrate in 100-μl volumes of 50 mM Tris, 0.1 M NaCl, 1 mM EDTA, and 0.01% Tween 80 (pH 7.5). Incubations were at 37°C, and absorbance readings at 405 nm were taken periodically over a 3-h period. Appropriate blanks consisting of all components except substrate were performed in parallel. Data were taken from time points having the best balance between adequate color development and continued linearity of the reaction.

Lineweaver-Burk analyses (35) of effects of synthetic inhibitors on high-molecular-weight human uPA were performed in direct (plasminogen-independent) assays based on the following modifications of the plasminogen-linked assay described immediately above. Briefly, 0–5 μM concentrations of inhibitors were tested against 25 IU/ml uPA and 0.4–4.0 mM concentrations of the synthetic uPA substrate benzoyl-β-alanine-glycine-arginine-*p*-nitroanilide (Pefachrome UK, Centerchem, Stamford, CT) in 100-μl volumes of 50 mM Tris, 0.1 M NaCl, 1 mM EDTA, and 0.01% Tween 80 (pH 7.5). Incubations were allowed to proceed at 37°C, and absorbances at 405 nm were read every 15 min for a 135-min period. A single time point representing maximal color development consistent with the linearity of all inhibitor and substrate combinations over time was then chosen for data acquisition. Data were plotted as $1/[S]$ *versus* $1/v$ for Lineweaver-Burk analysis, and inhibition constants (K_i values) were obtained from replots of the resultant slopes *versus* [I] (35). Although Dixon plotting (35) of the same data yielded essentially identical results, Lineweaver-Burk analysis consistently yielded K_i determinations with less ambiguity, so the decision was made to present the data in the latter format.

Effects of synthetic uPA inhibitors on chymotrypsin, elastase, kallikrein, thrombin, and trypsin activities were assessed as described above for plasmin except that the following enzyme and substrate combinations were used: chymotrypsin, 1 mg/ml bovine pancreas chymotrypsin A_4 (Boehringer Mannheim, Indianapolis, IN) and 1 mM succinyl-L-phenylalanine-*p*-nitroanilide (Suphepa, Boehringer Mannheim); elastase, 4 μg/ml human neutrophil elastase (Calbiochem, La Jolla, CA) and 1 mM *N*-succinyl-alanyl-alanyl-alanine-*p*-nitroanilide (Sigma Chemical Co., St. Louis, MO); kallikrein, 50 mU/ml human plasma kallikrein (Calbiochem) and 1 mM benzoyl-prolyl-phenylalanyl-arginine-*p*-nitroanilide (Chromozym PK, Boehringer Mannheim); thrombin, 10 mU/ml human plasma thrombin (Boehringer Mannheim) and 1 mM tosyl-glycyl-prolyl-arginine-*p*-nitroanilide (Chromozym TH, Boehringer Mannheim); trypsin, 0.1 μg/ml bovine pancreas trypsin (Boehringer Mannheim) and 1 mM carbobenzoxy-valyl-glycyl-arginine-*p*-nitroanilide (Chromozym TRY, Boehringer Mannheim).

Cells and Cell Culture. HT-1080 human fibrosarcoma cells were obtained from the American Type Culture Collection (Rockville, MD) and propagated in Eagle's minimum essential medium with Earle's salts and nonessential amino L-glutamine, 100 U/ml penicillin, and 100 μg/ml streptomycin. Cells were grown under standard tissue conditions at 37°C in a humidified atmosphere containing 5% CO_2. Cells were passaged twice weekly. For routine harvesting, cells were trypsinized using standard procedures. When cells were harvested for experiments they were released from plastic using Versene without trypsin (Gibco/BRL, Grand Island, NY) followed by washing with and resuspension in Hanks' balanced salt solution, serum-free Eagle's medium, or ITS-BSA, depending on experimental requirements. Quantification of cell number was made by hemacytometer counting, and viability determinations were made by standard trypan blue exclusion techniques.

Cell Surface uPA Activity Assay. Inhibition of HT-1080 cell surface receptor-bound uPA was assessed using a modification of the plasminogen-linked chromogenic uPA assay described above. Briefly, cells harvested with Versene were washed once in Hank's balanced salt solution and resuspended at 2×10^6 cells/ml. Twenty-five μl of this suspension were added to 75 μl containing appropriate antibodies or uPA inhibitors and all other components of the plasminogen-linked chromogenic uPA assay described above except uPA. Incubations were allowed to proceed at 37°C for 0–2 h, with periodic spectrophotometric readings. For all HT-1080 cell surface uPA assays, parallel points were performed using 0.5 IU/ml human uPA as a positive control for inhibitory activity; this 50-fold lower level of uPA relative to the standard assay described above was chosen empirically to correspond to the effective concentrations of HT-1080 cell surface uPA in these assays. Control experiments (not shown) indicated that inhibitor IC_{50} values obtained using either 0.5 or 25 IU/ml uPA were essentially identical; thus, both 0.5 and 25 IU/ml uPA fell within the linearity range of the assay. Inhibitor IC_{50} values obtained in HT-1080 cell surface uPA assays are therefore directly and quantitatively comparable to those obtained in standard assays using 25 IU/ml uPA as an enzyme source.

Preparation of [^{3}H]Fibronectin. [^{3}H]Fibronectin was prepared by tritiation of human fibronectin (Calbiochem) with [^{3}H]formaldehyde (80–100 Ci/mmol; New England Nuclear, Boston, MA) using the method of McAbee and Grinnell (36). Final product was stored frozen in small aliquots at −80°C in 0.1 M sodium phosphate buffer (pH 6.8) until use. Specific activities of several different lots of [^{3}H]fibronectin so prepared ranged from 11.1 to 14.3 μCi/mg.

Whole Cell [^{3}H]Fibronectin Degradation Assay. The ability of antibodies or synthetic inhibitors to block cell surface uPA-mediated, plasminogen-dependent degradation of [^{3}H]fibronectin by HT-1080 cells was assessed as follows. Microtiter plates were precoated with 50 μl of 20 μg/ml [^{3}H]fibronectin in 0.1 M sodium phosphate buffer (pH 6.8). After 18 h at 37°C, plates were washed three times with phosphate-buffered saline and placed on ice until needed. HT-1080 cells were harvested with Versene as described above and resuspended in ITS-BSA medium at 1×10^6 cells/ml. Subsequent incubations of cells in [^{3}H]fibronectin-coated plates were in 100-μl volumes of ITS-BSA containing 5×10^4 cells, 200 μg/ml plasminogen or 200 μg/ml additional BSA, and appropriate concentrations of synthetic inhibitors or anti-catalytic monoclonal antibodies (see below). Incubations were carried out for 2.5 h at 37°C in a humidified atmosphere containing 5% CO_2, sufficient time for cells to attach as judged by phase-contrast microscopy. Following incubation, plates were shaken gently on a rotating shaker for 5 min; 50-μl aliquots of supernatants were then taken for assessment of released radioactivity by liquid scintillation counting. Controls included cell-free incubations with and without 100 μg/ml human plasmin (American Diagnostica) to define the upper limit of releasable plasmin-sensitive radioactivity and background leaching of radioactivity from the plastic, respectively.

Anti-catalytic murine monoclonal antibodies to human uPA and tPA were obtained from American Diagnostica (products 394 and 374B, respectively). Control experiments demonstrated complete and cross-reactivity-free anti-catalytic specificities for purified human uPA and tPA, respectively (data not shown); virtually complete inhibition was obtained at concentrations of 10 μg/ml or greater with both antibodies. The anti-uPA antibody was found to be fully active against cell surface uPA (data not shown), as reported by the manufacturer.

RESULTS

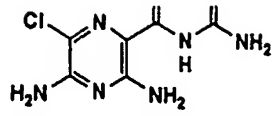

Amiloride

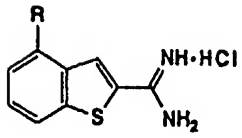

4-substituted benzo[b]thiophene-2-carboxamidines

Compound	-R
B392	-H
B428	-I
B623	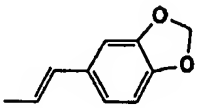

Fig. 1. Structures of amiloride and parental and 4-substituted benzo[*b*]thiophene-2-carboxamidine compounds B392, B428, and B623.

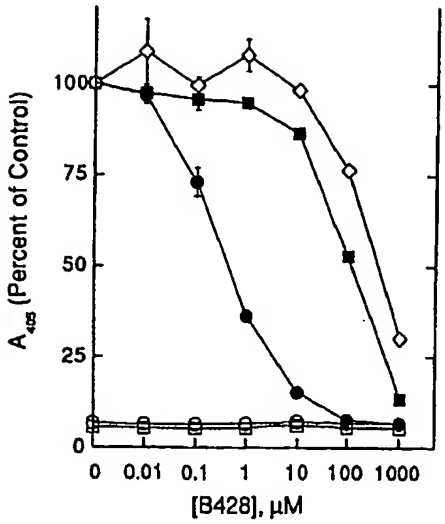

Fig. 2. Effects of B428 on uPA, tPA, and plasmin enzymatic activities. Plasminogen-linked uPA and tPA assays and a direct plasmin assay were performed simultaneously as described in "Materials and Methods." Effects of the indicated concentrations of B428 on uPA (●,○), tPA (■,□), and plasmin (◇) in the presence (●,■) or absence (○,□,◇) of plasminogen are shown. Data represent means ± range of duplicate determinations. After determination of plasminogen-dependent activities, B428 IC_{50} values against uPA and tPA were 0.35 and 95 μM, respectively, in this experiment; the corresponding IC_{50} value against plasmin was 331 μM. One hundred % absorbance values for uPA, tPA, and plasmin assays were 0.967 ± 0.011, 1.160 ± 0.012, and 0.960 ± 0.006, respectively.

Using this compound as a reference agent, we began a search of various mono- and bicyclic aromatic amidines and guanidines with the goal of identifying other selective uPA inhibitors of even greater potency. One bicyclic aromatic amidine, benzo[*b*]thiophene-2-carboxamidine (compound B392 in Fig. 1), was found to be twice as potent as amiloride itself (IC_{50} = 3.7 μM), while retaining high selectivity for uPA relative to tPA and plasmin (Table 1). Subsequent introduction of iodine at the 4 position of B392 yielded compound B428, which had an additional 10-fold increase in potency against uPA (IC_{50} = 0.32 μM; Table 1). Importantly, B428 maintained high selectivity for uPA relative to tPA and plasmin (Table 1), shown graphically in the representative titration of B428 against the three enzymes (Fig. 2). Fig. 2 serves to highlight several points. First, the inhibitory potency of B428 against both uPA and tPA is demonstrated using their natural physiological substrate, plasminogen. Thus, the 330-fold selectivity of B428 for uPA over tPA occurs within the physiologically relevant framework of plasminogen activation and is not just a phenomenon observed with low-molecular-weight synthetic substrates. Second, in the absence of plasminogen there is negligible direct cleavage of plasmin substrate by either uPA or tPA. Third, the observed inhibition of uPA by B428 cannot be accounted for by inhibition of plasmin, since the IC_{50} value of B428 against plasmin is 352 μM, greater than 1000-fold higher than the IC_{50} value against uPA. Results from several similar titrations of B428 are presented in Table 1. Overall, the development of B428 represented a 22-fold increase in potency over amiloride, with essentially no sacrifice in inhibitory selectivity for uPA relative to tPA and plasmin.

More than 90 additional 4-substituted benzo[*b*]thiophene-2-carboxamidines were subsequently synthesized and examined. The most potent of these, B623, has a benzodioxolanylethenyl side chain at the 4 position (Fig. 1). B623 has an IC_{50} value against uPA of 0.07 μM, an increase in potency of 4.6-fold over B428, and an overall 100-fold improvement in potency relative to the starting compound amiloride (Table 1). In addition, B623 maintains high selectivity for uPA over tPA and plasmin, with 340-fold and >3500-fold selectivity ratios, respectively (Table 1).

To investigate the effects of B428 and B623 on a larger spectrum of serine proteases, we tested the effects of these compounds on chymotrypsin, elastase, kallikrein, thrombin, and trypsin activities. As shown in Table 2, neither compound showed significant inhibitory effects against chymotrypsin, elastase, or thrombin, although both inhibited kallikrein and trypsin with IC_{50} values in the low micromolar range (Table 2). Thus, while moderately active against kallikrein and trypsin, B428 and B623 still show 15- to 40-fold greater potencies against uPA.

To examine the mechanism of uPA inhibition by B428 and B623, Lineweaver-Burk analyses were performed using the synthetic uPA substrate benzoyl-β-alanine-glycine-arginine-*p*-nitroanilide in direct (plasminogen-independent) chromogenic assays. As shown in Fig. 3, Lineweaver-Burk analysis of B428 yielded a *y*-axis intercept typical of a competitive inhibitory mechanism (35). Interestingly, similar analysis of B623 yielded a line intercept between the *y*- and *x*-axes, suggestive of mixed type competitive/noncompetitive inhibition (35).

Table 1 *Effects of 4-substituted benzo[b]thiophene-2-carboxamidines and amiloride on human uPA, tPA, and plasmin enzymatic activities*

	uPA		tPA		Plasmin	
Compound	IC_{50} (μM)[a]	*n*	IC_{50} (μM)[a]	*n*	IC_{50} (μM)[a]	*n*
Amiloride	7.2 ± 0.9	10	>1000[b]	2	>1000[b]	2
B392	3.7 ± 1.2	2	>1000[b]	2	>1000[b]	3
B428[c]	0.32 ± 0.02	14	107 ± 22	3	352 ± 30	2
B623	0.07 ± 0.01	18	24 ± 2	5	>250[d]	4

[a] Plasminogen-linked uPA and tPA assays and direct plasmin assay performed as described in "Materials and Methods." Values represent means ± SEM of IC_{50} determinations from *n* separate experiments, each experiment performed in duplicate.

Protease[a]	IC_{50}, μM	
	B428	B623
Chymotrypsin	S[b]	>250[c,d]
Elastase	>1000[e]	>250[c]
Kallikrein	8.8	3.0
Thrombin	850	>250[c]
Trypsin	4.9	2.8

[a] Protease assays performed as described in "Materials and Methods." For each protease, positive controls for inhibition of uPA by B428 or B623 were performed simultaneously; in all cases, expected anti-uPA potencies were observed.

[b] S, stimulatory at concentrations above 10 μM; 4-fold stimulation reached at 250 μM, and 7-fold stimulation reached at 1 mM (data not shown). Mechanisms of this repeatable stimulation of chymotrypsin are unknown.

[c] Limited solubility of B623 above 250 μM precludes higher IC_{50} determinations.

[d] No evidence of chymotrypsin stimulation by B623 at concentrations up to 250 μM.

[e] Less than 50% inhibition at 1 mM concentration.

this observation was confirmed in several separate experiments. Moreover, Lineweaver-Burk analyses of other 4-substituted benzo[*b*]-thiophene-2-carboxamidines having side chains intermediate in length between B428 and B623 consistently showed that the noncompetitive inhibitory component became more pronounced with increasing chain length (data not shown). However, the inclusion of 1 mg/ml BSA in the Lineweaver-Burk analyses eliminated the apparent noncompetitive inhibitory component without altering either K_i or V_{max} values (data not shown), indicating that it results from nonspecific interactions between B623 and urokinase based on the presence of the hydrophobic 4-position side chain. The lack of effect of BSA inclusion on either K_i or V_{max} rules out precipitation of uPA due to insolubility of B623/uPA complexes, and other control experiments indicate that precipitation of uPA substrate itself does not occur in the presence of B623 (data not shown). We conclude that B623 is a purely competitive uPA inhibitor and that the apparent noncompetitive inhibitory component is an artifact of nonspecific interactions between the compound's hydrophobic side chain and uPA.

Replotting of slopes from several Lineweaver-Burk experiments yielded mean K_i values of 0.53 ± 0.07 (SEM) μM and 0.16 ± 0.02 μM for B428 and B623, respectively (Table 3). These K_i values, obtained in plasminogen-independent assays using synthetic uPA substrates, are in close agreement with IC_{50} values obtained in the indirect plasminogen-linked uPA assays (Table 1).

Since it is cell surface, uPAR-bound uPA that is the primary form of the enzyme involved in cellular invasiveness, we tested the ability of B428 and B623 to inhibit cell surface uPA in whole cell, plasminogen-dependent chromogenic assays using HT-1080 human fibrosarcoma cells. These cells produce uPA and express uPAR on their cell surfaces (37). As shown in Fig. 4 (*left*), essentially all HT-1080 cell-associated PA activity can be inhibited by anti-uPA monoclonal antibodies in the same concentration range required for the inhibition of purified uPA. Anti-tPA antibodies and control antibodies against the CA125 tumor marker (38) had no effect on either HT-1080 cell-associated PA activity or purified uPA itself. Thus, HT-1080 cell-associated PA is uPA. Moreover, this cell-associated uPA is in fact cell surface uPA since there is virtually no detectable uPA secreted into conditioned media during the 2-h duration of this assay (data not shown). In a series of similar experiments, B428 and B623 inhibited HT-1080 cell surface uPA with mean IC_{50} values of 0.54 and 0.20 μM, respectively (Fig. 4, *right*), in good agreement with K_i values obtained using purified uPA (Table 3). In the same series of experiments, amiloride had a mean IC_{50} value of 16 μM against HT-1080 cell surface uPA (Fig. 4, *right*), or 30- to 80-fold less activity than that seen with B428 and B623, respectively.

The ability of B428 and B623 to block cell surface uPA-mediated (*left*), background release of radioactivity under cell-free conditions was very low in both the absence and presence of plasminogen, indicating a lack of contaminating plasmin in the plasminogen preparation. In contrast, addition of plasmin to cell-free wells led to large amounts of radioactivity release, demonstrating plasmin sensitivity of the [^{3}H]fibronectin layer. With cells, [^{3}H]fibronectin degradation was only seen if plasminogen was present during the 2.5-h cell attachment period; thus cells were incapable of degrading [^{3}H]fibronectin except via plasminogen-dependent mechanisms. Plasminogen-dependent cellular degradation of [^{3}H]fibronectin was completely blocked by the addition of anti-uPA monoclonal antibodies, whereas anti-tPA antibodies were without effect. Thus, plasminogen-dependent [^{3}H]fibronectin degradation occurring during HT-1080 cell attachment is mediated solely by cell surface uPA. This finding is in agreement with the studies of Fig. 4, which showed that HT-1080 cell-associated PA activity is in fact cell surface uPA. B428 and B623 both inhibited plasminogen-dependent, cell surface uPA-mediated [^{3}H]fibronectin degradation by HT-1080 cells in a dose-dependent manner (Fig. 5, *right*). IC_{50} values for B428 and B623 were 1.5 and 0.39 μM, respectively, slightly higher than those seen for the inhibition of cell surface uPA enzyme activity (Fig. 4, *right*) and K_i values obtained against purified uPA (Table 3). Nevertheless, B428 and B623 remain highly potent inhibitors of cell surface uPA-mediated cellular degradation of [^{3}H]fibronectin.

DISCUSSION

The role of uPA, and particularly cell surface uPA, as an initiator of ECM degradation and *in vitro* and *in vivo* cellular invasiveness is now well established (2–6, 10, 19, 23, 39–41). The most compelling evidence in support of this concept comes from experiments performed by many laboratories in which the enzymatic activity of cell surface uPA is blocked with anti-catalytic anti-uPA antibodies, PAI-1 or PAI-2, or in which uPA binding to uPAR is blocked with antibodies or peptide antagonists. For instance, the present study demonstrates the ability of anti-catalytic anti-uPA antibodies to block cell surface uPA-mediated degradation of [^{3}H]fibronectin by HT-1080 cells (Fig. 5). Similarly, degradation of [^{125}I]fibronectin by mouse melanoma cells is inhibited by anti-catalytic anti-uPA antibodies (10), and peptides corresponding to the uPAR binding region of the A-chain of uPA inhibit degradation of ^{125}I-laminin by colon carcinoma cells (11) and of whole ECM by mouse LB6 cells expressing human uPAR charged with human uPA (12). Anti-catalytic anti-uPA antibodies inhibit whole ECM degradation by human squamous carcinoma cells (13), and inhibitory effects of PAI-1 and PAI-2 on whole ECM degradation by HT-1080 cells (14) and human colon carcinoma cells (15), respectively, have been reported.

In vitro, anti-catalytic anti-uPA antibodies inhibit the invasiveness of human prostate carcinoma (16) and ovarian carcinoma (17) cells into ECM layers. Moreover, *in vitro* ECM invasion by human prostate and colon carcinoma cells is blocked by antibodies to the uPAR-binding A-chain of uPA (18) or peptides corresponding to the uPAR binding region of the A-chain (16, 19). Anti-catalytic anti-uPA antibodies, PAI-1 and PAI-2 have all been shown to inhibit *in vitro* invasion of human monocytes (20, 21) and lung carcinoma cells (22) into amniotic membranes. Similarly, anti-catalytic anti-uPA antibodies block chick chorioallantoic membrane invasion of HEp3 human carcinoma cells (23) and the above-mentioned mouse LB6 cells expressing human uPAR charged with human uPA (24).

In vivo, anti-catalytic anti-uPA antibodies inhibit metastases of HEp3 human carcinoma cells to chick embryo lung and heart (25, 26)

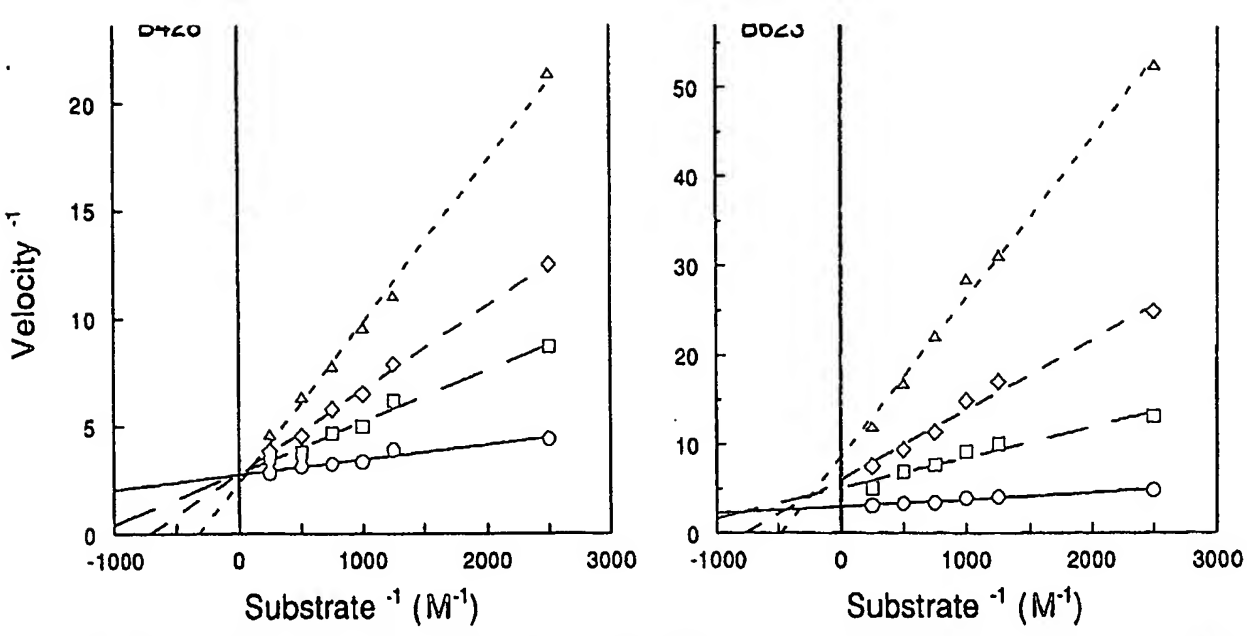

Fig. 3. Lineweaver-Burk analyses of B428 and B623 inhibition of uPA. Lineweaver-Burk analyses of inhibition of uPA by B428 (*left*) and B623 (*right*) were performed in direct chromogenic assays using the synthetic uPA substrate benzoyl-β-alanine-glycine-arginine-*p*-nitroanilide as described in "Materials and Methods." Substrate concentrations used were 0.4, 0.8, 1, 1.33, 2, and 4 mM; inhibitor concentrations were 0 (○), 1.25 μM (□), 2.5 μM (◇), and 5 μM (△). Data represent means of duplicate determinations. Replots of slopes from the experiments shown yielded K_i values of 0.50 and 0.14 μM for B428 and B623, respectively; mean K_i values obtained from a number of similar experiments are presented in Table 3.

Table 3 *Urokinase inhibition constants (K_i) for 4-substituted benzo[b]thiophene-2-carboxamidines*

Compound	K_i (μM)[a]	*n*
B428	0.53 ± 0.07	4
B623	0.16 ± 0.02	3

[a] K_i values determined from replots of slopes from Lineweaver-Burk analyses similar to those presented in Fig. 3. Data represent means ± SEM of determinations from *n* separate experiments.

in mice receiving B16 melanoma cells via tail vein injection (10), as well as local invasiveness and lung metastases in nude mice bearing subcutaneous MDA-MB-231 breast carcinoma tumors (42). Taken together, all of the preceding studies provide compelling evidence for the importance of cell surface uPA in ECM degradation, *in vitro* cellular invasiveness, and *in vivo* tumor metastasis and invasion. Inhibition of cell surface uPA is therefore an attractive pharmaceutical target for counteracting cellular invasiveness in numerous disease states such as cancer, arthritis, and pathological neovascularization.

Pharmaceutically useful uPA inhibitors must be specific for uPA relative to tPA and plasmin, since the inhibition of fibrinolysis mediated by the latter two enzymes would be an unacceptable side effect. Although many low-molecular-weight serine protease inhibitors will inhibit uPA, only three groups of such inhibitors are relatively free of inhibitory effects against tPA and plasmin, and unfortunately these show only moderate potency against uPA. The first group, the para-substituted benzamidines, is exemplified by *p*-aminobenzamidine, whose K_i value against uPA has been variously reported to be 17–82 μM (28–30). Second, the potassium-sparing diuretic amiloride selectively inhibits uPA ($K_i \approx 7$ μM) with virtually no effect on tPA or plasmin (31). Finally, 4-chloro- and 4-trifluoromethylphenylguanidine are approximately equipotent uPA inhibitors with amiloride ($K_i \approx 6$ μM), and neither compound has appreciable inhibitory effects on either tPA or plasmin (32).

Despite only moderate potencies, at least three reports suggest that uPA-selective inhibitors such as *p*-aminobenzamidine and amiloride can nevertheless inhibit cellular invasiveness *in vivo*. First, *p*-aminobenzamidine prolonged the survival of mice challenged with Ehrlich carcinoma cells (44). Finally, amiloride blocked prostaglandin E_1-induced neovascularization in the rabbit cornea (45). While uPA inhibition was not firmly established as a causative mechanism in these three studies, such observations nevertheless support the concept that, like anti-uPA antibodies, PAI-1, PAI-2 and uPAR peptide antagonists, low-molecular-weight synthetic uPA inhibitors can block cell surface uPA-mediated cellular invasiveness *in vivo* resulting in beneficial therapeutic effects.

Our search of a large number of monocyclic and bicyclic aromatic amidines and guanidines led to the finding that benzo[*b*]thiophene-2-carboxamidine, compound B392, was itself more potent than any previously described selective synthetic uPA inhibitor. Several simple substitutions at various positions on the molecule revealed that iodine at the 4 position (B428) increased potency by an additional factor of 10. Subsequent substitutions at the 4 position with over 90 different substituents led to even greater potencies, culminating in the synthesis of our most potent compound to date, B623.

Similar compounds in which the benzo[*b*]thiophene sulfur atom was replaced with carbon, oxygen, or nitrogen were less potent as uPA inhibitors, and 2-guanidino-benzo[*b*]thiophene was essentially devoid of activity. Thus, 4-substituted benzo[*b*]thiophene-2-carboxamidines appear to represent a clearly defined class of previously unknown, potent and selective uPA inhibitors. Moreover, the ability of compounds such as B428 and B623 to inhibit uPA without significant effects on tPA or plasmin underscores their potential utility as antiinvasiveness drugs, since thrombotic side effects secondary to inhibiting fibrinolysis would be avoided. While some inhibition of trypsin and kallikrein was observed with B428 and B623, potencies against these two enzymes were 15- to 40-fold less than those observed against uPA. Inhibition of trypsin and kallikrein by B428 and B623 suggests functional active site similarities between the three enzymes. Indeed, this is supported by the fact that amiloride itself is a known kallikrein inhibitor (46), and both 4-chloro- and 4-trifluoromethylphenylguanidine inhibit trypsin in the 60–120 μM range (32).

B428 and B623 inhibit free and cell surface uPA with similar potencies. This is important since cell surface uPA is the major form of the enzyme involved in extracellular proteolysis and cellular inva-

Fig. 4. Inhibition of HT-1080 cell surface uPA by anti-uPA antibodies, B428, B623, and amiloride. Cell surface uPA activity on whole living HT-1080 cells was assessed by chromogenic assay in the presence and absence of plasminogen as described in "Materials and Methods"; the results shown represent plasminogen-dependent activity only, which was calculated from the difference between these two incubations. *Left*, incubations with HT-1080 cells (——) or 500 mIU/ml uPA (– – – –) containing the indicated concentrations of anti-uPA (●), anti-tPA (■), or anti-CA125 (♦) monoclonal antibodies. *Right*, incubations with HT-1080 cells containing the indicated concentrations of B428 (⊞), B623 (△), or amiloride (⊠). Results represent means ± SEM of individual determinations from 5 separate experiments, each experiment having been performed in duplicate.

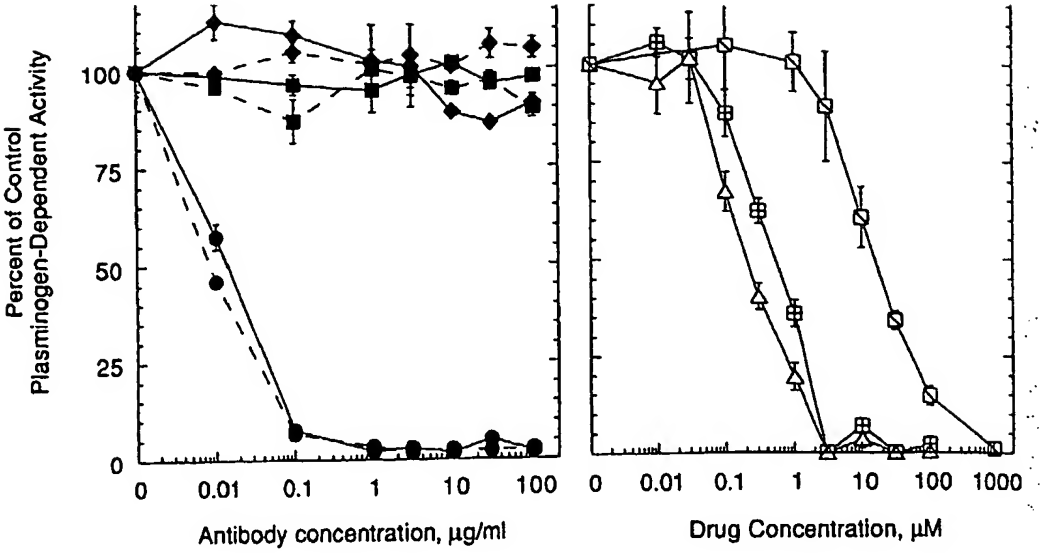

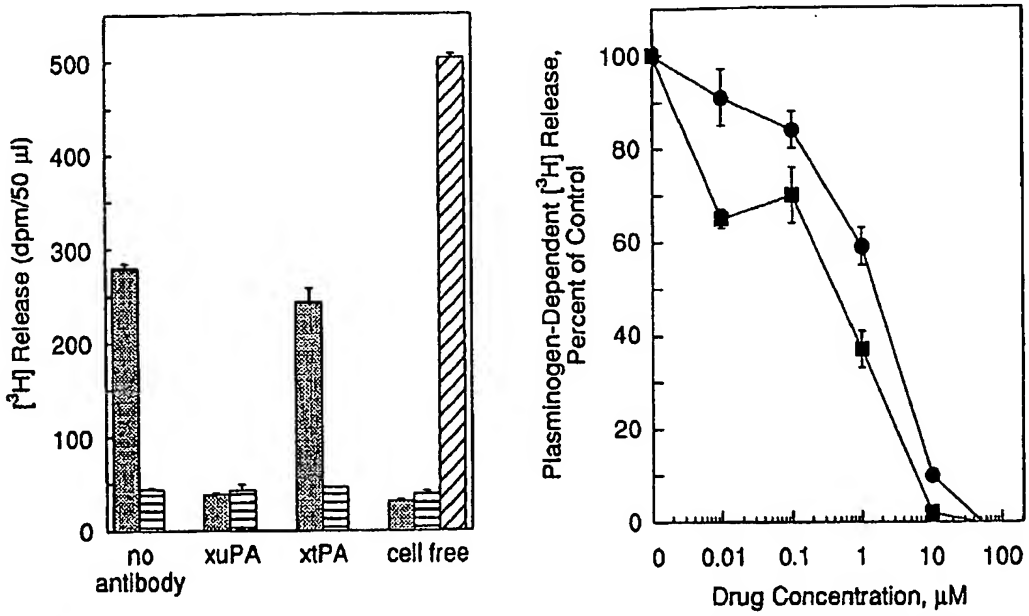

Fig. 5. Cell surface uPA-mediated degradation of [^{3}H]fibronectin by HT-1080 cells during cell attachment: inhibition by B428, B623, and anti-uPA antibodies. [^{3}H]Fibronectin degradation assays were performed as described in "Materials and Methods" during the first 2.5 h following seeding of HT-1080 cells into [^{3}H]fibronectin-coated 96-well plates. This time period was determined to be the length of time required for virtually all cells to become attached as judged by visual phase-contrast microscopy. *Left*, total ^{3}H release seen with cells with no antibody, cells with 10 μg/ml anti-uPA antibodies, cells with 10 μg/ml anti-tPA antibodies, or no cells, in the presence (⊟) or absence (▤) of plasminogen as indicated. Also included is a cell-free incubation with 100 μg/ml plasmin (▨) to demonstrate the plasmin sensitivity of the [^{3}H]fibronectin layer. *Right*, separate experiments for B428 (●) and B623 (■) were performed; results were normalized to percentage of control (no inhibitor) and plotted in the same graph for comparative purposes. Data represent differences in ^{3}H release between incubations with and without plasminogen, defined as plasminogen-dependent ^{3}H release. The B428 experiment was performed simultaneously with the control incubations shown on the *left*; 100% in the B428 experiment represents the plasminogen-dependent portion of ^{3}H release seen in the "no antibody" group of controls. Similar relative levels of plasminogen-dependent and plasminogen-independent ^{3}H release occurred in the B623 experiment, the controls of which are not shown. *Left* and *right*, data represent means ± SEM of triplicate determinations.

HT-1080 cells. Although there is some loss of inhibitory potency as one moves from inhibition of free uPA to cell surface uPA to cell surface uPA-mediated cellular function, these losses are not large and are probably related to metabolism, nonspecific adsorption to membranes, diffusion constraints, or other cell-dependent phenomena which might lower effective concentrations of the compounds.

In summary, we have shown 4-substituted benzo[*b*]thiophene-2-carboxamidines, exemplified by compounds B428 and B623, to be highly potent competitive inhibitors of uPA with excellent selectivity for uPA relative to tPA and plasmin. Both compounds block cell surface uPA activity as well as cell surface uPA-mediated cellular degradation of [^{3}H]fibronectin. Our results indicate that 4-substituted benzo[*b*]thiophene-2-carboxamidines such as B428 and B623 represent an important new class of potent and selective synthetic uPA

REFERENCES

1. Mullins, D. E., and Rohlich, S. T. The role of proteinases in cellular invasiveness. Biochim. Biophys. Acta, *695:* 177–214, 1983.
2. Danø, K., Andreasen, P. A., Grøndahl-Hansen, J., Kristensen, P., Nielsen, L. S., and Skriver, L. Plasminogen activators, tissue degradation, and cancer. Adv. Cancer Res., *44:* 139–266, 1985.
3. Saksela, O. Plasminogen activation and regulation of pericellular proteolysis. Biochim. Biophys. Acta, *823:* 35–65, 1985.
4. Testa, J. E., and Quigley, J. P. The role of urokinase-type plasminogen activator in aggressive tumor cell behavior. Cancer Metast. Rev., *9:* 353–367, 1990.
5. Blasi, F., Vassalli, J-D., and Danø, K. Urokinase-type plasminogen activator: proenzyme, receptor, and inhibitors. J. Cell Biol., *104:* 801–804, 1987.
6. Roldan, A. L., Cubellis, M. V., Masucci, M. T., Behrendt, N., Lund, L. R., Danø, K., Appella, E., and Blasi, F. Cloning and expression of the receptor for human urokinase plasminogen activator, a central molecule in cell surface, plasmin dependent proteolysis. EMBO J., *9:* 467–474, 1990.
7. Mignatti, P., Robbins, E., and Rifkin, D. B. Tumor invasion through the human amniotic membrane: requirement for a proteinase cascade. Cell, *47:* 487–498, 1986.

carcinoma collagenase through plasminogen activator. Life Sci., *26:* 1225–1231, 1980.
10. Flearing, V. J., Law, L. W., Corti, A., Appella, E., and Blasi, F. Modulation of metastatic potential by cell surface urokinase of murine melanoma cells. Cancer Res., *48:* 1270–1278, 1988.
11. Schlechte, W., Murano, G., and Boyd, D. Examination of the role of the urokinase receptor in human colon cancer mediated laminin degradation. Cancer Res., *49:* 6064–6069, 1989.
12. Quax, P. H. A., Pedersen, N., Masucci, M. T., Weening-Verhoeff, E. J. D., Danø, K., Verheijen, J. H., and Blasi, F. Complementation between urokinase-producing and receptor-producing cells in matrix degradation. Cell Regul., *2:* 793–803, 1991.
13. Niedbala, M. J., and Sartorelli, A. C. Plasminogen activator mediated degradation of subendothelial extracellular matrix by human squamous carcinoma cell lines. Cancer Commun., *2:* 189–199, 1990.
14. Cajot, J. F., Bamat, J., Bergonzelli, G. E., Kruithof, E. K. O., Medcalf, R. L., Testuz, J., and Sordat, B. Plasminogen-activator inhibitor type 1 is a potent natural inhibitor of extracellular matrix degradation by fibrosarcoma and colon carcinoma cells. Proc. Natl. Acad. Sci. USA, *87:* 6939–6943, 1990.
15. Baker, M. S., Bleakley, P., Woodrow, G. C., and Doe, W. F. Inhibition of cancer cell urokinase plasminogen activator by its specific inhibitor PAI-2 and subsequent effects on extracellular matrix degradation. Cancer Res., *50:* 4676–4684, 1990.
16. Hoosein, N. M., Boyd, D. D., Hollas, W. J., Mazar, A., Henkin, J., and Chung, L. W. K. Involvement of urokinase and its receptor in the invasiveness of human prostatic carcinoma cell lines. Cancer Commun., *3:* 255–264, 1991.
17. Kobayashi, H., Ohi, H., Sugimura, M., Shinohara, H., Fujii, T., and Terao, T. Inhibition of *in vitro* ovarian cancer cell invasion by modulation of urokinase-type plasminogen activator and cathepsin B. Cancer Res., *52:* 3610–3614, 1992.
18. Hollas, W., Blasi, F., and Boyd, D. Role of the urokinase receptor in facilitating extracellular matrix invasion by cultured colon cancer. Cancer Res., *51:* 3690–3695, 1991.
19. Schlechte, W., Brattain, M., and Boyd, D. Invasion of extracellular matrix by cultured colon cancer cells: dependence on urokinase receptor display. Cancer Commun., *2:* 173–179, 1990.
20. Kirchheimer, J. C., and Remold, H. G. Endogenous receptor-bound urokinase mediates tissue invasion of human monocytes. J. Immunol., *143:* 2634–2639, 1989.
21. Kirchheimer, J. C., Binder, B. R., and Remold, H. G. Matrix-bound plasminogen activator inhibitor type 1 inhibits the invasion of human monocytes into interstitial tissue. J. Immunol., *145:* 1518–1522, 1990.
22. Bruckner, A., Filderman, A. E., Kirchheimer, J. C., Binder, B. R., and Remold, H. G. Endogenous receptor-bound urokinase mediates tissue invasion of the human lung carcinoma cell lines A549 and Calu-1. Cancer Res., *52:* 3043–3047, 1992.
23. Ossowski, L. *In vivo* invasion of modified chorioallantoic membrane by tumor cells: the role of cell surface-bound urokinase. J. Cell Biol., *107:* 2437–2445, 1988.
24. Ossowski, L., Clunie, G., Masucci, M-T., and Blasi, F. *In vivo* paracrine interaction between urokinase and its receptor: effect on tumor cell invasion. J. Cell Biol., *115:* 1107–1112, 1991.
25. Ossowski, L., and Reich, E. Antibodies to plasminogen activator inhibit human tumor metastasis. Cell, *35:* 611–619, 1983.
26. Ossowski, L. Plasminogen activator dependent pathways in the dissemination of human tumor cells in the chick embryo. Cell, *52:* 321–328, 1988.
27. Ossowski, L., Russo-Payne, H., and Wilson, E. L. Inhibition of urokinase-type plasminogen activator by antibodies: the effect on dissemination of a human tumor in the nude mouse. Cancer Res., *51:* 274–281, 1991.
28. Stürzebecher, J., and Markwardt, F. Synthetische Inhibitoren der Serinproteinasen.
29. Christova, E., Yomtova, V., and Blagoev, B. Hydrophobic interactions in the urokinase active centre. Inhibitory action of alkyl ammonium and amidinium ions: comparison with trypsin. Int. J. Pept. Protein Res., *15:* 459–463, 1980.
30. Geratz, J. D., Shaver, S. R., and Tidwell, R. R. Inhibitory effect of amidino-substituted heterocyclic compounds on the amidase activity of plasmin and of high and low molecular weight urokinase and on urokinase-induced plasminogen activation. Thromb. Res., *24:* 73–83, 1981.
31. Vassalli, J-D., and Belin, D. Amiloride selectively inhibits the urokinase-type plasminogen activator. FEBS Lett., *214:* 187–191, 1987.
32. Yang, H., Henkin, J., Kim, K. H., and Greer, J. Selective inhibition of urokinase by substituted phenylguanidines: quantitative structure-activity relationship analyses. J. Med. Chem., *33:* 2956–2961, 1990.
33. Garigipati, R. S. An efficient conversion of nitriles to amidines. Tetrahedron Lett., *31:* 1969–1972, 1990.
34. Karlan, B. Y., Clark, A. S., and Littlefield, B. A. A highly sensitive chromogenic microtiter plate assay for plasminogen activators which quantitatively discriminates between the urokinase and tissue-type activators. Biochem. Biophys. Res. Commun., *142:* 147–154, 1987.
35. Segel, I. H. Enzyme Kinetics: Behavior and Analysis of Rapid Equilibrium and Steady-State Enzyme Systems, pp. 100–160. New York: John Wiley and Sons, 1975.
36. McAbee, D. D., and Grinnell, F. Fibronectin-mediated binding and phagocytosis of polystyrene latex beads by baby hamster kidney cells. J. Cell Biol., *97:* 1515–1523, 1983.
37. Stephens, R. W., Pöllänen, J., Tapiovaara, H., Leung, K-C., Sim, P-S., Salonen, E-M., Rønne, E., Behrendt, N., Danø, K., and Vaheri, A. Activation of pro-urokinase and plasminogen on human sarcoma cells: a proteolytic system with surface-bound reactants. J. Cell Biol., *108:* 1987–1995, 1989.
38. Karlan, B. Y., Amin, W., Casper, S. E., and Littlefield, B. A. Hormonal regulation of CA125 tumor marker expression in human ovarian carcinoma cells: inhibition by glucocorticoids. Cancer Res., *48:* 3502–3506, 1988.
39. Takahashi, K., Ikeo, K., Takashi, G., and Tanifuji, M. Local function of urokinase receptor at the adhesion contact sites of a metastatic tumor cell. Thromb. Res., (Suppl. 10): 55–61, 1990.
40. Estreicher, A., Mühlhauser, J., Carpentier, J-L., Orci, L., and Vassalli, J-D. The receptor for urokinase type plasminogen activator polarizes expression of the protease to the leading edge of migrating monocytes and promotes degradation of enzyme inhibitor complexes. J. Cell Biol., *111:* 783–792, 1990.
41. Masucci, M. T., and Blasi, F. The receptor for human urokinase: a potential target for anti-invasive and anti-metastatic therapy. Thromb. Res., (Suppl. 11): 49–60, 1990.
42. Brünner, N., Høyer-Hansen, G., Rømer, J., Ellis, V., Holst-Hansen, C., Spang-Thomsen, M., and Danø, K. Inhibition of intraperitoneal and metastatic spread of a xenotransplanted human breast carcinoma using a monoclonal antibody directed against the human urokinase-type plasminogen activator. Proc. Am. Assoc. Cancer Res., *33:* 61, 1992.
43. Verloes, R., Atassi, G., Dumont, P., and Kanarek, L. Tumor growth inhibition mediated by trypsin inhibitor or urokinase inhibitor. Eur. J. Cancer, *14:* 23–31, 1978.
44. Kellen, J. A., Mirakian, A., and Kolin, A. Antimetastatic effect of amiloride in an animal tumour model. Anticancer Res., *8:* 1373–1376, 1988.
45. Avery, R. L., Connor, T. B., Jr., and Farazdaghi, M. Systemic amiloride inhibits experimentally induced neovascularization. Arch. Ophthalmol., *108:* 1474–1476, 1990.
46. Margolius, H. S., and Chao, J. Amiloride inhibits mammalian renal kallikrein and a kallikrein-like enzyme from toad bladder and skin. J. Clin. Invest., *65:* 1343–1350, 1980.